

Role of the Ocean in the Global Carbon Cycle

Thesis submitted to

**The Maharaja Sayajirao University of Baroda
Vadodara, India**

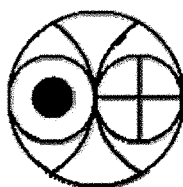
For the degree of

Doctor of Philosophy in Geology

By

Satya Prakash

April, 2008



**Planetary and Geosciences Division
Physical Research Laboratory,
Navrangpura, Ahmedbad-380 009,
India**

Certificate

I hereby declare that the work presented in this thesis is original and has not been formed the basis for the award of any degree or diploma by any university or institution.

Satya Prakash.

Satya Prakash (Author)

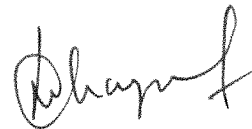
Planetary and Geosciences Division
Physical Research Laboratory
Navrangpura, Ahmedabad-380 009
India

Certified by:



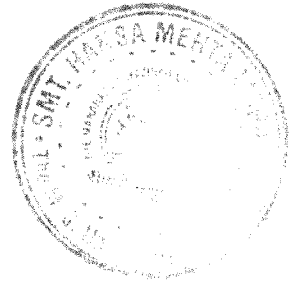
Prof. R. Ramesh (Guide)

Planetary and Geosciences Division
Physical Research Laboratory
Navrangpura, Ahmedabad-380 009
India



Prof. L.S. Chamyal (Co-guide)

Department of Geology
The Maharaja Sayajirao University of Baroda
Vadodara-390 002
India



Dedicated to

Bhaiya and Bhabhi
(Brother and Sister-in-law)



ABSTRACT

Nitrogen plays a key role in oceanic productivity and hence its unavailability can be a limiting factor. The present work uses nitrogen as a tool to estimate primary productivity of different parts of the Indian Ocean and thus assess its role in Global Carbon Cycle.

As the oceans play a major role in the global carbon cycle, it is required to quantify the amount of inorganic carbon taken up by the individual ocean basins. Also the assessment of different ocean basins as source/sink of carbon is important. The present study was carried out using the ^{15}N tracer technique which gives total production as a sum of new production (nitrate uptake) and regenerated production (ammonium and urea uptakes). The advantage of this technique lies in the quantification of new productivity which is a measure of carbon removed from the surface for significantly longer time periods (>1000 yrs). The present work is a comprehensive study of primary productivity in different regions of the Indian Ocean such as the Arabian Sea, equatorial Indian Ocean and Southern Indian Ocean. Though some study has been carried out previously in some selected parts of the Arabian Sea, most of them are concentrated on the north-western and central Arabian Sea. No study has been done in the equatorial Indian Ocean and Southern Indian Ocean. The present study concentrates on the north-eastern Arabian Sea and is the *first* to measure primary productivity in the *equatorial Indian* and *Southern Indian Oceans*.

The biogeochemistry of the Arabian Sea, one of the most biologically productive regions of the world ocean, is driven by seasonally reversing southwest and northeast monsoons; both the monsoons trigger high primary production but the underlying mechanisms are different. Results from the present study suggest that the Arabian Sea is characterized by the presence of two different biogeochemical provinces during the late winter monsoon: low productive southern province and highly productive northern province with an overall increasing trend from the south to the north. Total productivity in the southern region averaged around $5.5 \text{ mmolNm}^{-2}\text{d}^{-1}$ ($440 \text{ mgCm}^{-2}\text{d}^{-1}$) whereas in the north it was $19 \text{ mmolNm}^{-2}\text{d}^{-1}$ ($1520 \text{ mgCm}^{-2}\text{d}^{-1}$);

increase in productivity from the south to north was more than three fold. New productivity also increased on south-north transect, from $2.1 \text{ mmolNm}^{-2}\text{d}^{-1}$ ($168 \text{ mgCm}^{-2}\text{d}^{-1}$) in the south to $15.7 \text{ mmolNm}^{-2}\text{d}^{-1}$ ($1256 \text{ mgCm}^{-2}\text{d}^{-1}$) in the north. Increase in new productivity was more than 7-fold. The column integrated total production (x) and new production (y), show a significant correlation (Fig.2): for non-bloom stations: $y = (0.44 \pm 0.23) x - (0.30 \pm 1.38)$ (coefficient of determination, $r^2 = 0.43$); and for bloom stations, $y = (1.08 \pm 0.23) x - (4.68 \pm 4.46)$ ($r^2 = 0.91$). The slope of regression (i.e., 0.44 and 1.0 for non-bloom and bloom stations respectively) is the maximum possible value of the f -ratio.

During the early winter monsoon total productivity varied from $4.07 \text{ mmolNm}^{-2}\text{d}^{-1}$ ($326 \text{ mgCm}^{-2}\text{d}^{-1}$) to $23.31 \text{ mmolNm}^{-2}\text{d}^{-1}$ ($1865 \text{ mgCm}^{-2}\text{d}^{-1}$) with a mean of $8.65 \text{ mmolNm}^{-2}\text{d}^{-1}$ ($692 \text{ mgCm}^{-2}\text{d}^{-1}$). Productivity during this season was almost half of that during the bloom but was more than the productivity in the south during the late winter monsoon. New productivity showed a large variation; it varied from a low of $1.95 \text{ mmolNm}^{-2}\text{d}^{-1}$ ($156 \text{ mgCm}^{-2}\text{d}^{-1}$) to a high of $19.70 \text{ mmolNm}^{-2}\text{d}^{-1}$ ($1576 \text{ mgCm}^{-2}\text{d}^{-1}$). The f -ratio varied from 0.46 to 0.87. This suggests that 46-87% of the total productivity can be exported to the deep under a steady state condition. Relation between total and new productivity yielded a slope of 0.88 which suggests that at most 88% of the total productivity can be exported. Above results from the two seasons suggests that productivity in the Arabian Sea is heterogeneous in space and time but still this basin is capable of high export production and thus plays a significant role in global carbon cycle.

The first result from the equatorial Indian Ocean suggests that total N-uptake is very less in this basin: it varied from $0.66 \text{ mmolNm}^{-2}\text{d}^{-1}$ to $2.23 \text{ mmolNm}^{-2}\text{d}^{-1}$ in the pre-monsoon season. The mean N-uptake was $1.32 \text{ mmolNm}^{-2}\text{d}^{-1}$ ($105.6 \text{ mgCm}^{-2}\text{d}^{-1}$). New production along 77°E transect was $0.20 \text{ mmolNm}^{-2}\text{d}^{-1}$ ($16 \text{ mgCm}^{-2}\text{d}^{-1}$), almost half of the same $0.43 \text{ mmolNm}^{-2}\text{d}^{-1}$ ($34.4 \text{ mgCm}^{-2}\text{d}^{-1}$) along 83°E transect. Urea was the most preferred form of nitrogen for phytoplankton followed by ammonium. Nitrate was the least preferred. The f -ratio was also very low though it showed considerable spatial variation: it varied from 0.14 to 0.40. The f -ratio was low (mean = 0.18) along 77°E transect but was relatively high (mean = 0.29) along

83°E. In the equatorial Indian Ocean upper mixed layer had greater control on the productivity; since this layer was devoid of any nutrients, the productivity was less. Also due to strong stratification the export production was low.

The first comprehensive estimates of nitrogen based productivity from a large area in the Southern Indian Ocean suggest that Antarctic coastal zone, STF and equatorial Indian Ocean was relatively more productive than other parts of the Southern Ocean. Euphotic zone integrated total N-uptake rate varied from 1.73 mmolNm⁻²d⁻¹ (138 mgCm⁻²d⁻¹) to 12.26 mmolNm⁻²d⁻¹ (981 mgCm⁻²d⁻¹) in the Southern Indian Ocean; the highest rate was measured in the Antarctic coastal zone (69°S). New productivity varied from 0.92 mmolNm⁻²d⁻¹ (73.6 mgCm⁻²d⁻¹) to 7.7 mmolNm⁻²d⁻¹ (616 mgCm⁻²d⁻¹). The Antarctic coastal zone, equatorial region and STF had more new production compared to other regions of the Southern Ocean. The mean Column N-uptake rate at two equatorial stations sampled during this study was ~8 mmolNm⁻²d⁻¹. The *f*-ratio was almost the same (0.45) at both stations. Though a large part of the southern Ocean, HNLC region, is less productive, it can have high export production, almost 50% of the total. The *f*-ratio varied from 0.27 to 0.63 in the Southern Ocean with a mean of 0.50 and with an upper limit of 0.63. Compared to other data from similar regions the present study shows a shift in productivity regime from regenerated nutrient based production to nitrate based production. This means a slightly greater export production in this region than before. Again, a significant correlation between total and new productivity can provide a significant input for the estimation of carbon fluxes over a large region using satellite data.

Acknowledgements

At this point of time when I am summarizing my work at PRL for my Ph.D thesis, I would like to express my gratitude to many individuals who, with their sincere guidance and unconditional support made this thesis a reality.

First of all I would like to express my gratitude to my thesis supervisor Prof. R.Ramesh for his guidance, encouragement and support. He is the best teacher in the world who explains tough concepts in a simple way that straight-away goes into one's head and one can never forget the same. I have greatly benefited by him; otherwise learning complex phenomena of Ocean Science, whatever little I could learn, would have been very difficult for me. I also thank him for inviting me for innumerable parties at week-ends which helped me a lot in releasing my week's tension and starting afresh. I also thank Prof. L. S. Chamyal (Dept. of Geology, M.S. University of Baroda) for his interest in this work, and his help with university procedures.

I am indebted to the faculty of PGSDN here for their comments and suggestions during various phases of my work that certainly added to its quality. I specially thank Prof. S. Krishnaswami and Prof. M.M.Sarin whose questions, critical comments and suggestions during Area Seminars and 2nd and 4th year reviews helped me to improve this work. I also thank other members of the Academic Committee for their critical and positive comments.

I also thank Mr. R.M Dwivedi (Chief Scientist SS-222, SK-214), Dr. Prasanna Kumar (Chief Scientist SK-220) and Dr. M. Sudhakar (Chief scientist ABP-15) for giving me opportunities to participate in different cruises. Thanks are also due to Ms Mini Raman for providing me radiometer data of light measurements, Dr. Prabhu Matondakar and S.W.A Naqvi for Chl-*a* and nutrients data for Arabian Sea cruises, Dr. Sugandhini Sardesai for nutrient data for equatorial Ocean cruise and Dr. Rahul Mohan for Chl-*a* data for Southern Ocean cruise. I thank my friends Arvind, Thomas, Nagamani (all from SAC), Nuncio, Jeyu, Anil, Jyothi Babu and Madhu (all from NIO) for their help at various stages of my thesis work. Special thanks are due to Ravi Mishra, Meena, Anup, Amitabh, S.K.Singh for making "long and horrifying" Southern Ocean cruise memorable.

I specially thank Prof. UdayaKumar, Dr. M.S.Sheshshayee and Dr. Bindumadhava for their help during my stay at GKVK Bangalore for sample analysis. Thanks are also due to Bhushna for his help at GKVK. I still cherish those moments spent with them, especially parties in the evening, at Green Park.

I am grateful to Profs. Trevor Platt and Shubha Sathyendranath for giving me an opportunity to participate in POGO training programme and introducing me to satellite based oceanographic studies. I also thank all the participants of the training programme for making the stay in NIO RC-Kochi memorable.

I thank Dr. M. Sudhakar and Mr. Subrahmanyam of NCAOR Goa for all the help towards arranging different cruises. I also thank captain and crew members of FORV *Sagar Sampada* (SS-222), ORV *Sagar Kanya* (SK-214, SK-220) and *Akademik Boris Petrov* (ABP-15) for their help during this work.

This work would not have been possible without valuable helps from P.K Gopi (stores), Parul ben, Gandhi and Deekshitulu (accounts), Ravishankar (Purchase), Ghanshyam bhai (transport), P. K. Gopi (stores), Bhavsar Bhai (Chemistry lab) and Vaghela Bhai (C-14 lab). Computer Centre staff are also much appreciated. I thank Mrs Nistha Kumar and Uma ben of PRL library for their support. I also thank PRL canteen staff for providing good food that kept me going all these years.

Thanks are also due to colleagues at PRL especially M.G.Yadava, J.T Padia, R.A. Jani, D.K.Rao, R.D.Deshpande, Navin Juyal for their encouragement and support all through my stay at PRL. I also thank Deepak Dhingra and Neeraj Srivastava with whom I spent my initial days at PRL. I would especially thank veteran members of “post-lunch” tea club: Jyoti, Ravi, Sunil, Sudhir, Deepu da, Shukla ji, Panda, and Santosh. Help from seniors like Aniraban da, Prasanta da, Sanjeev, Dilip, Sudeshna, Jayesh, Nagar, Morthekai, Neeraj, Manoj, Charan, Manish, Lokesh, Amit, Gowda and Pathak are also appreciated. I also thank “regular” tea club members Sumita, Ashutosh, Ritesh, Kushu, Akhilesh, Santosh, Salman, Tyagi, Rehman, Ashwini, Gyana, Shuchita, Kripa, Alok, Vineet, Priyam, Jayati and many more. Juniors like Rohit, Naveen, Arvind and Amzad made life much easy and enjoyable at lab and hostel: special thanks to them. I will never forget n-number of *chai* by Hanuman and Jayesh.

This page will be incomplete without mentioning my batch mates with whom I have shared all my feelings and frustrations. Shreyas and Subimal were always there with me in my good and bad times; Sanat and Uma, without pulling whose legs I never started my day; hard work of Sasadhar most often frustrated me. Cooking and eating veg and non-veg dishes with Shreyas, Subimal, Anirban da, Dilip, Jayesh, Archita and Santosh will always remain in my heart.

I can not forget to thank my cute little sis Neha (Dr. Neeharika Verma) who was always with me with her supporting words and relaxing laughter when it needed the most. Hours that we have spent talking to each other about our thesis and making plans to finish it on time, though I am a bit late, will always remain with me. At last I would like to thank my parents, brothers and sisters for their long wait to see this thesis. Being a Bihari I know what matters there at home is a government job and for my family the patience to wait for this thesis is unimaginable. I whole-heartedly thank them all for their support and encouragement. Tons of thanks to *bhaiya* and *bhabhi* who brought me so far since childhood that I could do Ph.D; thanks to *bhaiya* and *bhabhi* for everything they did for me. Mannu and Goldi, my two sweet nieces, always waited for this day to come, so a sincere thanks to them as well.

Contents

	List of tables.....	iv-v
	List of figures.....	vi-ix
Chapter 1	Introduction	1-17
1.1	Marine Primary Production.....	2
1.2	Estimation of new and regenerated productivity.....	5
1.2.1	Different methods for measuring new and export production.....	5
1.2.2	Merits of using nitrogen as a tracer for estimating new and regenerated productivity.....	6
1.3	N-uptake rates and <i>f</i> -ratios in different parts of the world's ocean.....	6
1.4	Indian Ocean and its biogeochemical properties.....	9
1.5	Carbon budget of the Indian Ocean.....	12
1.6	Previous ¹⁵ N based studies in different parts of Indian Ocean.....	13
1.7	Scope of the present work.....	14
1.8	Outline of the thesis.....	15
1.9	Scientific questions addressed.....	16
Chapter 2	Sampling Location, Seasons and Experimental Techniques	18-46
2.1	Introduction.....	19
2.1	Ocean colour studies.....	20
2.2.1	Analysis of ocean colour data.....	20
2.2.2	Study Area.....	21
2.2.3	Limitation of ocean remote sensing.....	22
2.3	Primary Production.....	22
2.3.1	Arabian Sea.....	23
2.3.2	Equatorial Indian Ocean.....	26
2.3.3	Southern Indian Ocean.....	28
2.4	Experimental Procedures.....	29
2.4.1	Sample collection.....	29
2.4.2	Tracer Preparation.....	31
2.4.3	Ambient nutrient measurement.....	31
2.4.4	Addition of tracers.....	32
2.4.5	Incubation.....	32
2.4.6	Filtration.....	33

2.5	Instruments and analysis.....	34
2.5.1	Instrumentation.....	35
2.5.2	Con-flo.....	36
2.5.3	Mass spectrometer.....	36
2.5.4	Calibration of mass spectrometer.....	37
2.5.5	Estimation of uptake rate.....	40
2.5.6	Equation used for the estimation of uptake rates.....	41
2.6	Iron experiment.....	42
2.6.1	Experimental procedure.....	43
2.6.2	Iron tracer preparation.....	45
2.6.3	Chlorophyll measurement.....	45
2.7	Quality Control.....	46

Chapter 3 The Northeastern Arabian Sea 47-88

3.1	Introduction.....	48
3.2	Remote sensing studies.....	51
3.3	Chlorophyll- <i>a</i> , nutrients and physical parameters during February-March 2004 in the northwestern Arabian Sea.....	59
3.3.1	Chlorophyll- <i>a</i>	59
3.3.2	Nutrients.....	61
3.3.3	Hydrographic conditions.....	63
3.4	¹⁵ N based Productivity study during the late winter monsoon (Feb.-March 2004).....	65
3.4.1	Total Production.....	65
3.4.2	New Production.....	67
3.4.3	Regenerated Production.....	70
3.4.4	<i>f</i> -ratios in the eastern Arabian Sea during Feb.-March 2004.....	71
3.5	Chlorophyll- <i>a</i> , nutrients and physical parameters during December-2004 in the northwestern Arabian Sea...	72
3.5.1	Chlorophyll- <i>a</i>	72
3.5.2	Nutrients.....	74
3.5.3	Hydrographic conditions.....	76
3.6	¹⁵ N based Productivity study during the early winter monsoon (December 2004).....	78
3.6.1	Total Production.....	78
3.6.2	New Production.....	79
3.6.3	Regenerated Production.....	81
3.6.4	<i>f</i> -ratio during December-2004.....	82
3.7	Effect of winter cooling on the <i>f</i> -ratio.....	84
3.8	Export flux in the Arabian Sea during the winter monsoon..	85
3.9	Conclusions.....	86

Chapter 4 The Equatorial and Southern Indian Ocean 89-128

4.1	Introduction.....	90
4.2	Physical parameters, Chlorophyll-a and nutrients in the equatorial Indian Ocean during pre-monsoon season 2005.....	92
4.2.1	Hydrographic Conditions.....	92
4.2.2	Nutrients.....	93
4.3	¹⁵ N based productivity studies in the equatorial Indian Ocean during pre-monsoon 2005.....	96
4.3.1	Total Production.....	96
4.3.2	New Production.....	98
4.3.3	Regenerated production.....	100
4.3.4	<i>f</i> -ratios in the equatorial Indian Ocean.....	103
4.4	Southern Ocean.....	104
4.5	Summary of the earlier work.....	108
4.6	Chlorophyll-a, nutrients and physical parameters during Feb-March 2006 in the southern Indian Ocean.....	110
4.6.1	Chlorophyll-a.....	110
4.6.2	Nutrients.....	112
4.6.3	Hydrographic Conditions.....	113
4.7	¹⁵ N based productivity during late austral summer 2006.....	114
4.7.1	Total production.....	114
4.7.2	New Production.....	117
4.7.3	Regenerated Production.....	119
4.7.4	<i>f</i> -ratios in the Southern Ocean.....	120
4.8	Iron Experiment.....	122
4.9	Conclusions.....	126

Chapter 5 Conclusions and Scope for Future Work 129-134

5.1	The northeastern Arabian Sea.....	130
5.2	The equatorial Indian Ocean.....	132
5.3	The southern Indian Ocean.....	133
5.4	Scope for future work.....	134

References 137-151

List of Tables

Tables	Page
1.1 New or export production ($\text{mmol Nm}^{-2}\text{d}^{-1}$) and f -ratio in different regions	7
1.2 Annual balance of carbon (Tg C yr^{-1}) for the Indian Ocean and sub-regions.....	12
2.1 Details of the cruises undertaken for this study	19
2.2 Sampling location along with dates of sampling during the Arabian Sea cruise in late winter (Feb-March 2004).....	24
2.3 Sampling depths during Feb-March 2004.....	25
2.4 Sampling location along with dates of sampling during the Arabian Sea cruise in early winter (Dec-2004)	26
2.5 Sampling depths during Dec-2004.....	26
2.6 Sampling location along with dates of sampling during the equatorial Indian Ocean cruise in pre-monsoon season (May-June 2005).....	27
2.7 Sampling depths during SK-220 (May-June 2005).....	28
2.8 Sampling Location along with dates of sampling during the Southern Indian Ocean cruise (Jan-April 2006).....	28
2.9 Sampling depths during the Southern Indian Ocean cruise (Jan-April 2006).....	29
2.10 Table showing overall precision, based on the standard measurements, during the analysis of the samples	40
2.11 Difference between duplicates	40
2.12 The locations of the stations for Iron enrichment experiments along with the date of sampling. IEE stands for Iron Enrichment Experiment.....	43
3.1 ^{15}N based productivity and f -ratios during Feb.-March 2004 (late winter monsoon) in the eastern Arabian Sea.....	72

Tables		Page
3.2	¹⁵ N based productivity and <i>f</i> -ratios during December 2004 (early winter monsoon) in the eastern Arabian Sea.....	83
3.3	Sea Surface Temperature (SST) and salinity a) during Feb.-March 2004 (late winter monsoon) b) during Dec-2004 (early winter monsoon) in the eastern Arabian Sea. PP1 to PP 11 represent stations during the late winter monsoon and PP'1 to PP'11 represent station during the early winter monsoon. PP is different from PP'	84
4.1	Nitrate, ammonium and urea uptake and the <i>f</i> -ratios at station IEE 1 under controlled and enriched iron conditions	124
4.2	Nitrate, ammonium and urea uptake and the <i>f</i> -ratios at station IEE 2 under controlled and enriched iron conditions	124

List of Figures

Figures		Page
1.1	Schematic representation of primary production, new production and regenerated production in the photic zone.....	4
1.2	Monsoon wind-stress field over the northern Indian Ocean for July (summer monsoon) and January (winter monsoon).....	10
2.1	Study Area for Ocean color studies	22
2.2	Block diagram showing steps involved in estimation of new and regenerated production	23
2.3	The cruise track along which sampling was done during SS-220. PP denotes primary productivity stations.....	24
2.4	The cruise track along which sampling was done during SK-214. PP denotes primary productivity stations	25
2.5	The cruise track along which the sampling was done during SK-220.....	27
2.6	The cruise track along which sampling was done for the present study in the Southern Ocean (ABP15).....	29
2.7	Go-Flo bottles attached to a CTD rosette used to collect sea-water samples from different depths	30
2.8	Author filtering samples in dark on board R/V Akademik Boris Petrov in the Arabian Sea.....	34
2.9	Some typical examples of (a.) calibration curve obtained immediately after putting fresh chemicals in the oxidation/reduction chambers and (b.) examples of calibration curve used for the estimation of particulate organic nitrogen in the post incubation sample.....	39
2.10	Schematic representation of the sampling adopted in the present study for iron enrichment experiment.....	44
3.1	Monsoon wind stress field from the NCEP climatology for a) January, b) April, c) July and d) November	49
3.2	Satellite derived Chl- <i>a</i> over zone 1.....	53

Figures		Page
3.3	Satellite derived SST over zone 1.....	53
3.4	Satellite derived Chl- <i>a</i> over zone 2.....	54
3.5	Satellite derived SST over zone 2.....	55
3.6	Satellite derived Chl- <i>a</i> data and SSTs from May to September from the region 52°E to 57°E and 5°S to 10°N	55
3.7	Satellite derived wind speed over zone 1.....	56
3.8	Satellite derived wind speed over zone 2.....	57
3.9	Satellite derived Chl- <i>a</i> data and SSTs over Zone 1 in winter (October to March).....	57
3.10	Satellite derived Chl- <i>a</i> data and SSTs over Zone 2 in winter (October to March).....	58
3.11	Vertical profiles of Chl- <i>a</i> at different stations in the eastern Arabian Sea during late winter monsoon (Feb.-March 2004).....	60
3.12	Euphotic zone integrated chl- <i>a</i> concentration at all the stations during Feb.-March 2004.....	61
3.13	Vertical profiles of nutrients at different stations during the present study (cruise SS#222).....	62
3.14	SST and salinity at different stations in the eastern Arabian Sea during Feb-March 2004.....	64
3.15	Temperature-depth profiles at different stations obtained using CTD data during Feb.-March 2004.....	65
3.16	Station-wise column-integrated total N-uptake for eastern Arabian Sea during the present study	66
3.17	New production at different stations in the eastern Arabian Sea during the late winter monsoon.....	68
3.18	Relationship between total N uptake rate and nitrate uptake rate in the eastern Arabian Sea during the late winter monsoon.....	69
3.19	Ammonium and urea uptake rates at different stations in the eastern Arabian Sea during the late winter monsoon.....	70
3.20	<i>f</i> -ratios at different stations in the Eastern Arabian Sea during the late winter monsoon.	71

Figures		Page
3.21	Station-wise column integrated chlorophyll concentration during Dec-2004.....	73
3.22	Vertical profiles of Chl- <i>a</i> at different stations in the eastern Arabian Sea during the early winter monsoon (Dec - 2004).....	74
3.23	Vertical profiles of nitrate at different stations during December-2004	75
3.24	SST and salinity at different stations in the eastern Arabian Sea during early winter monsoon (Dec-2004).....	76
3.25	Temperature-depth profiles at different stations obtained using CTD data during December 2004.....	77
3.26	Total N-uptake rate (new production) at different stations in the eastern Arabian Sea during December 2004.....	78
3.27	Nitrate uptake rate (new production) at different stations in the eastern Arabian Sea during December 2004.....	80
3.28	Relationship between total N-uptake during the early winter monsoon (December) in the eastern Arabian Sea.....	81
3.29	Ammonium and urea uptake rates at different stations in the Eastern Arabian Sea during early winter monsoon.....	82
3.30	<i>f</i> -ratio at different stations in the eastern Arabian Sea during the early winter monsoon.....	83
4.1	Figure showing wind stress field for the Indian Ocean during January, April, July and October.....	90
4.2	SST (°C) at all stations along 77°E and 83°E transects	92
4.3	Salinity at all stations along 77°E and 83°E transects.....	93
4.4	Photic zone integrated nitrate at different stations in the equatorial Indian Ocean	94
4.5	Depth profiles of nitrate at different stations in the equatorial Indian Ocean during pre-monsoon 2005.....	95
4.6	Total N-uptake rates at different stations in the equatorial Indian Ocean during pre-monsoon 2005.....	96
4.7	Mixed layer depth integrated total N-uptake rates at different stations in the equatorial Indian Ocean during pre-monsoon 2005.....	97

Figures		Page
4.8	Photic zone integrated total nitrate uptake rates (new production) at different stations in the equatorial Indian Ocean during pre-monsoon 2005.....	98
4.9	Station-wise mixed layer depth integrated nitrate uptake rates (new production) at different stations in the equatorial Indian Ocean during pre-monsoon 2005.....	99
4.10	Relation between mixed layer integrated total N-uptake rate and nitrate uptake rate in the equatorial Indian Ocean during pre-monsoon 2005.....	100
4.11	Mixed layer depth integrated ammonium uptake rates at different stations in the equatorial Indian Ocean during pre-monsoon 2005.....	102
4.12	Mixed layer depth integrated urea uptake rates at different stations in the equatorial Indian Ocean during pre-monsoon 2005.....	103
4.13	<i>f</i> -ratios at different stations in the equatorial Indian Ocean.....	104
4.14	The aerial extent of the Southern Ocean (left) and the cartoon of the Antarctic Circumpolar Current (ACC; right).....	105
4.15	Vertical profiles of Chl- <i>a</i> (left panel) and column integrated Chl- <i>a</i> (right panel) at different stations in the Southern Indian Ocean.....	110
4.16	Vertical profiles of ambient nitrate concentrations at different stations in the Southern Indian Ocean.....	112
4.17	SST (in °C) at different stations in the Southern Indian Ocean	113
4.18	Temperature-depth profiles at different stations in the Southern Indian Ocean. The stations in the south had deeper mixed layers compared to those in the north.....	114
4.19	Total N-uptake rates at different stations in the Southern Indian Ocean.....	115
4.20	New production at different stations in the Southern Indian Ocean ...	118
4.21	Relationship between total N uptake and nitrate uptake in the Southern Indian Ocean	119
4.22	Ammonium and urea uptake rates at different stations in the Southern Indian Ocean.	120
4.23	<i>f</i> -ratios at different stations in the Southern Indian Ocean.....	122

Chapter One

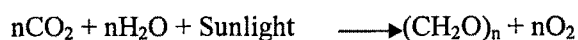
Introduction

One of the major roles of contemporary oceanographers is to understand the role of ocean in the carbon cycle and thus in Global Change. According to an estimate, the concentration of CO₂ in the atmosphere has increased by 35% during the last 150 years compared to the pre-industrial level (from 280 ppm in pre-industrial era to 379 ppm in 2005) (IPCC AR IV-2007) and it is projected to double in the coming century. Carbon dioxide is a greenhouse gas which can trap the longer wave radiation emitted by the earth and hence causes increase in the earth's temperature; the global temperature has increased by $0.74 \pm 0.18^\circ\text{C}$ during the last century (IPCC AR IV-2007). One of the main causes of increase in concentration of CO₂ is the increased human activities like fossil fuel burning, change in agricultural patterns, deforestation etc. However, its growth rate, at present, is less than half of the expected if all the CO₂ released by fossil fuel burning and land-use pattern change had remained in the atmosphere. This is because the growth rate of atmospheric CO₂ depends not only on the human activities but also on the different biogeochemical and climatological processes which lead to its drawdown from the atmosphere to different earth reservoirs (Falkowaski et al., 2000). A rapid and continuous exchange of CO₂ takes place between atmosphere and the ocean and terrestrial ecosystems. Oceans, in particular, take up considerable amount of CO₂ through physico-chemical and biological processes and acts as a "sink" of atmospheric CO₂ (Sarmiento and Gruber, 2002) but the complex processes affecting it are still poorly understood (Ittekkot 1991). A major part of the atmospheric CO₂ is also taken up by the terrestrial and oceanic biota; it has been estimated that a total of 104.9 Gt of carbon is fixed per year by the terrestrial and oceanic biota, out of which about 46.2% (48.5 Gt) is taken up by ocean (Field et al., 1998).

1.1 Marine primary production

Ocean biota mainly consist of single celled micro-organisms called phytoplankton. They are the first link in ocean food-web and have the same mode of nutrition as terrestrial plants, but are short-lived, free floating and have no supporting structure to maintain unlike terrestrial plants. They are present in the upper sunlit

layer of the ocean called the photic zone i.e., the depth at which the ambient light intensity becomes 1% of that the ocean surface. In the presence of sunlight phytoplankton convert atmospheric inorganic CO₂ into organic carbon through photosynthesis.



The amount of carbon thus fixed by these phytoplankton through synthesis of organic carbon, measured in units of 'amount of carbon per volume of water per unit time (mgC l⁻¹ hr⁻¹ or mgC m⁻³ d⁻¹)' is called primary production. A major part of this primary production is recycled in the photic zone itself, through microbial decay or is eaten by zooplankton, and thus enters the food web but still some part of newly synthesized organic matter is also transported to the deep via sinking. They escape from the upper ocean to the thermocline and below and thus get removed from the atmosphere for longer times. This is termed as 'export production' and the process is known as the "biological pump".

Availability of sunlight is one of the major limiting factors of primary productivity, as light intensity decreases with depth. The general limit of light penetration, even in open ocean waters, is approximately 100-150 m (1% of surface intensity). Since photosynthesis depends on light, primary production takes place within this zone. Apart from sunlight, CO₂ and H₂O, some elements such as N, P, Fe, Si etc are also essential for phytoplankton growth (Toggweiler 1999), absence of which limits photosynthesis and primary production. These are called nutrients. All these nutrients occur in small amounts.

Among all the other nutrients supply of nitrogenous nutrients is considered as a major limiting factor that regulates the oceanic primary production (Harrison et al., 1987). On the basis of the source of nitrogen, primary production can be divided into two: New Production and regenerated production (Dugdale and Goering 1967). New production is fuelled by newly-borne nitrogen, mainly in the form of nitrate, into the photic zone. The main sources of this nitrogen are upwelling of nitrate rich deep waters, aeolian deposit and through lateral advection. Regenerated production is supported by nitrogen derived from recycling of organic matter in the photic zone itself (Fig 1.1). This nitrogen is mainly in the form of ammonium or urea.

Ammonium and urea can circulate indefinitely under a quasi-steady state condition or an ideal closed system if there is no loss from the phytoplankton population. But there are losses through the sinking of particulate matter, mixing and by predation by zooplankton in the real ocean and in such cases other sources of nitrogen is necessary to maintain the system. The sum of the losses, in the form of export production, is balanced by nitrate uptake, by nitrogen fixation or by any other possible source of non-regenerated nitrogen. Therefore on a longer timescale export production is equal to new production under steady state condition (Eppley and Peterson, 1979).

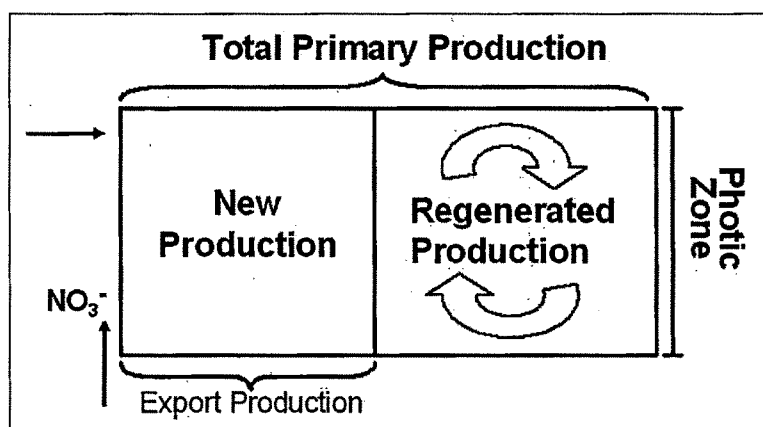


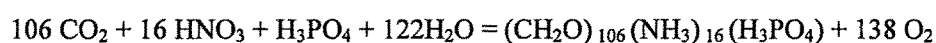
Figure 1.1. Schematic representation of primary production, new production and regenerated production in the photic zone.

The ratio of new to total production is called the f -ratio (Eppley and Peterson 1979). It represents the probability that a nitrogen atom is assimilated by phytoplankton due to new production; likewise $(1-f)$ is the probability of assimilation by regenerated production. $(1-f)/f$ provides a measure of number of times nitrogen recycles in the photic zone before sinking out of the system as particulate matter (Eppley and Peterson, 1979).

Phosphorus is another element the availability of which is believed to limit primary production especially in the open ocean (Tyrell and Law 1997, Tyrell 1999). It is present in seawater in the form of dissolved phosphate (PO_4^{3-}), enters the ocean through rivers as a product of continental weathering (Toggweiler 1999) and is removed from ocean waters through sedimentation. Geochemists argue (Broecker 1982) that since its only source is through river discharge; its concentration in open

ocean waters is low and limits productivity. This is very unlikely because the residence time of PO_4^{3-} in the ocean is around 50,000 years (Van Cappelan and Ingall 1994). Also PO_4^{3-} is unique in a sense that it escapes burial in sediments: only 1% of the phosphorous taken up by phytoplankton is trapped in sediments (Brocker and Peng 1982). High residence time and low burial rate implies a high standing stock of phosphorus in the oceanic water.

The traditional stoichiometric formula for the composition of marine phytoplankton organic matter:



Phytoplankton take up C, N and P in a fixed ratio of 106:16:1 known as the Redfield ratio (Redfield 1934). It is the molecular ratio of carbon, nitrogen and phosphorus in marine organic matter (Falkowaski et al., 1998) and it is remarkably close to ratio of these elements in the seawater. Any variation that exists in the natural environment are likely to be small, under the normal marine pH condition.

1.2 Estimation of new and regenerated productivity

1.2.1 Different methods for measuring new and export production

New and regenerated productivity are measured using the ^{15}N tracer technique, originally proposed by Dugdale and Goering (1967), modified by the JGOFS (1996). Uptake rates of ^{15}N labeled nitrate, ammonium and urea are measured in the post-incubated samples; nitrate uptake rate gives an estimate of new production whereas a sum of ammonium and urea uptake rates gives a measure of regenerated production. New production is also measured from rate of change of nitrate concentration in the upper water column (Allen et al., 1996). Nitrogen-fixation also provides new nitrogen to the water column (Capone et al., 1997; Karl et al., 1997) and hence is referred as new production. Nitrification of regenerated nutrients such as ammonium and urea, taking place generally below (Dore and Karl 1996) and within the photic zone (Fernandez et al., 2005; Rees et al., 2006), is also a source of new nitrogen. On the other hand release of DO^{15}N , and reduced forms of nitrogen such as ammonium from cells during incubation results in an underestimation (Bronk et al. 1994) but it is significant only when samples are

incubated for longer durations (~12 hrs) (Glibert et al., 1982). For the present study, the ^{15}N tracer technique is used to estimate new and regenerated productivity; experimental details are given in Chapter 2. Export production is measured using sediment traps (Nair et al., 1989) and ^{243}Th deficiency in the water column (Buesseler 1991, 1998; Ramaswamy et al., 2005). Sediment traps are generally deployed in the open ocean, at a depth ranging from 200 m to more than 1000 m where they collect particulate matter exported to the deep, the major limitation being export flux severely overestimated in the coastal region, where the sediment flux is high. Particulate organic matter sticks to these sediments while settling down, which tends to overestimate it. In the ^{234}Th technique downward flux of organic matter is estimated using the ratio of carbon to ^{234}Th and this does not take care of advection of DOM and the vertical migration of zooplankton. It has been found that trap-derived and ^{234}Th derived export flux differ by a factor of 3-10 (Buesseler 1991) which suggests that these methods may be of limited significance to accurate measure of particle flux to the deep.

1.2.2 Merits of using nitrogen as a tracer for estimating new and regenerated productivity

Nitrogen is one of the essential elements for the growth of phytoplankton. It is a major structural component of their body cells. It is present in oceanic waters in various forms which allows us to distinguish it on the basis of its source and thus provides a tool to measure different components of productivity i.e., new and regenerated productivity. In other words, use of nitrogen as a tool to measure productivity gives a better insight of the biogeochemistry of ocean.

1.3 N-uptake rates and f -ratios in different parts of the world's ocean

Since the formulation of concept of new and regenerated productivity by Dugdale and Goering (1967) and use of new productivity as a measure of export production (Eppley and Peterson, 1979), ^{15}N tracer technique has been extensively used to characterize the biogeochemistry of the surface ocean and to assess the ocean's role in carbon sequestration. Global scientific programmes have been carried out in the past

to estimate the relationship between new and export productivity. Some of the major programmes are: VERTEX (Vertical exchange processes) in the north Pacific, WECOMA in the equatorial Pacific (Barber 1992), ANTARKTIS in the Atlantic and Indian Sector of the Southern ocean (Semeneh et al., 1998), Research on Antarctic Coastal Ecosystem Rates (RACER; Huntley et al., 1991), Subarctic Pacific Ecosystem research (SUPER) in the north Pacific (Miller et al., 1991; Miller 1993), time series experiments at Bermuda (BATS) and Hawaii (HOT) (Lohrenz et al., 1992; Malone et al., 1993; Roman et al., 1993), 1988 Black Sea Expedition (Murray 1991), POMME in the Atlantic ocean (Fernandez et al., 2005) and BOBPS (Bay of Bengal Processes Studies) in the Bay of Bengal (Sanjeev Kumar et al., 2004; Sanjeev Kumar and Ramesh, 2005).

Region/season	Nitrate uptake	<i>f</i> -Ratio	Reference
HOT	0.6	0.10	Michaels et al. (1994)
BATS	0.9	0.15	Emerson et al. (1997)
NABE	7.0	0.51	Bender et al. (1992); McCarthy et al. (1996)
Equatorial Pacific (150°W)			
November	0.5-2.7	0.08-0.21	Raimbault et al. (1999)
August	0.5-4.8	0.05-0.2	McCarthy et al. (1996)
Sub-Arctic Pacific			
Station-P winter	1.0-4.5		Varela and Harrison (1999)
Station-P summer	0.8-4.0		Wheeler and Kokkinakis (1990)
Peru	18.3-24.2	0.30-0.42	Wilkerson et al., (1987)
Sub-Arctic Atlantic			
Iceland Basin-July	0.9-5.8		Sambrotto et al. (1993)
North Atlantic	3-9	0.25-0.56	Fernandez et al., (2005)
Greenland polynya	2.5	0.56	Smith et al., (1997)
Southern Ocean			
170°W /summer	0.9-12.5	0.05-0.48	Sambrotto and Mace (2000)
Ross Sea			
Arabian Sea			
Spring Intermonsoon	0.1-3.0	0.04-0.35	Sambrotto (2001)
Southwest Monsoon	3.0-9.0	0.05-0.42	Sambrotto (2001)
Early NE Monsoon	0.8-6.0	0.15	McCarthy et al. (1999)
Late NE Monsoon	0.7-3.0	0.13	McCarthy et al. (1999)
Bay of Bengal			
Late SW Monsoon	0.4-8.8	0.34-0.81	Sanjeev Kumar et al., (2004)
Early SW Monsoon	1.0-3.3	0.48-0.78	Sanjeev Kumar et al., (2004)

Table 1.1 New or export production ($\text{mmol Nm}^{-2} \text{d}^{-1}$) and *f*-ratio in different regions (Source: Falkowski et al. 2003 and Sambrotto and Mace 2000); NABE = North Atlantic Bloom Experiment.

During JGOFS (Joint Global Ocean Flux Studies), different parts of the worlds ocean e.g., the equatorial Pacific (Barber et al., 1994), the Arabian Sea (Smith 2001;

Sambrotto 2001), the Southern ocean (Sambrotto and Mace 2000), the North Atlantic (Ducklow and Harris 1993) were studied in detail to get a better estimate of carbon fluxes in these oceans. The nitrate uptake rate (new production) and f -ratio obtained from different programmes/areas using different methods is listed in Table 1.1.

The global ocean can be subdivided into three main categories on the basis of new production (Ducklow 1995): (i) regions where nitrate is depleted in spring but is again renewed in winter every year and (ii) regions where surface water contains high concentrations of nitrate throughout year (iii) regions where nitrate is permanently depleted in the surface waters. In some part of the world ocean nitrate is transported to the upper layer due to vertical mixing during the winter; this increases productivity of the basin, sometimes leading to initiation of phytoplankton bloom. Such regions are coastal and shelf regions (Townsend et al., 1992; Hansell et al., 1993); Southern Ocean (Holm-Hansen and Mitchell 1991; Sullivan et al., 1993), northern Arabian Sea (Dwivedi et al., 2006) and North Atlantic (Sambrotto et al., 1993). Occurrence of bloom in such regions leads to episodic increase in the export of biomass (Honjo and Manganini 1993). There are regions such as the subarctic north Pacific, central equatorial Pacific and the Southern Ocean where surface nitrate is high yet the productivity is low. Because of this property these are described as a “High Nutrient Low Chlorophyll” or HNLC regions (Minas et. al., 1986). In general new production has been reported to be low in HNLC (Dugdale et al., 1992). Several causes including low temperature, low specific growth rate, grazing control, sun-light limitation, trace metal toxicity and Fe-limitation, have been proposed to explain the “HNLC” condition. In the oligotrophic gyres, the surface ocean is almost devoid of nitrate, but is known to maintain a significant new production even in the absence of new nitrate from deeper layers. The other sources suggested for such significant new production are nitrate enriched buoyant mats of diatoms (Villareal et al., 1993) or atmospheric inputs of nitrogen species. However, the latter causes only 1-2% of global new production. Sometimes the atmospheric inputs of nutrients can drive local blooms (Michaels et al. 1993) or can stimulate new production in nutrient poor waters (DiTullio and Laws 1991).

Some major international scientific programmes such as JGOFS aimed at assessing the role of global ocean in the carbon cycle. India also actively participated in this programme and a number of studies were carried out during the Indian JGOFS in the eastern Arabian Sea to assess its role in the global carbon cycle and to determine whether it is a “source” or “sink” of CO₂. A large part of the Indian Ocean such as the equatorial and the Southern Indian Ocean still remains unexplored from this point of view.

1.4 Indian Ocean and its biogeochemical properties

The Indian Ocean, the third largest ocean, caters to the large population of the southern and eastern Asia. It plays an important role in the global ocean system as a modulator of heat and salinity transport (Bates et al., 2006a). As a large population inhabits the coasts of the Indian Ocean, it is more likely to be affected by human impacts and other anthropogenic causes. Most of this population survives on resources derived from this ocean such as fishing and trade. Ever increasing population, different types of chemicals dumped by them into the coastal areas and also changes in the riverine discharge and composition due to human activities may affect the chemistry of the Indian Ocean. According to a study Indian Ocean is warming faster than any other ocean basin (Levitus et al., 2000). This makes the northern Indian Ocean an important region of the world ocean for the oceanographic studies to study and understand the effect of human activities on ocean biogeochemistry.

The Indian Ocean has got a unique geographical setting; it is landlocked on its northern side and is connected to the Southern Ocean and Antarctica on the south. The winds over the northern Indian Ocean *i.e.*, north of 10°S, reverse direction twice a year; it blows from the southwest during May–September (known as summer monsoon) and from the northeast during November–February (known as winter monsoon) (see Fig 1.2). During March–April and October winds are generally weak and are in transition phase. The winds during the summer monsoon are much stronger than the winter monsoon.

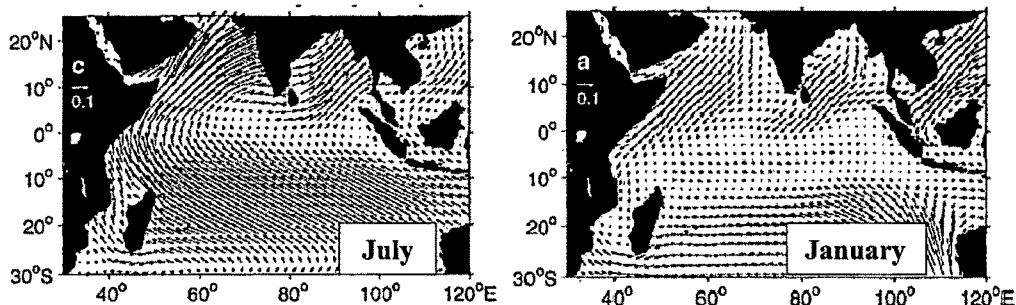


Fig 1.2 Monsoon wind-stress filed over the northern Indian Ocean for July (summer monsoon) and January (winter monsoon) (Source Shankar et al., 2002).

The seasonally reversing monsoon winds over the northern Indian Ocean forces a seasonally reversing circulation in the upper ocean (Shankar et al., 2002) which is mainly controlled by the land-sea temperature contrast between the Eurasia and the northern Indian Ocean. Change in wind direction and reversal of upper ocean circulation patterns makes the Indian Ocean a unique basin and also different from the other two major ocean basins i.e., the Pacific and Atlantic basins. The Indian peninsula divides the northern Indian Ocean into two: the Bay of Bengal and Arabian Sea. Though they are situated at the same latitude they are entirely different in oceanographic properties such as sea surface temperature (SST), mixed layer depth (MLD), nutrients, productivity etc. The Bay of Bengal receives a large quantity of fresh water through the rivers and experiences more precipitation than evaporation. This leads to formation of less saline water on the surface causing a strong vertical stratification. This inhibits the transport of nutrients from the deeper layer to the surface, which in turn, decreases the productivity of this basin. The Arabian Sea, on the other hand, receives significantly less amount of fresh water through rivers. Also, evaporation exceeds precipitation in the Arabian Sea resulting in the formation of high saline water known as Arabian Sea High Salinity Water (ASHSW) and spreads as salinity maximum just beneath the upper mixed layer (Schott and Fischer 2000). The equatorial Indian Ocean is characterized by semiannual strong eastward surface wind (Wyrтки 1973), known as Wyrтки jets, during the transition seasons between the monsoons i.e., April to June (spring intermonsoon or SIM) and October to December (fall intermonsoon or FIM) (Schott and McCreary 2001). The Wyrтки jet carries

equatorial warm surface water towards the east causing a decrease in the mixed layer depth in the west but an increase in the east (Rao et al., 1989).

The Arabian Sea is one of the most productive regions in the world oceans (Banse 1987; Nair et al., 1989; Madhupratap et al., 1996; Smith 2001) and is characterized by strong, seasonal oscillations in the biological production (Burkill et al., 1993) which is attributed to the strong seasonal oscillation in the oceanic circulation forced by the monsoons. In summer, the strong southwest monsoon causes intense upwelling in the western Arabian Sea along the Somalia and Oman coasts and also along the western Indian coast. Increase in the mixed layer due to strong winds during the southwest monsoon brings ample nutrients into the surface layer and causes phytoplankton blooms. During the winter monsoon, cool dry air from Himalaya causes enhanced evaporation which results in the deepening of mixed layer due to convective mixing. This again brings nutrients into the surface layer and trigger blooms during the later phase. The spring and fall inter-monsoons are characterised by well stratified surface water with shallow mixed layer devoid of nutrients and low productivity in the Arabian Sea. The southwest monsoon current advects to the southern Bay of Bengal through the south of Sri Lanka and triggers high biological productivity in the Bay (Vinaychandran et al., 2004).

Other important features of the Indian Ocean are the biogeochemical cycling of carbon and other important elements, its response to natural and anthropogenic changes, geographical constraints on vertical mixing, seasonally reversing monsoon (Hood et al., 2006), globally significant oceanic biological production particularly in the northern Arabian Sea (Madhupratap et al., 1996), intense denitrification as Arabian sea alone contributes ~40% (Bange et al., 2005) of the global denitrification (in this process bacteria begin to utilize NO_3 instead of O_2 as an oxidant for decomposing organic debris when the ambient O_2 concentration is close to zero; Naqvi et al., 1982; Naqvi and Jayakumar 2000), fixation of N_2 by cyanobacteria (Capone et al., 1997) and high export production despite low productivity in the Bay of Bengal (Sanjeev Kumar et al., 2004).

1.5 Carbon budget of the Indian Ocean

The Indian Ocean has been identified as a net sink for atmospheric CO₂ (Takahashi et al., 2002). It takes up ~330-430 Tg C yr⁻¹, which accounts for nearly 20% of the global oceanic uptake of CO₂. Most of this air-to-sea CO₂ flux occurs south of 20°S. This is because sea surface temperature decreases drastically south of 20°S, to reach below zero near the Antarctic coast and CO₂ is more soluble in cold water compared to warm water. Contribution of the equatorial and the northern Indian Ocean is yet to be assessed. Bates et al., (2006a) has identified the northern Indian Ocean (north of 35°S) as a net source of CO₂ to the atmosphere. They estimated an annual loss of ~240 Tg C yr⁻¹ of CO₂ to the atmosphere from the sea. Subregions of the Indian Ocean affected by seasonally reversing monsoons are perennial sources of CO₂ to the atmosphere (Hood et al., 2006) despite having episodic high biological productivity. Though the surface layer of the Indian Ocean is strongly autotrophic, biological uptake of CO₂ by the Indian Ocean has been estimated to be ~750-1320 Tg C yr⁻¹ by Bates et al., (2006b), it can not compensate for the loss of CO₂ to the atmosphere *via* upwelling of deeper cold water. Sabine et al., 2000 and Hall et al., 2004 have proposed an estimate of 150-500 Tg C yr⁻¹ of CO₂ loss to the atmosphere by the warm northern Indian Ocean. Table 1.2 summarizes the annual air-sea CO₂ fluxes for the Indian Ocean and its subregions.

Region	CO ₂ flux	Net Production	River input	Vertical Diffusion	Upwelling/ Advection
Indian Ocean	-237	-1572 (-802)	+30	+437	+1342 (+572)
Arabian Sea	-64	-150 (-80)	+2	+58	+154 (+84)
Bay of Bengal	-13	-150 (-94)	+25	+25	+113 (+57)
10°N-10°S	-180	-486 (-304)	+1	+178	+ 487 (+304)
10°S-20°S	-110	-349 (-72)	+1	+97	+361 (+84)
20°S-35°S	+130	-437 (-95)	+1	+95	+211 (+26)

Table 1.2. Annual balance of carbon (Tg C yr⁻¹) for the Indian Ocean and subregions. “Negative” and “positive” terms are “loss from” and “gain to” the surface layer (0-100 m) respectively. (Source: Hood et al., 2006)

1.6 Previous ^{15}N based studies in different parts of Indian Ocean

^{15}N based productivity has been reported for the western and central Arabian sea by a few authors (Owens et al., 1993; McCarthy et al., 1999, Watts and Owens, 1999; Sambrotto, 2001) but only a few results are available from the eastern Arabian Sea (Sanjeev Kumar et al., 2008). Owens et al., (1993) reported a large variation in the total N-uptake rates, from $23.1 \text{ mmolNm}^{-2}\text{d}^{-1}$ in the central Arabian Sea to $96.7 \text{ mmolNm}^{-2}\text{d}^{-1}$ in the coastal upwelling region during the late summer monsoon. The f -ratio varied from a low of 0.09 at an open ocean station to as high as 0.92 at a coastal station. McCarthy et al., (1999) reported N-uptake rates varying from $9.2 \text{ mmolNm}^{-2}\text{d}^{-1}$ to $40 \text{ mmolNm}^{-2}\text{d}^{-1}$ during winter monsoon and from $3.9 \text{ mmolNm}^{-2}\text{d}^{-1}$ to $24 \text{ mmolNm}^{-2}\text{d}^{-1}$ during the late summer/early winter monsoon for the central Arabian Sea. Here the N-uptake rate was significantly higher in the winter ($\sim 26 \text{ mmolNm}^{-2}\text{d}^{-1}$) than the late summer ($11 \text{ mmolNm}^{-2}\text{d}^{-1}$). The f -ratio varied from 0.03 to 0.31 and from 0.04 to 0.29 during winter and the late summer monsoons respectively. Watts and Owens (1999) also reported large variations in the N-uptake rate; it varied from $1.1 \text{ mmolNm}^{-2}\text{d}^{-1}$ to $23.6 \text{ mmolNm}^{-2}\text{d}^{-1}$ for the northwestern Arabian Sea during an intermonsoon period. They found f -ratios varying from a low of 0.07 in the open ocean region to a high of 0.92 at a coastal station. A large variation in the N-uptake rate, ranging from $0.1 \text{ mmolNm}^{-2}\text{d}^{-1}$ to $13 \text{ mmolNm}^{-2}\text{d}^{-1}$ has also been reported by Sambrotto (2001) during the spring intermonsoon and the summer monsoon for the northern Arabian Sea. Sustained observations over several years are required to get a meaningful average of ^{15}N based export productivity. This thesis is important in this context.

^{15}N based productivity measurements in the Indian sector of the Southern Ocean are limited in time and space. Slawyk (1979) was the first to report nitrate uptake rates from the Kerguelen Island area of the Southern Ocean; nitrate uptake rates were low and varied from $0.03 \text{ mmolNm}^{-2}\text{d}^{-1}$ to $0.12 \text{ mmolNm}^{-2}\text{d}^{-1}$ with a mean of $0.06 \text{ mmolNm}^{-2}\text{d}^{-1}$. Probyn and Painting (1985) reported N-uptake rates for the surface waters from the coastal regions between Cape Ann and Mawson. The N-uptake rates reported by them were significantly high; they varied from $2.16 \text{ mmolNm}^{-3}\text{hr}^{-1}$ to $5.41 \text{ mmolNm}^{-3}\text{hr}^{-1}$ with a mean of $4.47 \text{ mmolNm}^{-3}\text{hr}^{-1}$. They

reported a preference for reduced nitrogen (ammonium and urea) over nitrate by the phytoplankton of the Antarctic coastal waters. Mengesha et al., (1998) studied the N-uptake characteristics of the Southern Ocean waters over two seasons, spring and austral summer 1994, for a small area near the Kerguelen Island. During spring specific and absolute nitrate uptake dominated over ammonium and urea uptakes whereas during summer ammonium uptake was more than nitrate uptake. The specific nitrate uptake during spring was 0.0048 hr^{-1} which reduced to 0.0011 hr^{-1} in the summer. Ammonium uptake increased slightly during the summer, from 0.0015 hr^{-1} in spring to 0.0018 hr^{-1} in summer. The f -ratio also decreased in the summer but showed considerable variations. It varied from 0.68 to 0.85 in spring and from 0.17 to 0.63 in summer. Specific nitrate and ammonium uptake rates reported for the surface waters by Semeneh et al., (1998) was an order of magnitude lower than the rates earlier reported rates; specific nitrate and ammonium uptake rates were 0.001 hr^{-1} and 0.0004 hr^{-1} respectively in the Prydz Bay area in 1991. The absolute total N-uptake rate and f -ratio were $0.038 \text{ mmolNm}^{-3}\text{d}^{-1}$ and 0.68 respectively. He also reported N-uptake rates from a longitudinal transect along 62°E . The specific nitrate uptake rates from this region was also (0.001 hr^{-1}) low but ammonium uptake rate was high (0.0019 hr^{-1}). The Absolute total N-uptake rate was almost double of the rate from Prydz Bay but the f -ratio was low (0.034).

No data exist on the biological productivity of the equatorial Indian ocean except a documentation on the anomalous phytoplankton bloom, using ocean colour data, in eastern part of the Indian Ocean during an Indian Ocean dipole year (Murtugudde et al., 1999).

1.7 Scope of the present work

The present work investigates the biological productivity and f -ratio characteristics of the Arabian Sea, equatorial Indian Ocean and the Southern Ocean using the ^{15}N tracer technique with following objectives:

1. Estimation of total productivity, new productivity and f -ratio characteristics of the northeastern Arabian Sea during winter monsoon and to compare

changes in the N-uptake rate due to occurrence of a phytoplankton bloom dominated by *Noctiluca scintillans* (autotrophic variety).

2. The aim was also to compare the total and new productivity of bloom and non-bloom areas and to know the extent of different biogeochemical provinces, if any, present in this part of the world ocean
3. To know the extent of intra-seasonal variability in the N-uptake rates and *f*-ratio during the winter monsoon and to assess the effect of winter cooling on them.
4. New production estimation in the equatorial Indian Ocean. This would help in assessing the role of this equatorial region in the global carbon cycle. The result will also help in examining it as a possible source/sink for atmospheric CO₂.
5. Productivity measurements in equatorial Indian Ocean have been made along two transects: 77°E and 83°E. This will help understanding latitudinal variation in biological productivity.
6. The estimation of new productivity and *f*-ratio in the Southern Ocean, a globally significant HNLC region. This would help quantify the extent of export production taking place here.
7. The Southern Ocean is characterized by the presence of various current systems which play a major role in its biogeochemistry. The present study covers stations in different current regimes. This will help in ascertaining role of various current systems on the biological and export productivity of the Southern Ocean, especially the Indian Sector.

1.8 Outline of the thesis

This thesis has been divided into five chapters. Their contents are as follows:

Chapter 1 describes the role of the ocean in the global carbon cycle. It also describes, in detail, the concepts of ocean productivity, new and regenerated production and a brief review of literature in the world ocean and study area.

Chapter 2 deals with the sampling details during the cruises and experimental methods followed during present study.

Chapter 3. discusses the results obtained during present study from the Arabian Sea. It discusses the effect of winter cooling on the total and new production and f -ratio. It also compares N-uptake rates and f -ratios of bloom and non-bloom areas and discusses the effect of occurrence of *Noctiluca* bloom on nitrogen uptake rates.

Chapter 4 deals with the results of present study for the equatorial Indian Ocean and the Southern Indian Ocean. It includes the results of new and regenerated production measurements along two transects in the equatorial Indian Ocean. It also investigates the N-uptake and f -ratio characteristics of the Southern Ocean and discusses the effect of the presence of different current systems on the productivity of this basin.

Chapter 5 synthesizes the results obtained in the present study, highlighting the important findings. It also deals with the scope for future work that may further improve our understanding of nitrogen and carbon cycle in this region.

1.9 Scientific questions addressed

The present study has attempted to address the following scientific questions:

The northeastern Arabian Sea:

- Has global warming increased productivity in the northeastern Arabian Sea?
- How much is the total productivity in the northeastern Arabian Sea during the winter monsoon?
- How much is the new and regenerated productivity in this basin during the winter monsoon?
- How does f -ratio vary in the northeastern Arabian Sea?
- What is the effect of winter cooling on the total and new productivity and also on the f -ratio?
- What is the intra-seasonal variability in productivity in this basin during the winter monsoon?
- How much does the productivity increase because of the occurrence of *Noctiluca* bloom? Does it also affect the f -ratio?
- Is there any identifiable productivity based biogeochemical divide in the Arabian Sea during the winter monsoon?

The equatorial and southern Indian Ocean:

- How much is the new and regenerated productivity in the equatorial Indian Ocean?
- What is the magnitude of f -ratio in this basin?
- Is there any longitudinal or latitudinal variation in productivity regime of the equatorial Indian Ocean?
- What is the magnitude of export production here? Is it able to export a significant part of productivity despite being an oligotrophic region?
- How much is the primary production in the Southern Indian Ocean which is otherwise considered as iron limited?
- How much is the f -ratio and the export production?
- Which is the preferred nutrient in this HNLC area?
- What is the role of different water fronts present in this area on biological productivity?
- Is there is shift in productivity regime due to global warming?
- What is the effect of iron enrichment on N-uptake rates?

In short, this thesis investigates the N-uptake and f -ratio characteristics of different parts of the Indian Ocean and evaluates its role in the Global Carbon Cycle.

Chapter Two

Sampling Locations, Seasons and Experimental Techniques

2.1 Introduction

The main aim of this thesis is to characterize the Indian Ocean on the basis of new production and f -ratio and to evaluate its role in the Global Carbon Cycle. To achieve this goal, three different methods were used:

1. Satellite based Ocean color studies of northeastern Arabian Sea
2. ^{15}N measurements in the same region of the Arabian Sea. Measurements were also done in the equatorial and the southern Indian Ocean
3. Small scale iron enrichment experiment in the southern Indian Ocean

Recent observations based on ocean colour show that the summer productivity in the western Arabian Sea has been increasing during the last seven years, reportedly due to the warming of the Eurasian landmass (Goes et al., 2005). Ocean color data from SeaWiFS (Sea-viewing Wide Field of view Sensor) for the Arabian Sea were analyzed to assess the role of global climate change on the productivity of the eastern Arabian Sea.

For ^{15}N measurements four cruises were undertaken: two cruises in the eastern Arabian Sea and one each in the equatorial Indian Ocean and the Southern Indian Ocean. The details of the cruises with the region of study, cruise number, duration and the ships on which studies were carried out are listed in Table 2.1.

Region	Cruise No.	Duration	Ship
Arabian Sea	SS- 222	20 th Feb to 11 th March-2004	FORV <i>Sagar Sampada</i>
Arabian Sea	SK- 214	4 th Dec to 16 th Dec- 2004	ORV <i>Sagar Kanya</i>
Equatorial Indian Ocean	SK- 220	10 th May to 6 th June-2005	ORV <i>Sagar Kanya</i>
Southern Ocean	ABP- 15	25 th Jan to 1 st April- 2006	<i>Akademik Boris Petrov</i>

Table 2.1 Details of the cruises undertaken for this study

Iron is believed to be a limiting nutrient in the southern ocean. In the southern Indian Ocean small scale iron enrichment experiments were also done, for the first

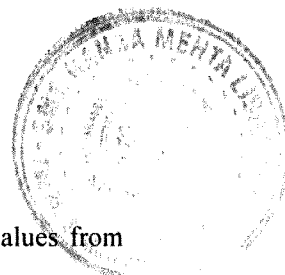
time, to assess the effect of iron enrichment on the N-uptake rates in this part of the world ocean.

2.2 Ocean colour studies

The only possible way to monitor the variation in the biological properties of the ocean on a larger spatial scale is by remote sensing. Ocean colour remote sensing is a method of collecting information about the constituents of water using optical signals in the visible range. It is well established that the concentration of phytoplankton influences the colour of the ocean water. Chlorophyll-a, which is the main photosynthetic constituent in the phytoplankton, absorbs more in blue than in green; as the concentration of phytoplankton increases, the backscattered light progressively shifts towards the green. This property is successfully used to derive the Chl-a concentration with the help of a sensor in a satellite. In the tropics, where variation in sunlight is not significant on an interannual scale, variation in chlorophyll concentration can indicate the variation in primary production. Satellite ocean colour data provides the spatial and temporal variations in phytoplankton biomass and hence in the primary production on a larger scale. Since the launch of SeaWiFS (Sea-viewing Wide Field of view Sensor) in August 1997, global ocean colour data are available to the science community on a regular basis.

2.2.1 Analysis of ocean colour data

For present study, monthly composites Level-3 Version 49-km resolution mapped SeaWiFS chlorophyll images were taken. From these images chlorophyll values were obtained using SEADAS software (provided by NASA for ocean colour image processing). SeaWiFS uses OC2 algorithm (O'Reilly et. al., 1998) for deriving Chl-a values from the recorded radiance. Sensitivity studies on the algorithm for Chl-a retrieval from measured sensor detected radiances show that the retrieved Chl-a values have the accuracy of $\sim 30\%$ (the radiance has an error of $\sim 1\%$). For this analysis, pixel values more than 5 mgm^{-3} were not considered because, OC2 algorithm which is used for deriving Chl-a values from the recorded radiance overestimates Chl-a when it is more than 1.5 mg m^{-3} . Apart from that, in our analysis pixels having more than 1.5 mgm^{-3} correspond to coastal waters which are case 2



waters. It is well established that the algorithms used to derive Chl-*a* values from case 1 waters i.e., open ocean waters, break down in the case 2 waters (Subha Sathyendranath, IOCCG report no 3). Case 2 waters are influenced not only by the phytoplankton but also by the inorganic suspended particles and dissolved organic matter. Presence of these in coastal waters interferes with the phytoplankton signals and algorithm OC2 tends to overestimate the Chl-*a*.

The seasonality of the north-east Arabian Sea SST (Sea Surface Temperature) is also inspected over the same region for the same time period in order to analyse the effect of sea surface cooling due to upwelling on the chlorophyll-*a* concentration. Monthly composite SST data are taken from AVHRR (Advanced Very High Resolution Radiometer) pathfinder version 5 (June-1997 to Dec-2004) and MODIS (Moderate Resolution Imaging Spectro-radiometer) data (Jan-2005 to June-2005). We have also analyzed version-3 QuickScat data in order to monitor change, if any, in wind speed over past 6 years (1999-2005).

2.2.2 Study area

The remote sensing studies were done for the eastern Arabian Sea. We have divided the eastern Arabian Sea into two zones (Fig. 2.1): Zone 1 extends from 20°N to 25°N and 62°E to 75°E and zone 2 extends from 20°N to 10°N and 62°E to 75°E. This division into two different zones is based on the observed physical forcing responsible for the high production in each zone. Our aim, here, is not to subdivide the basin into different hydrographic regimes but to see the change in production in the basin as a whole. The proposed subdivision allows us to monitor any change over this area.

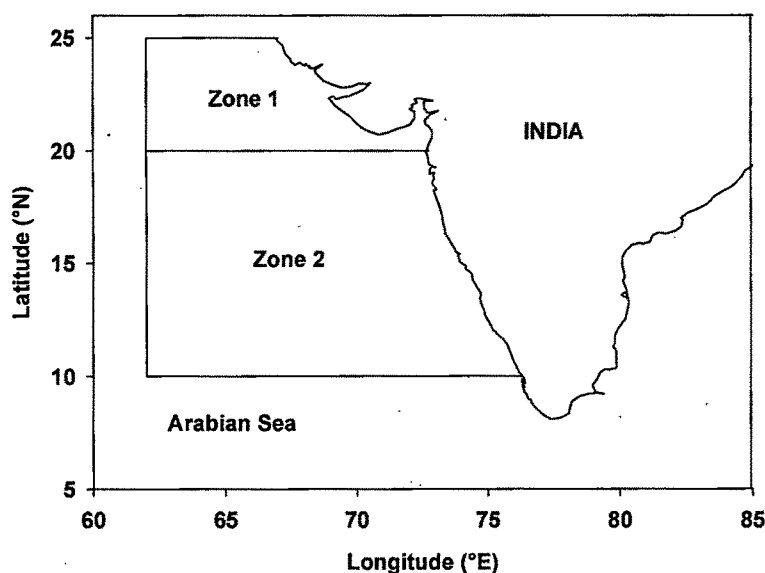


Fig. 2.1 Study Area for Ocean color studies

2.2.3 Limitations of Ocean remote sensing

One of the major limitations of the ocean colour remote sensing is that it is very sensitive to the meteorological conditions. The present sensors used in SeaWiFS and MODIS give abnormal values when cloud cover or some other interference like land etc is present. We could not get enough data for the months of June, July and August because of very dense cloud cover in this area. However, since the zone 2 encompasses a large area we could get some cloud free pixels which certainly could not be neglected. Therefore some chlorophyll values have been obtained in these months.

2.3 Primary Production

Joint Global Ocean Flux Study (JGOFS) protocol (Fig 2.2) was followed for the estimation of total primary production which is the sum of new and regenerated production. For the present study nitrate uptake rate is considered as new production and a sum of ammonium and urea uptake rates as regenerated production. New production is measured as the uptake rate of ^{15}N -labelled nitrate by the phytoplankton during deck incubation and regenerated production as a sum of ^{15}N -

labelled ammonium and urea uptake rates. Though the objectives and the research teams were different during different cruises, the same experimental procedures were followed, which are discussed in detail in the following subsections.

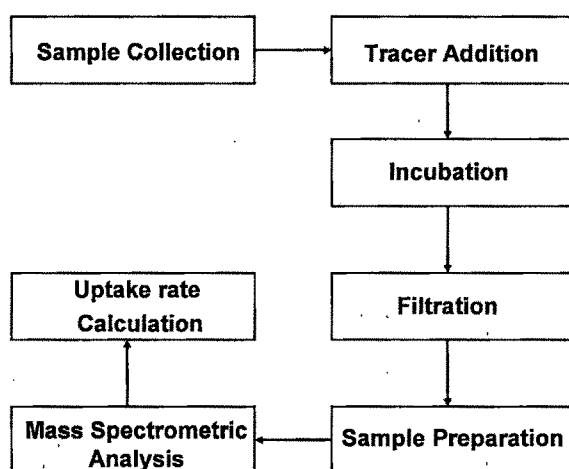


Fig. 2.2 Block diagram showing steps involved in estimation of new and regenerated production

2.3.1 Arabian Sea

India launched its first Ocean Color Sensor called Ocean Color Monitor (OCM) on Indian Remote Sensing Satellite IRS P4 in May 1999. The cruises in the Arabian Sea were a part of satellite ocean-color data validation cruises for OCM and were undertaken in collaboration with Space Application Centre (SAC), Ahmedabad. Cruises were undertaken in two seasons: during the late winter monsoon (Feb.-March 2004) and during the early winter monsoon (Dec-2004). During the late winter monsoon sampling was done in the eastern Arabian Sea onboard *FORV Sagar Sampada* (SS-222). Water samples were collected at 11 different stations, shown in Fig. 2.3. Here PP1 to PP11 denote primary productivity stations 1 to 11. The details of sampling locations along with dates of sampling and sampling depths are listed in Tables 2.2 and 2.3, respectively.

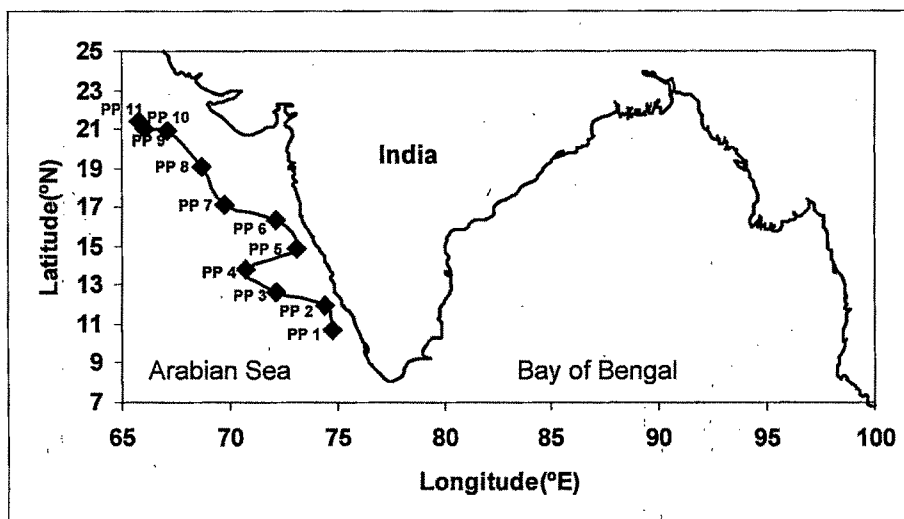


Fig. 2.3 The cruise track along which sampling was done during SS-220. PP denotes primary productivity stations

New Production Stations	Latitude(°N)	Longitude(°E)	Date
PP1	10.72	74.78	22/02/2004
PP2	12.01	74.45	23/02/2004
PP3	12.65	72.16	24/02/2004
PP4	13.81	70.73	25/02/2004
PP5	14.84	73.11	26/02/2004
PP6	16.38	72.16	27/02/2004
PP7	17.10	69.79	28/02/2004
PP8	19.08	68.71	29/02/2004
PP9	20.91	67.08	01/03/2004
PP10	21	66.08	02/03/2004
PP11	21.41	65.82	03/03/2004

Table 2.2 Sampling location along with dates of sampling during the Arabian Sea cruise in late winter (Feb-March 2004)

%Light	Sampling Depths (m)										
	PP 1	PP 2	PP 3	PP 4	PP 5	PP 6	PP 7	PP 8	PP 9	PP10	PP11
100	0	0	0	0	0	0	0	---	---	---	---
80	4	4	2	1.5	2	2	1.5	0	0	0	0
64	7	7	4	3.5	5.5	5	4.5	2.5	3	3	2.5
20	30	17	27	19	30	11	18	15	11	11	9
5	57	45	51	51	55	---	40	35	26	25	16
1	95	83	100	81	115	---	130	67	55	55	25

Table 2.3 Sampling depths during Feb-March 2004

During the early winter monsoon (Dec-2004) sampling was again done at 11 stations, again in the eastern Arabian Sea onboard *ORV Sagar Kanya* (SK-214) but this time the sampling locations (Fig. 2.4), though in the same region, were different from the earlier ones. The details of the sampling locations for this cruise, with sampling dates are given in Table 2.4 and sampling depths are given in Table 2.5.

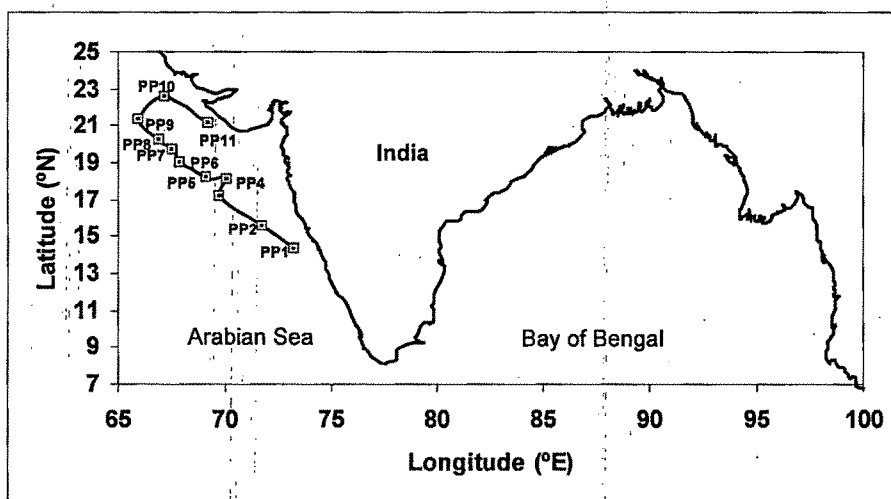


Fig. 2.4 The cruise track along which sampling was done during SK-214. PP denotes primary productivity stations

New Production Stations	Latitude(°N)	Longitude(°E)	Date
PP1	14.33	73.28	05/12/2004
PP2	15.58	71.73	06/12/2004
PP3	17.20	69.72	07/12/2004
PP4	18.10	70.08	08/12/2004
PP5	18.17	69.14	09/12/2004
PP6	19.00	67.92	10/12/2004
PP7	19.74	67.54	11/12/2004
PP8	20.22	66.96	12/12/2004
PP9	21.30	65.94	13/12/2004
PP10	22.59	67.22	14/12/2004
PP11	21.17	69.18	15/12/2004

Table 2.4 Sampling location along with dates of sampling during the Arabian Sea cruise in early winter (Dec-2004)

%Light	Sampling Depths (m)										
	PP 1	PP 2	PP 3	PP 4	PP 5	PP 6	PP 7	PP 8	PP 9	PP10	PP11
100	0	0	0	0	0	0	0	0	0	0	0
80	3	3	2.5	3	3	4	3	3	3	2	2.5
64	6	6	5	6	6	7	6	6	6	4	5
20	21	21	18	21	21	25	21	22	22	14	19
5	40	40	33	40	40	46	40	42	42	26	35
1	60	60	51	60	60	70	60	64	64	40	54

Table 2.5 Sampling depths during Dec-2004

2.3.2 Equatorial Indian Ocean

This cruise was aimed at studying equatorial Indian Ocean processes, in which a thorough measurement of physical, chemical and biological properties were carried out jointly by scientists from the Physical Research Laboratory (PRL), Ahmedabad and the National Institute of Oceanography (NIO), Goa, India.

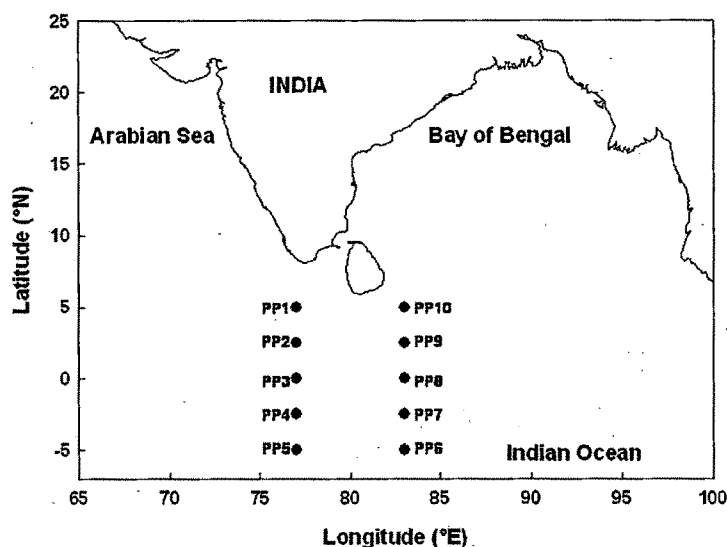


Fig. 2.5 The cruise track along which the sampling was done during SK-220.

In the equatorial Indian Ocean measurements were made in the pre-monsoon season (May-June 2005) on board *ORV Sagar Kanya* (SK-220). Here we collected samples from 10 stations along two transects, 77°E and 83°E (Fig. 2.5). Sampling was done at every 2.5° starting from 5° N to 5° S, with 5 stations along each transect. The details of the sampling locations for this cruise, with sampling dates are given in Table 2.6 and sampling depths are given in Table 2.7.

New Production Stations	Latitude	Longitude	Date
PP1	5 °N	77 °E	12/05/2004
PP2	2.5 °N	77 °E	14/05/2004
PP3	0 °N	77 °E	16/05/2004
PP4	2.5 °N	77 °E	19/05/2004
PP5	5 °N	77 °E	22/05/2004
PP6	5 °N	83 °E	25/05/2004
PP7	2.5 °N	83 °E	27/05/2004
PP8	0 °N	83 °E	31/05/2004
PP9	3 °N	83 °E	03/06/2004
PP10	5 °N	83 °E	04/06/2004

Table 2.6 Sampling location along with dates of sampling during the equatorial Indian Ocean cruise in pre-monsoon season (May-June 2005)

%Light	Sampling Depths (m)									
	PP 1	PP 2	PP 3	PP 4	PP 5	PP 6	PP 7	PP 8	PP 9	PP10
100	0	0	0	0	0	0	0	0	0	0
80	6	5	6	7	5	8	6	6	5	6
64	12	10	12	15	11	15	12.5	12	11	12
20	43	36	43	53	39	55	45	43	39	41
5	80	66	80	99	72	102	84	80	72	76
1	124	101	124	152	111	157	129	124	111	117

Table 2.7 Sampling depths during SK-220 (May-June 2005)

2.3.3 Southern Indian Ocean

The Southern Ocean cruise was a part of second expedition to the Southern Ocean and Larsemann Hills, Antarctica. The main task was to make a bathymetric survey of the approach channel to the proposed new station of India at the Antarctica. We carried out our experiments at a few selected sites on our way to Antarctica. Sampling was done in the late austral summer (Feb-March 2006), on board *RV Akedemik Boris Petrov* (ABP-15), at eight different stations (details of sampling locations and with dates are given in Table 2.8) covering a large area from the equator (0°) to the Antarctic coast (69°S) along the track shown in the Fig 2.6. Details of the sampling depths are listed in Table 2.9.

New Production Stations	Latitude(°S)	Longitude(°E)	Date
PP 1	69	76	24/02/2006
PP 2	65	56.3	03/03/2006
PP 3	58	50	06/03/2006
PP 4	43	48	13/03/2006
PP 5	40	48	15/03/2006
PP 6	35	48	17/03/2006
PP 7	7.5	61	02/02/2006
PP 8	0°	64	30/01/2006

Table 2.8 Sampling Location along with dates of sampling during the Southern Indian Ocean cruise (Jan-April 2006)

%Light	Sampling Depths (in Meter)							
	PP 1	PP 2	PP 3	PP 4	PP 5	PP 6	PP 7	PP 8
100	0	0	0.5	1	1	0	1	1
80	6	6	1.5	5	5	5	5	6
64	12	12	3	10	10	10	10	11
20	43	43	10	35	30	35	35	41
5	80	80	19	65	60	65	70	75
1	124	124	29	100	90	100	100	115

Table 2.9 Sampling depths during the Southern Indian Ocean cruise (Jan-April 2006)

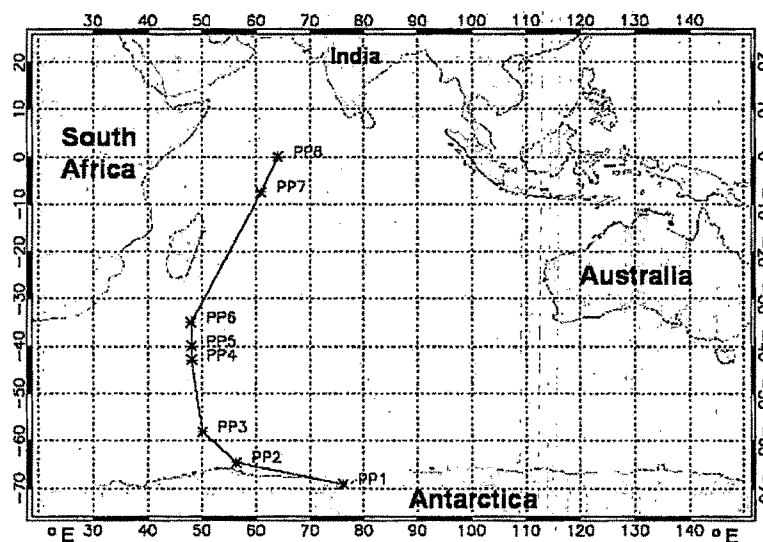


Fig. 2.6 The cruise track along which sampling was done for the present study in the Southern Ocean (ABP15).

2.4 Experimental Procedures

2.4.1 Sample collection

Common sampling procedure was followed during all the four cruises. Water samples were collected from six different depths to cover the entire photic zone. The depth of the photic zone i.e., the depth at which light falls to 1% of the surface level, was estimated using an underwater radiometer (Satlantic Inc.). Based on these light measurements six different depths were chosen for collecting water samples. The corresponding light levels are 100%, 80%, 64%, 20%, 5% and 1% of the surface

value. During all the cruises water samples were collected using clean Go-Flo bottles (General Oceanic, Miami, Florida, USA) attached to a CTD rosette (Fig. 2.7).

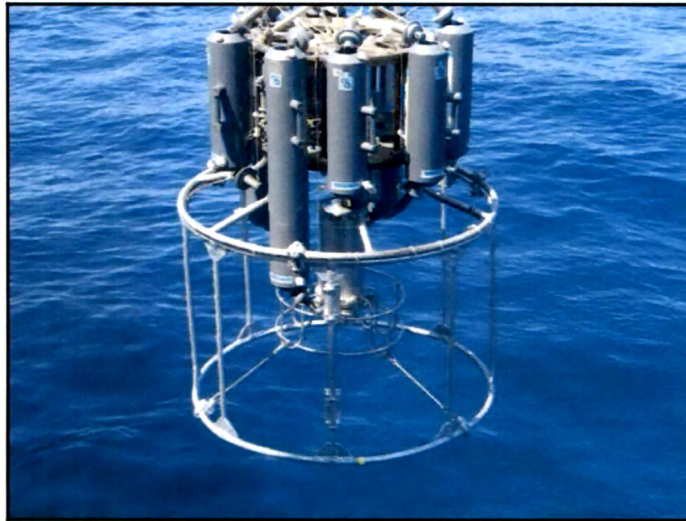


Fig. 2.7 Go-Flo bottles attached to a CTD rosette used to collect sea-water samples from different depths

An electronic CTD (Sea-Bird) was used to obtain conductivity-temperature-depth profiles. The temperature and pressure (*i.e.*, depth) sensors were calibrated before the cruise. The SEASOFT software package was used to process the raw CTD data. The CTD attached rosette was first lowered to the lowest desired depth and water samples were collected while hauling up by closing the bottles one by one at the desired depths. To ensure that the samples are collected from the desired depths, the CTD rosette was allowed to stabilize at that particular depth for some time, generally for one minute. Once the rosette was hauled back to the deck, the samples were immediately transferred to pre-washed polycarbonate Nalgene bottles of two (or one) liter capacity. Individual water samples were taken for nitrate (2L volume), ammonium (2L) and urea (1L) enrichment experiments. This was followed by the addition of ^{15}N (99 atom %) enriched tracer followed by incubation. Details of preparation of tracer solution, addition of tracer and incubation are discussed in following subsections.

2.4.2 Tracer preparation

^{15}N enriched nitrate, ammonium and urea tracers were made by dissolving ^{15}N -labelled (99 atom% enriched) dry nitrate, ammonium and urea salts, procured from Sigma-Aldrich (USA). First of all, stock solution of higher concentration for each tracer was made. 43.5 mg of nitrate (molecular weight ~ 85.98 g), 27.3 mg of ammonium (molecular weight ~ 54.48 g) and 16.8 mg of urea (molecular weight ~ 62.04 g) salt were dissolved separately in 250 ml of double distilled water in three different, well cleaned flasks, to make a stock solution of concentration ~ 2 mM. This stock solution was diluted to make working solutions of lower concentrations. To make a working solution of concentration $0.01 \mu\text{mole/ml}$, 5 ml of stock solutions of each compound was added to 995 ml of double distilled water. One ml of this solution, when added to one liter of sample, raised the concentration of respective tracers in the sample by $0.01 \mu\text{M}$. Another working solution of nitrate of concentration $0.1 \mu\text{mole/ml}$ was made by adding 12.5 ml of the stock solution in 237.5 ml of double distilled water. 1 ml of the resultant solution contains $0.1 \mu\text{mole}$ of nitrate and when added to a litre of sample, increased the concentration of nitrate in that sample to $0.1 \mu\text{M}$. Each stock and working solution was then kept in separate 250 ml Nalgene bottles. The weighing of the salts was done on Sartorius microbalance (Model No. MC-5; Germany) using Thomas Scientific weighing paper.

2.4.3 Ambient Nutrient Measurement

Nitrate, ammonium and urea were the nutrients of interest for the present study. During the Arabian Sea and Southern Ocean cruises, water samples (~ 100 ml) from each depth were taken in separate bottles and preserved in deep freezer to carry out the nitrate measurements at Dr. S. W. A. Naqvi's lab at NIO, Goa at the end of the cruise using an autoanalyzer. During the equatorial Indian Ocean cruise, nitrate was measured by onboard by Dr. Sugandhini Sardesai of NIO, Goa and her colleagues using an autoanalyzer. Ambient ammonium and urea could not be measured because of logistic reason but was calculated indirectly using regeneration rates for ammonium and urea by the mesozooplankton given by Mullin et al. (1973). Mesozooplankton was converted into dry weight using equation of Weibe et al. (1975). Using average excretion rates of 0.59 and $0.32 \text{ mg at-N (g dry wt.)}^{-1} \text{ d}^{-1}$, the

release rates were calculated for 12 hrs residence time of mesozooplankton in the mixed layer. According to this calculation the average ammonium and urea concentration in the upper layer were 0.017 μM and 0.009 μM respectively. These values could be at the detection limit ($\sim 0.01 \mu\text{M}$) if we take the uncertainties involved in the calculation into consideration and therefore, for the present study it was assumed that the tracer added was the only source for the planktons. Hence the uptake rates calculated here for ammonium and urea are conservative estimates.

2.4.4 Addition of tracers

Tracers were added to the samples just before the start of the incubation. For the Arabian Sea and Southern Ocean cruises, since the ambient nutrient measurement was not done onboard, a prefixed amount of nitrate was added. The nitrate concentration for these regions is well documented, so an attempt was made to add less than 10% of the possible ambient value. The actual nitrate measurements, which were done after the end of cruise, were used to calculate the uptake rates. During the equatorial Indian Ocean cruise, although nutrient measurements were done onboard, due to some logistics problems ambient nitrate value was not available on the day of sampling but was available only towards the end of the cruise. So here also prefixed concentrations of nitrate were added. Ambient ammonium and urea were not measured, so constant amount of ammonium and urea tracers were added; 0.01 μM during the Arabian Sea and equatorial Ocean cruises and 1 μM during southern ocean cruises (except at PP8 and PP9 which were in the equatorial region and hence 0.01 μM of each was added). During the Southern ocean cruise 1 μM ammonium and urea were added following Reay et al., (2001). Addition of high concentration of ammonium, here, may lead to the overestimation of ammonium uptake and hence the underestimation of the *f-ratio* (Binachi et al., 1997; Osion et al., 1980)

2.4.5 Incubation

Addition of tracers was followed by incubation. Soon after the addition of tracers, appropriate neutral density filters were put on the bottles. This was done in order to simulate the in-situ light condition. The neutral density filter was chosen in

such a way that the samples receive the same amount of sunlight that was available at the depth from which samples were taken. The filters were well calibrated using lux-meter in both dry and wet conditions. Once the filters were put on, the samples were left for incubation on the deck for four hours, symmetric to the local noon i.e., from 10.00 Hrs to 14.00 Hrs. A similar procedure was followed during the Arabian Sea and the equatorial Ocean cruises. For the Southern Ocean stations incubation was done for 6 hrs, except at two equatorial stations (PP7 and PP8). Since the quantum efficiency (production per unit chlorophyll per unit time) is very low in the case of Southern Ocean phytoplankton because of low sea surface temperature ($\sim 1^{\circ}\text{C}$), six hours incubation was done to ensure that the phytoplankton get enough time for photosynthetic production.

Flowing sea water from 5 m depth was continuously maintained into the incubation crates during the whole incubation period to regulate the temperature. After the incubation i.e., exactly after 4 hrs (6 hrs in case of Southern Ocean stations), samples were transferred to the shipboard laboratory for filtration and were kept wrapped in a thick black blanket in a dark cabin and were kept in dark till the filtrations were over. Filtrations were finished within 2 hours after the incubation.

2.4.6 Filtration

All samples are filtered subsequently through 47 mm diameter and $0.7\ \mu\text{m}$ pore size Whatman GF/F filters. These filters were calcinated for 4 hours at 400°C . Before calcination, filters were wrapped in an aluminium foil; one set of foil containing six filters. Well cleaned forceps were used to handle these filters as a precautionary measure to avoid any contamination. Samples were filtered under low vacuum ($<100\ \text{mm Hg}$) using a manifold unit procured from Millipore, USA. Samples treated with nitrate, ammonium and urea tracers were filtered using separate glass cups. After filtration, filter papers were "washed" using filtered sea-water to remove any left over ^{15}N . Filter papers were taken out carefully, after the filtration, with the help of forceps. Separate forceps were used for nitrate, ammonium and urea treated plankton samples. Filter papers were then kept in pestrislide boxes (Millipore make, procured from Millipore, USA). This was followed by keeping filters in an oven, at 50°C for 12 hrs, for drying and bringing to shore for isotopic analysis.



Fig. 2.8 Author filtering samples in dark on board R/V *Akademik Boris Petrov*

2.5 Instruments and analysis

In the recent years, improvement in mass spectrometry has revolutionized the application of different stable isotopes, especially the use of ^{15}N as a tracer to understand the oceanic processes and their role in the global carbon cycle. ^{15}N , a stable isotope of nitrogen, has an important application in the estimation of oceanic export production but low concentrations of nitrogen in waters had limited its use in the marine applications. Methods such as wet chemical sample preparation and isotope ratio mass spectrometry requires large amount of nitrogen ($\sim 100\ \mu\text{mole}$) and is mainly used in agricultural research. Another method, emission spectroscopy, is suitable for measuring low amounts of nitrogen ($< 1\ \mu\text{mole}$) and is suitable for marine applications but the precision is low.

With improved electronics, vacuum system and ion optics, even low concentrations of nitrogen ($< 1\ \mu\text{mole}$) can be measured with sufficiently high precision using an isotope ratio mass spectrometer. For the present study, all samples were analysed using a *CarloErba* elemental analyser interfaced via conflo III to a *Finnigan Delta Plus* mass spectrometer, using a technique for sub-microgram level ^{15}N determination (Owens and Rees, 1989).

2.5.1 Instrumentation

As discussed earlier, samples were analysed using an elemental analyser interfaced with a mass spectrometer. Elemental analyser is based on the Dumas principle of high temperature flash combustion. It consists of two reactors: a combustion or oxidation chamber and a reduction chamber. Both, the combustion and reduction chambers, are prepared in quartz tubes (length 41 cm); combustion chamber is prepared by filling silvered cobaltous oxide and chromium oxide, separated by quartz wool. Reduction chamber is filled with reduced copper with quartz wool at the top and bottom. Quartz wool was also used at the top and bottom of the chamber. Quartz wool separates different chemicals used and second, being porous it allows free movement of gas. The chemicals required for combustion and reduction chambers were procured from Courtage Analyses Services (France).

Before analysis, the filter containing the sample is packed into a pellet using a silver foil. Well cleaned forceps are used for packing the samples which were then loaded in a turret on the top of the oxidation chamber. At a time a maximum of 50 samples could be loaded. There is a well between the turret and the oxidation chamber where the pellet falls. There the sample is purged with pure He gas (grade 5, 99.999%, procured from Hydragas, Bangalore). This is followed by allowing the sample to fall into the oxidation chamber. As soon as the sample falls, a one-second pulse of oxygen is given at a flow rate of 175 ml/sec. The temperature of the oxidation chamber is maintained at 1060°C but as soon as the sample falls and oxygen pulse is given, this temperature increases to 1800°C for a moment, which leads to the combustion of the sample with a flash. Combustion in the presence of a large quantity of oxygen results into production of oxides of nitrogen, CO₂ and H₂O. Helium acts as a carrier gas and carries these gases to the reduction chamber. The reduction chamber contains reduced copper at 680°C. Here different oxides of nitrogen are reduced to N₂ gas. The gases, which now contain N₂, CO₂ and H₂O, are then passed through magnesium perchlorate, which absorbs moisture and water vapor present in the gas mixture. The remaining gases are then carried to gas chromatographic column (maintained at 60°C) which contains a molecular sieve. The sample gas, here a mixture of N₂ and CO₂, passes in a gas stream (called as the *mobile phase*) at different rates in the gas chromatographic column depending on

their various chemical and physical properties and their interaction with a specific column filling, called the *stationary phase* (here the molecular sieve). The function of the stationary phase in the column is to separate different components, causing each one to exit the column at a different time, called the retention time. The retention time of N₂ is less than CO₂, as a result of which N₂ moves faster than CO₂ and comes out earlier from the chromatographic column. Once the N₂ exits from the column, it is injected into the mass spectrometer through the Con-Flo.

2.5.2 Con-Flo

Con-Flo is an interface between the elemental analyzer and the mass spectrometer. N₂ released from the chromatographic column is introduced into the mass spectrometer through Con-Flo. It contains two inlets and one outlet capillary tube; one inlet each for the reference and the sample gases and one common outlet. Thus the Con-Flo transfers the reference or the sample gas into the mass spectrometer.

2.5.3 Mass Spectrometer

Analysis was done using a Finnigan Delta Plus stable isotope ratio mass spectrometer. This has an impact ionization source where ions are generated in high vacuum by electron impact. The energy of the ionizing electrons is 80eV. The ions, once produced, are accelerated towards the magnetic sector by a 3 KV potential. The ion beam exits the ion source through a slit with a width of 0.3 mm and then enters the magnetic sector where the magnetic field strength is 0.75 Tesla. The direction of the magnetic field is perpendicular to the direction of the moving ions. The geometry of the magnetic sector is such that the ion beam enters the magnetic sector at an angle of 26.5° and also exits the magnetic sector at the same angle. This is done in order to maintain the radius of curvature of flight at 9 cm. This mass spectrometer has a resolution ($m/\Delta m$) of 95 for C, N and O. The collector system consists of three Faraday cups connected to amplifiers.

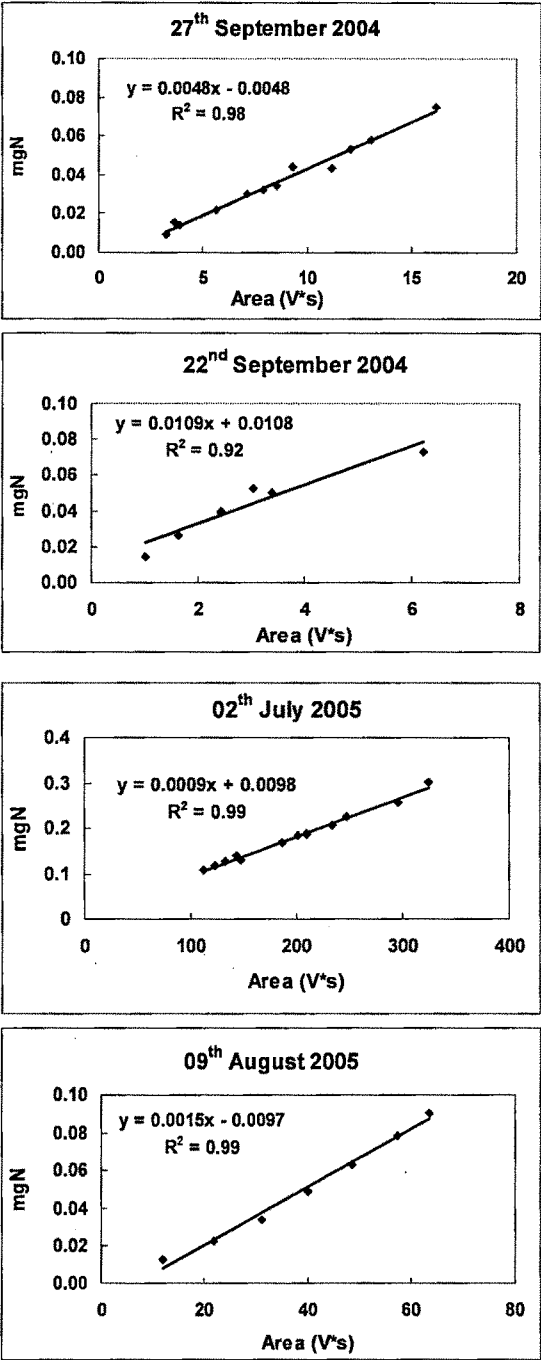
The elemental analyzer and mass spectrometer are fully automated and are controlled by the Finnigan MAT software ISODAT. Important instructions such as the opening and closing of sample and reference valves, their timings, time of helium

dilution and oxygen pulse rate etc. are controlled using this software. The typical data acquisition time for a sample is 450 seconds. Reference gases are introduced into the mass spec after the 37th and 87th seconds respectively. Sample gas is introduced at the ~150th second and analysis is continued till the ~225th second. Nitrogen peaks appear at the 187th second. The rest of the time is used for He flushing to minimize the memory effect. Ratio of 29/28 and 30/28 are used to calculate the ¹⁵N atom% and the total area under peaks 28, 29 and 30 is used to calculate the nitrogen content.

2.5.4 Calibration of the mass spectrometer

The aim is to measure the total organic nitrogen content of natural and enriched samples and the atom% ¹⁵N. To this end, it is important to check the stability and working of the mass spec. For this, the mass spec is calibrated using some standard material, inorganic as well as organic, of known nitrogen content. Main standards used are: Potassium nitrate, ammonium sulphate, acetone and BSA (an organic compound) which contain 13.8, 21.2, 10.3 and 17.8% nitrogen respectively. Since the typical concentration of particulate organic nitrogen is very less (typically 1 μ mole), weight of the standards is taken in such a range that it contains similar concentrations of nitrogen (generally 0.10 to 0.50 mg). For each such standard, the total area (a sum of area under the 28, 29 and 30 peaks in Vs) is plotted against the nitrogen content and a regression equation is derived. Some typical examples of such plots are given below (Fig. 2.9a):

a.



b.

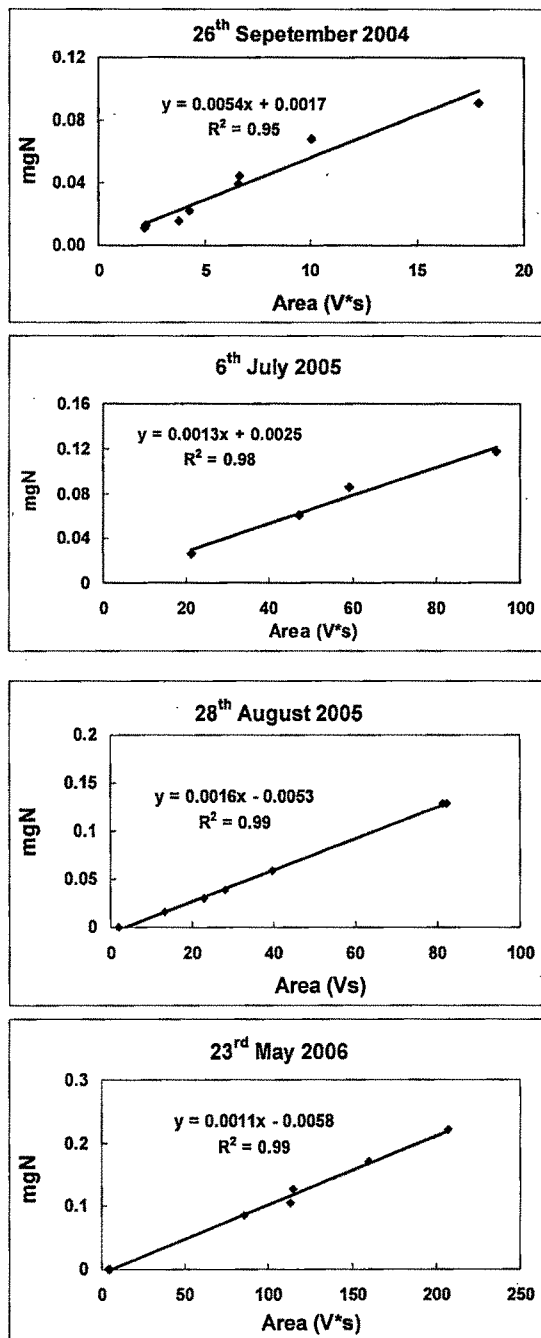


Fig. 2.9 Some typical examples of (a.) calibration curve obtained immediately after putting fresh chemicals in the oxidation/reduction chambers and (b.) examples of calibration curve used for the estimation of particulate organic nitrogen in the post incubation sample.

Only when the stability of the mass spec is confirmed, the sample analysis is started. In a set of 50 samples loaded in the turret for analysis, eight standards (8 standards + 42 samples) are also analyzed to check for possible stability change, if any. Overall precision on the basis of the standards measured during the analysis of the samples are shown in Table 2.10. These calibrations are used to calculate the organic nitrogen content of the sample. Some examples of such plots and equations are shown in Fig. 2.9b.

Standards Used	Quoted isotopic ratio	Values obtained during the present analysis
(NH ₄) ₂ SO ₄ (IAEA-N-2)	0.3753	0.3751 ± 0.0009 (n=22)
KNO ₃ (USGS 32)	0.4340	0.4329 ± 0.0012 (n=16)
KNO ₃ (IAEA-NO-3)	0.3695	0.3689 ± 0.0004 (n=11)

Table 2.10 Table showing overall precision, based on the standard measurements, during the analysis of the samples

During the Arabian Sea and equatorial Indian Ocean cruises only nitrate assimilation experiments was done in duplicates but during the Southern Indian Ocean cruises all the three i.e., nitrate, ammonium and urea, were done in duplicates. Table 2.11 shows the upper limit of the error in the PON estimation and atom % for the primary and duplicates.

Cruises	PON	Atom %
SS 222	< 35 %	< 0.5%
SK 214	< 9 %	< 5.5 %
SK 220	< 7%	< 2 %
ABP 15	< 0.3%	< 3%

Table. 2.11 Difference between duplicates

2.5.5 Estimation of uptake rate

Nitrogen uptake by the phytoplankton is estimated from ¹⁵N incorporation in the particulate organic matter. Several equations have been given in the past (Nees et al., 1962; Dugdale and Goering, 1967; Eppley et al., 1977) to estimate the uptake rate using ¹⁵N labeled techniques but all equations are based on some primary assumptions which fail under some conditions. The general equation for the

estimation of nitrogen uptake rate is derived from the concept of isotopic mass balance at the end of the incubation and was first shown by Collos and Slawyk (1985). According to the isotopic balance the number of ^{15}N atoms in the final particulate organic nitrogen is equal to the sum of the number of ^{15}N atoms in the initial particulate matter and the number of ^{15}N atoms taken up.

If C_p : ^{15}N atom % in the particulate phase after incubation
 C_d : ^{15}N atom % in the dissolved phase before incubation
 C_o : ^{15}N atom % in the particulate phase before incubation
 N_o : Concentration of particulate nitrogen before incubation
 N_f : Concentration of particulate nitrogen after incubation

And ΔN : Nitrogen taken up during incubation

Then isotope mass balance equation can be written as:

$$C_p * N_f = C_o * N_o + C_d * \Delta N \quad \text{.....(1)}$$

Since $N_f = N_o + \Delta N$

Equation (1) can be rewritten as

$$C_p * N_f = C_o * (N_f - \Delta N) + C_d * \Delta N \quad \text{.....(2)}$$

$$\text{Or } C_p * N_f = C_o * N_f - C_o * \Delta N + C_d * \Delta N$$

$$\text{Or } \Delta N * (C_o - C_d) = N_f * (C_o - C_p)$$

$$\text{Or } \Delta N = N_f * (C_o - C_p) / (C_o - C_d)$$

$$\text{Or } \Delta N = N_f * (C_p - C_o) / (C_d - C_o)$$

If Δt is the time of incubation, then the uptake rate is given as:

$$\Delta N / \Delta t = N_f * (C_p - C_o) / \Delta t * (C_d - C_o) \quad \text{..... (3)}$$

2.5.6 Equation used for the estimation of uptake rates

During the present study uptake rates were calculated using the equation of Dugdale and Wilkerson (1986):

$$\text{Uptake rate} = [\text{PON} * ^{15}\text{N}_{\text{xs}}] / [^{15}\text{N}_{\text{enrich}} * t]$$

Where PON = particulate organic nitrogen content of the sample in unit of $\mu\text{molN/L}$

$^{15}\text{N}_{\text{xs}}$ = Excess ^{15}N in post-incubation samples. This is calculated as difference in atom % between measured ^{15}N in the post-incubation sample and ^{15}N natural abundance (0.36781 atom %).

$^{15}\text{N}_{\text{enrich}}$ = ^{15}N enrichment in the dissolved fraction relative to the ambient

$^{15}\text{N}_{\text{enrich}}$ is calculated as:

$$^{15}\text{N}_{\text{enrich}} = \left[\frac{(99 * \text{tracer conc.}) + (^{15}\text{N}_{\text{natural}} * \text{ambient conc.})}{(\text{tracer conc.} + \text{ambient conc.})} \right] - ^{15}\text{N}_{\text{natural}}$$

And t = time of incubation

The above formula takes two parameters for the estimation of uptake rates: Particulate nitrogen and ^{15}N atom % in the post-incubation samples. These two parameters are measured on the same sample during mass spectrometer analysis and therefore this method gives the most accurate estimation of uptake rates. The hourly uptake rate is converted into daily uptake rate by multiplying it by day length *i.e.*, 12 hours, for nitrate and urea, as no nitrogen fixation takes place during night from nitrate and urea. For ammonium, the daily uptake rate is calculated by multiplying it by 18 hrs (Dugdale and Wilkerson, 1986). The nitrogen uptake rate is converted into carbon uptake rate using the Redfield ratio ($\text{C/N} = 6.62$), ignoring small variations in this ratio. Finally the f -ratio is calculated as:

$$f\text{-ratio} = \text{nitrate uptake} / \text{total N-uptake}$$

where the total uptake rate is the sum of nitrate, ammonium and urea uptake rates.

2.6 Iron Experiment

In the Southern Ocean, apart from ^{15}N experiments, bottle scale iron enrichment experiments were also done. The productivity of the southern Ocean is believed to be limited by the presence of the micro nutrient “Iron” (Martin and Fitzwater 1988, Martin et al., 1990). Iron helps in plant metabolism (Geider and La Roche 1994), and lack of iron may cause a decline in the photosynthetic electron transfer (Geider and La Roche 1994; Hutchins 1995) and this may decrease the photosynthetic efficiency of phytoplankton present there. Martin and his colleagues (Martin and Fitzwater, 1988) measured the concentration of iron in the waters of Gerlache strait (Antarctic coastal water) and Drake passage (off shore) and concluded that off shore location is less productive because it is not having enough iron to facilitate the consumption of nitrate present in the water whereas the coastal stations receive iron from continental margins, which are rapidly consumed in the surrounding water which is very productive and this iron is not getting transported to the open ocean (Martin et al., 1990). The idea of iron limitation got momentum when

it was shown, through bottle scale Fe enrichment experiments carried out for the first time at station PAPA (50°N, 145°W) by Martin and colleagues, that there is rapid increase in chlorophyll concentration and nitrate was totally consumed after 4 days since iron enrichment (Martin and Fitzwater 1988). This was followed by a number of iron enrichment experiments both in equatorial Pacific (IronEx I and IronEx II) and Southern ocean (EisenEx, SOIRE, SOFeX, EIFEX). No iron enrichment experiment has been done so far in the Indian sector of the Southern Ocean. We, for the first time, did bottle scale iron enrichment experiment in the Southern Indian Ocean at two different stations, the locations of which are shown in Table 2.12.

Station Name	Geographical Location		Date of sampling
IEE 1	43°S	48°E	13/03/2006
IEE 2	35°S	48°E	17/03/2006

Table 2.12 The locations of the stations for Iron enrichment experiments along with the date of sampling. IEE stands for Iron Enrichment Experiment

2.6.1 Experimental Procedure

Sampling was done in late austral summer (Feb-March 2006), on board *Akademik Boris Petrov* (ABP-15). Water samples from a fixed depth (in this case depth corresponding to deep chlorophyll maxima) were collected, using pre-cleaned Go-Flo bottles attached to a CTD rosette, to carry out the iron enrichment experiment. Samples were transferred directly into 1L Nalgene bottles to avoid any trace metal contamination. Samples were collected in eighteen 1L Nalgene bottles. These bottles were divided into two sets (set 1 and set 2) of 9 bottles each (Fig. 2.10). Further, each set of 9 bottles were subdivided into subsets of three bottles each (subset 1N, 2N and 3N) one bottle each for nitrate, ammonium and urea uptake rates (henceforth referred as ‘control experiment’). This was followed by addition of respective nutrients tracers. The second set was also treated similarly but along with nutrient tracers, iron solution was also added in each bottle (henceforth referred as ‘Fe experiment’). The purpose was: samples where only ¹⁵N labelled tracers were added help calculate the total uptake during the whole incubation period (the control experiment), whereas the samples where iron tracer was also added help monitor the

change in production, if any, because of the iron addition. 1 μM of ^{15}N enriched (99%) nitrate, ammonium and urea tracers were added to the respective water samples. The nitrate tracer added corresponded to $\sim 6\%$ and $\sim 18\%$ of the ambient concentration at station IEE1 and 2 respectively. Ambient ammonium and urea were not measured because of logistic reasons and it was assumed, for the calculation of uptake rates, that the tracer added was the only source available to planktons. In the surface waters of the open ocean, which is well oxygenated, the ambient concentrations of ammonium ($\sim 0.2 \mu\text{M}$; Binachi et al., 1997) and urea are low but still a high concentration of ^{15}N enriched tracer of ammonium and urea were added. This was done in order to artificially simulate the ammonium and urea uptake rates.

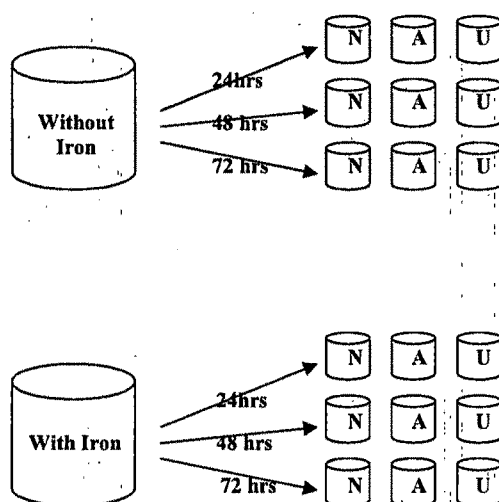


Fig 2.10 Schematic representation of the sampling adopted in the present study for iron enrichment experiment. (N = Nitrate tracer; A = Ammonium tracer; U = Urea tracer. All tracers were 99% enriched in ^{15}N)

The above methodology allowed us to monitor the effect of iron enrichment on nitrate, ammonium and urea uptake rates as well as on the f -ratio. This also helped to determine the preferred nutrient taken up during the iron enrichment experiment. It is very well established, now, through a number of iron enrichment experiments that there is some time-lag between the addition of iron and the consequent increase in production. To establish the role of the time of incubation on the iron and nitrogen

uptake kinetics, the three sets were incubated for three different time periods; subsets 1, 2 and 3 were incubated for 24, 48 hours and 72 hours respectively.

2.6.2 Iron tracer preparation

Iron exists mainly in two oxidation states: Fe (II) and Fe (III) but only Fe (II) is soluble in seawater and thus is bio-available. Even though Fe (II) is soluble in water, it precipitates at the present day sea water pH, *i.e.*, ~8. As a result of which its concentration in surface water decreases and becomes insufficient to meet the demand of phytoplankton to sustain biological production. To dissolve Fe in adequate concentration the pH of sea water must be lower. For tracer preparation 2L of surface water sample (pH 7.76) was taken from a station in the Southern Ocean and its pH was reduced to 1.91. This was followed by addition of 0.5 g of Iron (II) sulphate 7-hydrate ($\text{FeSO}_4 \cdot 7\text{H}_2\text{O}$, molecular weight 278.02, procured from VWR International Limited, UK). The concentration of the resulting solution was 0.93 mM. 1ml of this solution (*i.e.*, 930 nmol of Fe) was added to 1 L of the sea water sample for the iron enrichment experiment. This has already been shown that addition of iron increases productivity. Thus our aim of the present study was not to test whether addition of Fe increases the productivity but to check what happens to the new and regenerated productions because of the Fe addition. According to Michaelis-Menten kinetics, the effect of iron will saturate for large concentrations of Fe, which we have added. In addition, some experiments have shown that the effect of Fe addition is not immediate; rather it takes a few days. To see the effect of iron enrichment within a day or two on potential uptakes of nitrate, ammonium and urea, we increased the Fe concentration.

2.6.3 Chlorophyll measurement

In situ chlorophyll measurements were made by scientists from NCAOR (National Centre for Antarctic and Ocean Research), Goa, using a submersible fluorescence probe (*FluoroProbe*, *bbe-Moldaenke*, Kiel, Germany) for the determination of chlorophyll-a. This probe contains five light emitting diodes (450, 525, 570, 590, and 610 nm) for the excitation of pigments present in the phytoplankton. Chlorophyll fluorescence was measured at 685 nm. The excitation

spectrum obtained was compared to normal curves stored in the probe and the amount of chlorophyll was then calculated.

2.7 Quality Control

Special care was taken during experiments to avoid any contamination. For collection of samples Teflon coated Go-Flo bottles were used to avoid any trace metal contamination. These bottles were rinsed thoroughly before using them for sample collection. Samples were directly transferred from Go-Flo bottles to polycarbonate Nalgene bottles. No other plastic cans or pipes were used as a precautionary measure to avoid contamination. Always new and separate pipette tips were used for different tracers. Running seawater was used during incubation to maintain the temperature. Samples were immediately transferred to the ship-board laboratory after incubation and kept covered under dark cloths till the filtration was over. Filtration cups were thoroughly washed with milliQ water before the filtration and were rinsed properly once the filtration of each sample was over. This was done to restrict cross contamination. Filter papers were handled using well cleaned and separate forceps for each tracer. After filtration each bottles were washed thoroughly using 10% HCl, followed by fresh water for the next experiment. For the mass spectrometric analysis samples were packed in clean silver foils. Blanks with only silver foils were run in the mass spectrometer during every batch.

Chapter Three

The Northeastern Arabian Sea

3.1 Introduction

The northern Indian Ocean is divided into two major ocean basins by the Indian Peninsula: The Arabian Sea in the west and the Bay of Bengal in the east. The Arabian Sea has a unique geographical setting: it is surrounded by the Arabian and African continents in the north and west and by the Indian peninsula in the east. The presence of a huge landmass in the form of Indian peninsula, Eurasian continent and Arabia makes the oceanic and atmospheric circulation of the northern Indian Ocean different from the other two major oceans *i.e.*, the Atlantic and the Pacific. Unlike the other two major oceans upwelling does not occur along the equator in the Indian Ocean, but rather in the northern hemisphere off Somalia, Oman and the western coast of India, and that too is limited to the boreal summer (Schott et al., 2002). The Arabian Sea constitutes the northwestern part of the Indian Ocean. It is comparatively small in its aerial extent: assuming equator as its lower boundary it encompasses an area of about 6.2×10^6 km². It is one of the most biologically productive regions of the world ocean (Madhupratap et al., 1996; Smith, 2001) and is characterized by a range of biogeochemical provinces such as eutrophic, oligotrophic and oxygen deficient zones, based on atmospheric forcing due to the seasonally reversing monsoons: Southwest (summer) and Northeast (winter) monsoons (Bange et al., 2000; Wiggert et al., 2000; Prasanna Kumar et al., 2001a; Wiggert et al., 2002) and thus is an ideal laboratory for the oceanographic studies. Both the monsoons trigger high biological production but the underlying mechanisms are different. Fig 3.1 shows wind stress field over the Arabian Sea during different seasons. During the southwest monsoon, from May to September, strong south-westerly wind causes strong upwelling off Somalia and Oman and also along the western Indian coast, which enhances nutrients in the upper layers and causes high primary production. During the winter monsoon, cool dry air from the Himalaya enhances evaporation in the northern Arabian Sea causing surface cooling and convective mixing; this deepens the upper mixed layer causing entrainment of nutrients from the deeper to the upper layers triggering high primary production (Prasanna Kumar et al., 2001b), sometimes leading to the initiation of phytoplankton bloom.

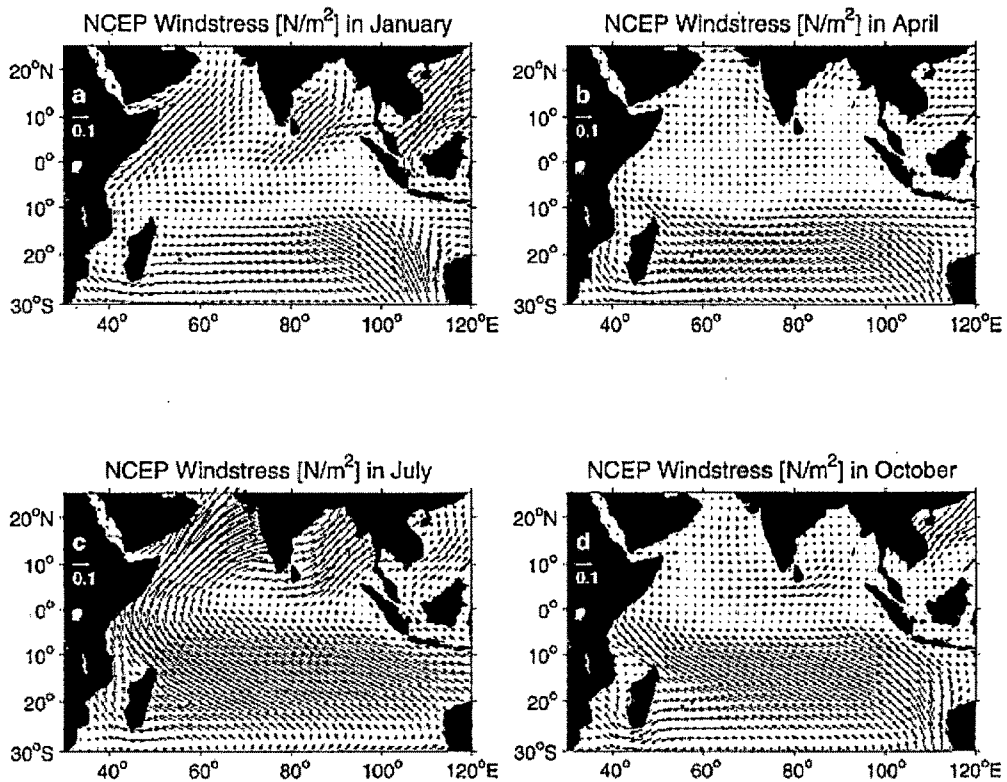


Fig 3.1 Monsoon wind stress field from the NCEP climatology for a) January, b) April, c) July and d) November (Source: Schott and McCreary 2001)

The total production during the bloom can reach up to $\sim 2 \text{ gCm}^{-2}\text{d}^{-1}$ (Sanjeev Kumar et al., 2008). The spring and fall intermonsoon seasons are characterized by weak winds and surface heating, which results in oligotrophy. These monsoonal circulations have also established a permanent gradient in terms of biological productivity in the Arabian Sea, from highly productive Oman coast to the oligotrophic central Arabian Sea (Pfannkuche and Lochte 2000). Because of the above reasons the Arabian Sea has always been a centre of attraction for the oceanographers and has been studied in detail during the past few decades. During the US and Indian JGOFS a detailed study of the Arabian Sea was carried out. Most work was concentrated on studies of nutrients (De Souza et al., 1996), chlorophyll and productivity (Bhattathiri et al., 1996), denitrification (Bange et al., 2000) and

physical forcing responsible (Madhupratap et al., 1996; Prasanna Kumar and Prasad, 1996). The main aims of JGOFS were as under:

1. To understand different physical processes controlling the biogeochemistry of the Arabian Sea.
2. To assess the variation in the primary production and the flux of carbon through the water column during different seasons
3. To assess the role of Arabian Sea in CO₂ air-sea exchanges. Does it act as a source or sink for the atmospheric carbon?
4. What is role of zooplankton in the overall transport of carbon to the deeper ocean?

Despite past major oceanographic programmes, limited data is available for the winter monsoon, especially for rates of primary and new production, as compared to the data available for the southwest monsoon in the Arabian Sea. As mentioned earlier the entrainment of nutrients into the surface layer during the winter monsoon leads to initiation of bloom in the northern Arabian Sea. The bloom during late winter monsoon is dominated by *Noctiluca scintillans*, a large and conspicuous dinoflagellate. This species is common in coastal areas worldwide and its most widely spread form is completely heterotrophic, survives on a wide range of prey such as phytoplankton and micro-zooplankton (Hansen et al., 2004). Heterotrophic red *Noctiluca scintillans* had been reported from the eastern Arabian in the month of September i.e., during the late summer/early winter monsoon (Sahayak et al., 2005). In the tropical and subtropical areas of the Southeast Asia, particularly in the northeastern Arabian Sea during late winter monsoon, a green form of *Noctiluca scintillans* is also found which can do photosynthesis and survive on itself under light for at least a month (c.f Sweeney 1971). The appearance of *Noctiluca* bloom in the northeast Arabian Sea is well documented in the literature (Dwivedi et al., 2006, Parab et al., 2006) but data available on the nitrogen uptake and *f*-ratios is limited (e.g. Sanjeev Kumar et al., 2008). The present study is mainly concentrated on the estimation of total and new productivity in the northeastern Arabian Sea during the



winter monsoon. The measurements carried out during the late winter monsoon also include productivity measurement in the *Noctiluca* dominated bloom areas.

Two different methodologies are used for the present study: 1) remote sensing study and 2) measurement of total and new productivity using the ^{15}N tracer technique over a large area in the eastern Arabian Sea.

3.2 Remote sensing studies

As discussed in the earlier section, the only possible way to monitor the variation in the biological properties of the ocean on a larger spatial scale is by remote sensing. Gregg et al. (2005) were the first to report an increase in the primary production of northern Indian Ocean using ocean color remote sensing data. They analyzed a 6 years time series of remotely-sensed global ocean chlorophyll data and reported an increase of 37.2% in the chlorophyll concentration in the western Indian Ocean (Somalian shelf) and 20.1% and 16.7% decrease in central Indian gyre and Bay of Bengal respectively. Goes et al. (2005) also reported an increasing trend in the chlorophyll concentration, and hence in the productivity, in the western Arabian Sea (47°E to 55°E & 5°S to 10°N and 52°E to 57°E & 5°S to 10°N). They attributed the cause to be the warming of the Eurasian landmass: the melting of the Himalayan snow cover in the recent past due to global warming apparently resulted in the enhancement of the land-sea contrast in summer temperature, thus enhancing monsoon winds. Though Gregg et al., 2005 also reported an increase in the chlorophyll concentration along the Somalian shelf, they did not attribute the cause to global warming. It is now well established through literature on palaeo-monsoon (Dupelssy, 1982; Sarkar et al., 1990) that whenever the southwest monsoon weakened (e.g. during the last glacial maximum circa 21,000 years ago), the northeast monsoon strengthened and *vice versa*. If this is taken in conjunction with Goes et. al., (2005) result one would expect a decreasing trend in the winter productivity in the north-eastern Indian Ocean. To verify this we have analysed the chlorophyll data over a period of eight years (1997 to 2005), obtained from SeaWiFS to characterize the interannual variation in the north eastern Arabian Sea, where winter cooling in the north and upwelling in the south are very prominent, causing an

increase in the primary production. Our analysis of 8 years record of satellite ocean colour data over north-eastern Arabian Sea (Fig. 3.2.), from September 1997 to June 2005, suggests that chlorophyll concentration has not changed significantly with time but two seasonal peaks can be seen clearly; one during the winter monsoon (Feb/March) and other during summer monsoon (September). There is no monotonic increase in the chlorophyll-a concentration as reported for the southwest Arabian Sea. On the other hand the southwest Arabian Sea, where the chlorophyll distribution is not bimodal.

In zone 1, 1997-2005, the chlorophyll concentration has remained more or less similar during October to December (Fig. 3.2.). In most years there is a seasonal increase from January to March. This is because of the input of nutrients from the deeper level to the surface layer due to the deepening of the mixed layer caused by the winter cooling and convective overturning. Also, wind blowing from the continent to the ocean supplies nutrients and iron dust. According to a previous study (Bange et al., 2000) the NH_4^+ input was the highest ($0.69 \pm 0.31 \mu\text{g}/\text{m}^3$) during the declining phase of NE monsoon (March). The increased input of nutrients into the photic zone through convective mixing and atmospheric input causes the increase in the productivity in Feb/March sometimes leading to blooms. The average Chl-a concentration in March over the last 8 years is $1.45 \text{ mg Chl}/\text{m}^3$, the maximum being $1.96 \text{ mg Chl}/\text{m}^3$ in 2002 and the minimum $0.92 \text{ mg Chl}/\text{m}^3$ in 2004. After March again Chl-a concentration starts decreasing till the onset of the summer monsoon. Because of dense cloud cover very little data is available for the months of June, July and August. From September onwards as the cloud cover decreases it is easier to obtain remotely sensed Chl-a data. In September the chlorophyll concentration is fairly high (but less relative to Feb/March) because of the input of nutrients due to upwelling in the southwest Arabian Sea and possible lateral advection (Prassana Kumar et al., 2001a).

The sea surface temperature, an indicator of vertical mixing, has remained almost the same (Fig. 3.3.) over past eight years. Thus the SST data do not show a significant reduction in the winter cooling. In this zone, during winter a significant fall in the SST can be seen ($3\text{-}4^\circ\text{C}$). The decrease in SST is due to the mixing of the

deeper water with the surface water. This causes increase in the productivity. The decrease in SST can also be seen during SW monsoon when moderate upwelling takes place although it is not that prominent in this zone. During summer too the SST falls but the magnitude of decrease is less (1-2°C). This clearly suggests that winter cooling has more control on the productivity than upwelling in this zone.

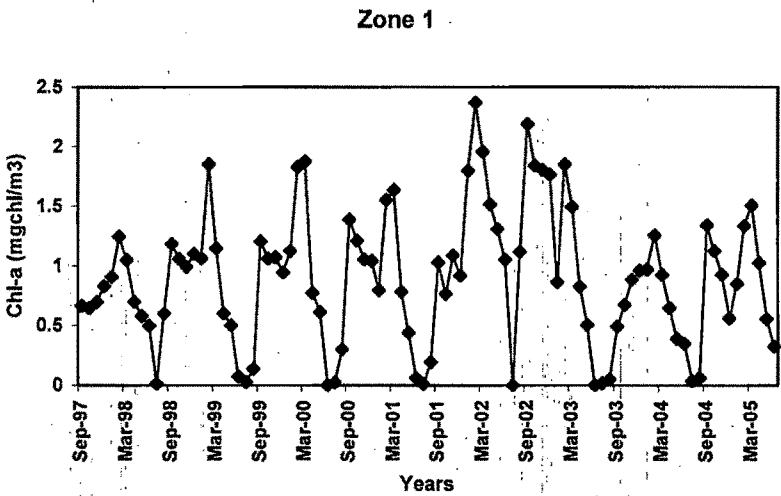


Fig. 3.2. Satellite derived Chl-*a* over zone 1.

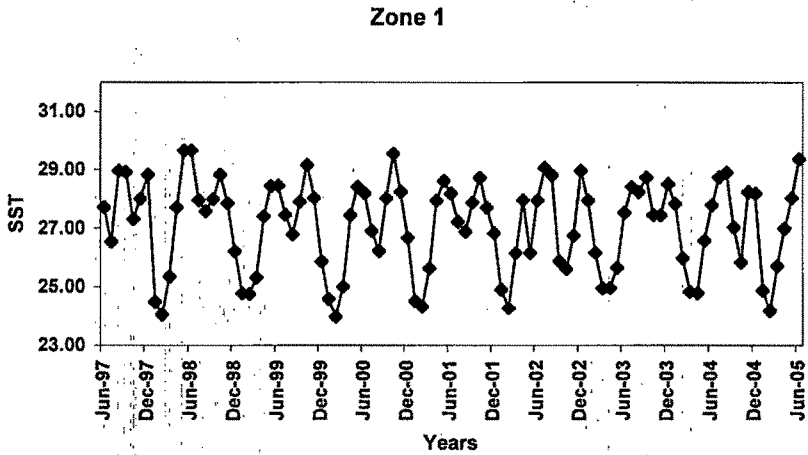


Fig. 3.3. Satellite derived SST over zone 1

In zone 2 the chlorophyll concentration remains low compared to zone 1, throughout the year. However, two prominent peaks can be seen every year (Fig. 3.4); one in the month of September when upwelling/vertical mixing takes place and the other, in the months of Feb/March, when winter cooling in the north triggers high production. Chlorophyll concentration is the highest in the month of September. The average value during 1997-2005 in September is 0.52 mg Chl/m^3 , the maximum being 0.69 mg Chl/m^3 (2004) and the minimum being 0.33 mg Chl/m^3 (1997). The chlorophyll concentration is also high during October to March, being the highest in March. The average chlorophyll concentration in March is 0.33 mg Chl/m^3 . In this part of Arabian Sea the satellite derived sea surface temperature shows a bimodal temperature cycle with lows during SW (2-3°C) and NE (1-2°C) monsoons (Fig. 3.5.). This change in temperature has a profound effect on the mixed layer through change in water density. The increase in the mixed layer depth causes the transport of nutrients rich colder water from the deeper level to the surface and supply of nutrients for production. This enhances the Chl-a value in this region during these months.

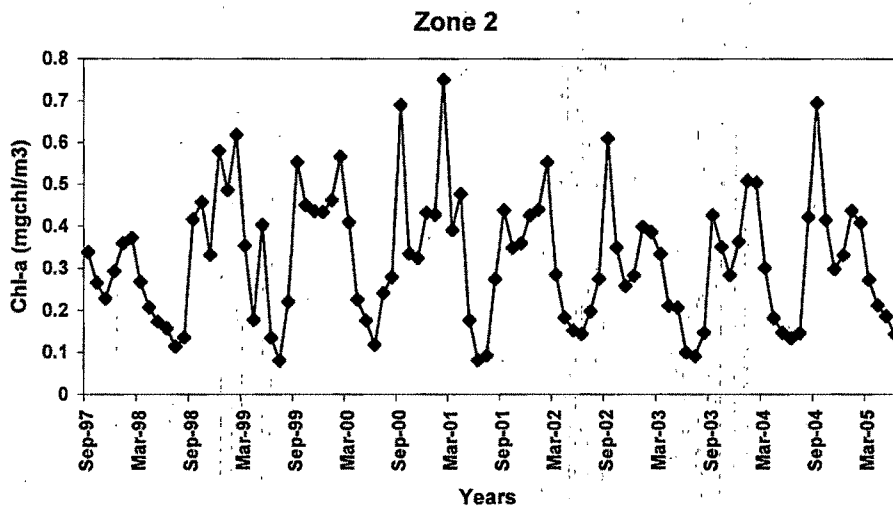


Fig. 3.4. Satellite derived Chl-a over zone 2

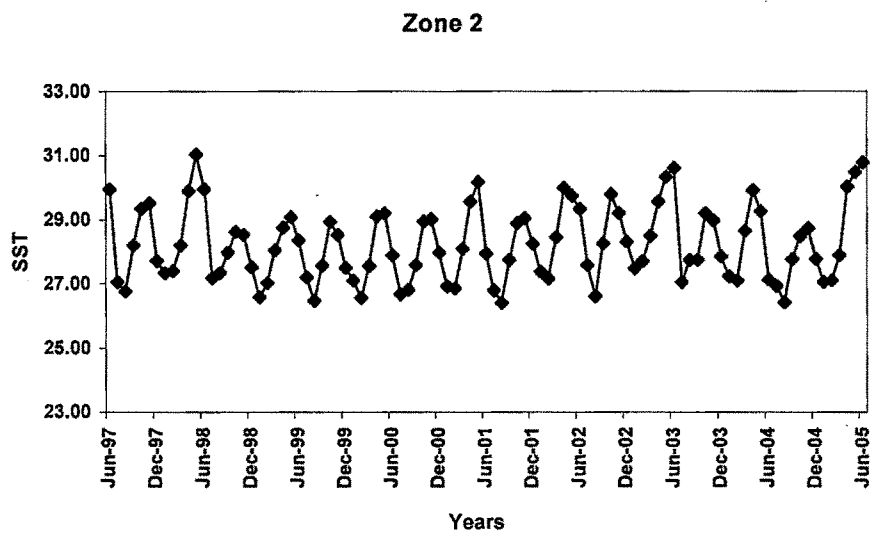


Fig. 3.5. Satellite derived SST over zone 2

Goes et. al., 2005 have argued, on the basis of the correlation between SST and satellite derived chlorophyll (Fig. 3.6, $R^2 = 0.70$), that the summer productivity has increased over the years due to increasing monsoon winds.

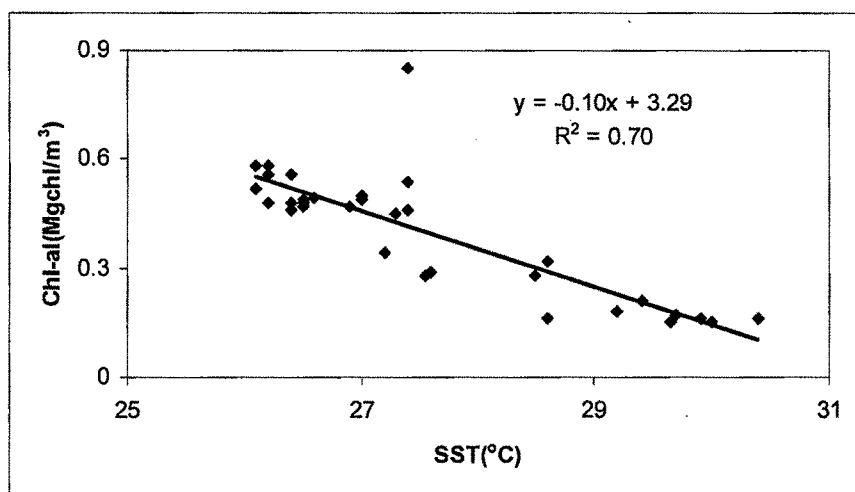


Fig. 3.6. Satellite derived Chl-*a* data and SSTs from May to September from the region 52°E to 57°E and 5°S to 10°N (Source: Goes et. al., 2005)

We also analysed the correlation between SSTs and Chl-a over Zone 1 and Zone 2 for the boreal winter i.e. October to March for the same time period and have observed that the slopes of the regressions are similar (~ -0.10) for all the three regions. Our analysis of sea surface wind data also does not show any significant change in the wind speed over north-eastern Arabian Sea (Fig. 3.7 and 3.8). In zone 2 we do not find any change in the wind strength. Wind speed pattern, over this region, has remained more or less constant during 1999-2005. Some small variations in wind speed can be seen in zone 1 but certainly there is no significant secular trend. These small changes can not be attributed to global warming because had it been due to temperature contrast between Eurasian plate and Arabian Sea, it should have affected both the zones. It is also difficult to relate these changes to decadal-scale oscillatory events using these data sets.

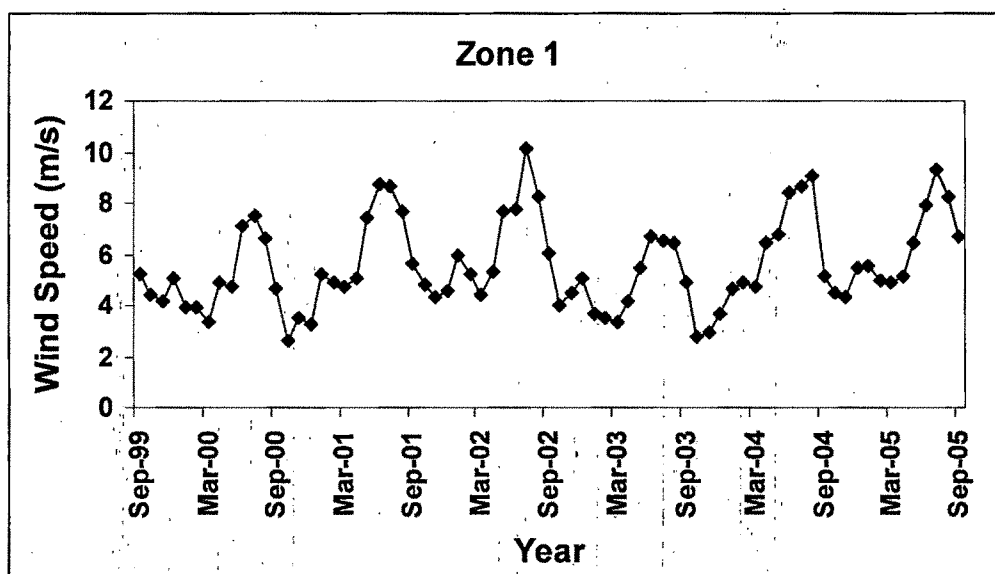


Fig. 3.7. Satellite derived wind speed over zone 1

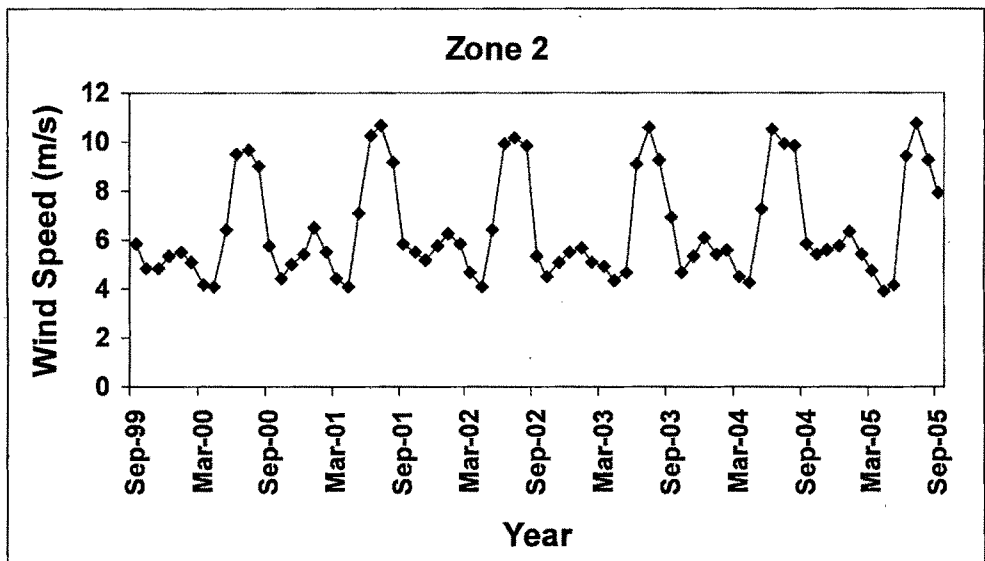


Fig. 3.8. Satellite derived wind speed over zone 2

The satellite derived chlorophyll and SST do not show significant correlation in winter in zone 1 (Fig. 3.9, $R^2 = 0.18$) but a significant correlation in zone 2 (Fig. 3.10, $R^2 = 0.44$).

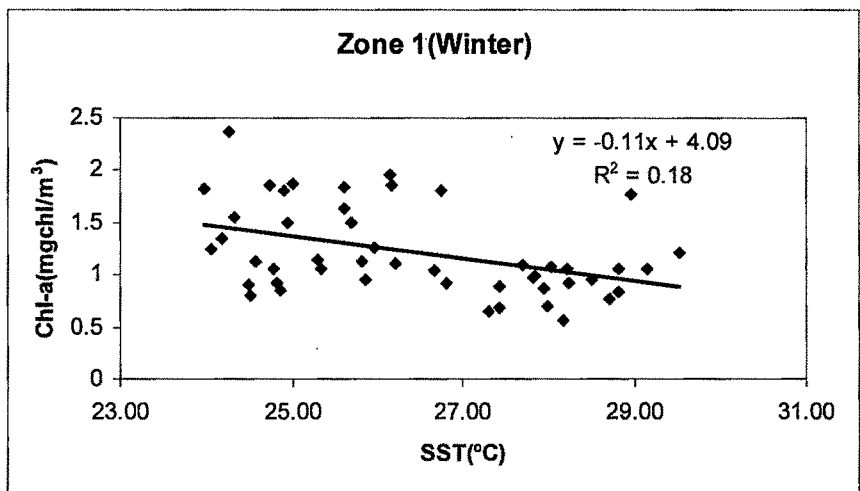


Fig. 3.9. Satellite derived Chl-*a* data and SSTs over Zone 1 in winter (October to March)

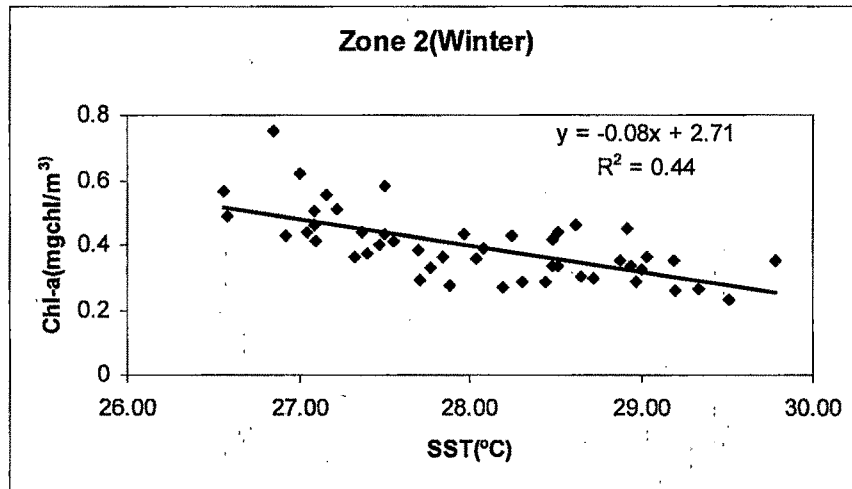


Fig. 3.10. Satellite derived Chl-*a* data and SSTs over Zone 2 in winter (October to March)

This suggests that both upwelling (SW monsoon) and convective mixing (NE monsoon) are responsible for a seasonal high productivity in this zone. Transportation of the deeper, colder, nutrient rich water to the surface triggers high production in the Western as well as in the Northern Arabian Sea. The average chlorophyll concentration in zone 1 is thrice the average concentration in zone 2 suggesting a greater control of winter cooling for the observed high production in this area. Although winter cooling has greater control on the production in the northeast Arabian Sea, it is not the only factor.

In summary, the interannual, remotely sensed, monthly composite chlorophyll data suggest high chlorophyll concentrations in the eastern Arabian Sea. The chlorophyll concentration in the north-eastern part of Arabian Sea is thrice that in the south-east. March is the most productive month due to winter cooling, while September is the most productive month during the summer monsoon. This is due to the difference in the physical forcing. The south-eastern Arabian Sea is equally productive in both summer and winter whereas the north-eastern part is more productive in winter than in summer. Overall, winter cooling has a more pronounced effect on the chlorophyll concentration and hence on the productivity in the eastern Arabian Sea compared to the summer monsoon. Although we see some seasonal variations in different parts of the Arabian Sea there is no significant secular trend.

Our analysis also shows that the trend reported by Goes et al., 2005 in the Western Arabian Sea is not observed in the eastern Arabian Sea. The increase in the chlorophyll reported by the Goes et al. 2005 is probably restricted to the west. Also their proposal that the intensification of southwest monsoon due to global warming has caused the increase in the productivity appears untenable, as we fail to observe any corresponding decreasing trend in the productivity of the north-eastern Arabian Sea. Any change in the monsoonal pattern because of land-sea temperature contrast should affect the north-eastern Arabian Sea in a bigger way because of its close proximity to the Himalaya as compared to the south-western Arabian Sea, which is not borne out by our analysis.

3.3 Chlorophyll-*a*, nutrients and physical parameters during February-March 2004 in the northwestern Arabian Sea

3.3.1 Chlorophyll-*a*

Chlorophyll concentration was measured at all the stations during this cruise. The surface waters at the stations in the south had less surface chlorophyll as compared to the stations in the north. It varied from 0.13 to 0.53 mgChlm⁻³ at the stations in the south (non-bloom area) i.e., PP1 to PP6 and PP8, where as in the north, where the *Noctiluca* bloom was present i.e., from PP7 and PP9 to PP11, surface chlorophyll concentration was very high; it varied from 0.96 to 2.74 mgChlm⁻³. The vertical profiles of Chl-*a* at different stations are shown in Fig. 3.11. In non-bloom areas, most of the station had a deep chlorophyll maximum. At PP1 the surface chlorophyll concentration was 0.15 mgChlm⁻³ which increased to 0.37 mgChlm⁻³ at 57 m. PP2 and PP4 had similar chlorophyll profiles; at both stations the chlorophyll concentration decreased slightly at 3-4 m but again increased to a maximum at 45-50 m. At PP5 the chlorophyll concentration increased from 0.29 mgChlm⁻³ at surface to 0.39 mgChlm⁻³ at 55 m, which decreased with depth to a low of 0.029 at 115 m. PP6, being a shallow station (<20 m) because of the presence of a sub-surface bank, relatively high surface Chl (0.53 mgChlm⁻³) but had low integrated chl concentration of 3.29 mgChlm⁻³ because of less column depth. PP7 had high chl concentration (0.96 mgChlm⁻³) at surface, which decreased rapidly at 1.5m to 0.27

mgChlm⁻³ but again increased to 0.69 mgChlm⁻³ at 40 m. PP8, despite being in the bloom zone this area was away from the actual bloom patch. The surface chlorophyll concentration, here, was significantly less (0.24 mgChlm⁻³) compared to PP7. The deep chlorophyll maximum was at 35 m and had concentration of 0.43 mgChlm⁻³. Station PP9, 10 and 11 was in the northeast Arabian Sea. These stations had high surface chlorophyll concentrations (> 1 mgChlm⁻³). The dominant species was *Noctiluca*. The concentration of *Noctiluca* was so high (1.2-2.7 mglm⁻³) that a significant amount of light (~ 22 %) got absorbed near the surface. As a result of this the depth of photic zone in this area decreased (mean photic depth ~ 50 m).

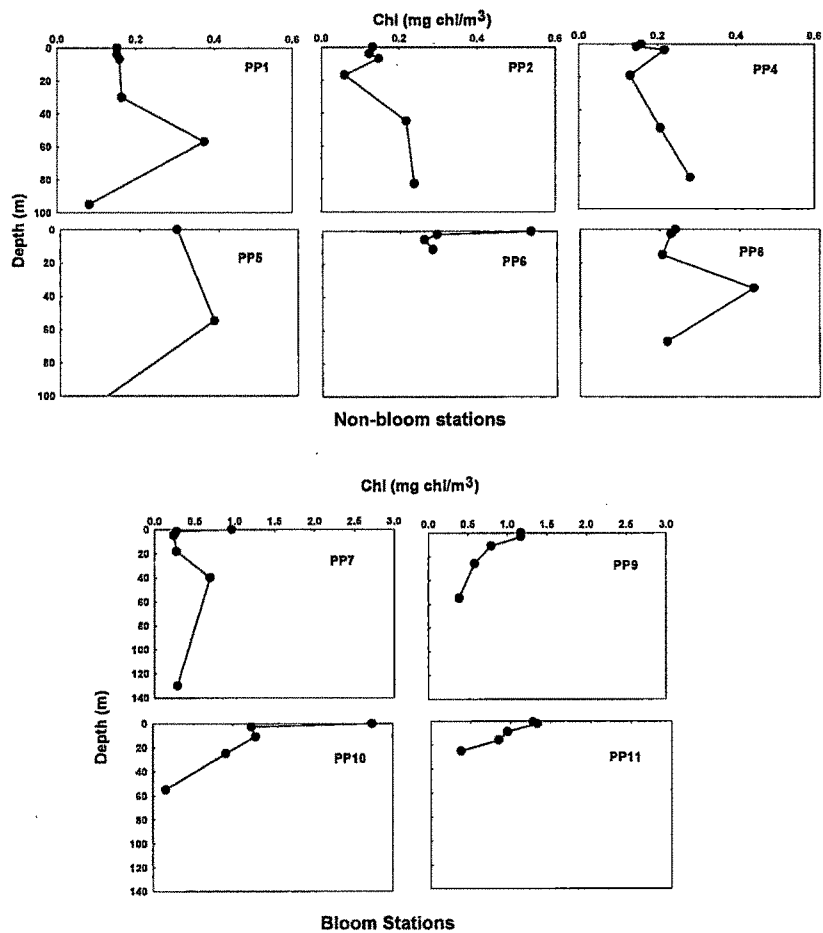


Fig 3.11. Vertical profiles of Chl-*a* at different stations in the eastern Arabian Sea during late winter monsoon (Feb.-March 2004)

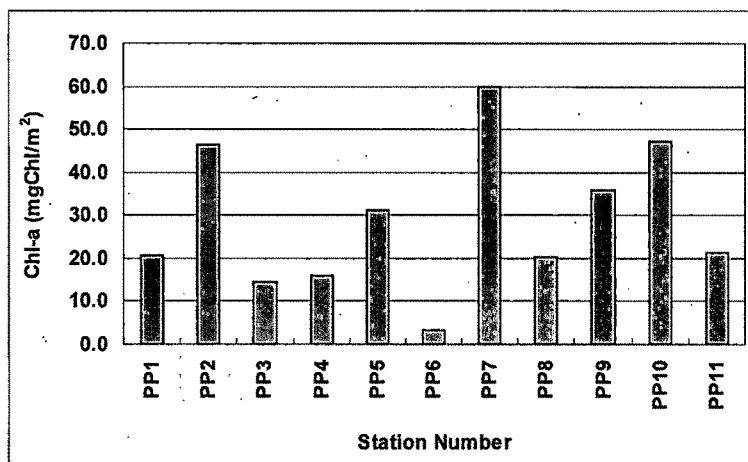


Fig. 3.12 Euphotic zone integrated chl-*a* concentration at all the stations during Feb.-March 2004.

The average column integrated Chl-*a* concentration during the study period was 27.04 mgChl^m⁻²; the maximum column integrated Chl-*a* concentration of 59.72 mgChl^m⁻² was found at PP7 and a minimum of 14.53 mgChl^m⁻² at PP2 (Fig 3.12).

3.3.2 Nutrients

Samples from all stations and all depths were analyzed for ambient nitrate concentration using an autoanalyzer. The surface layer had almost no nitrate at the southern stations i.e., from PP1 to PP6. The vertical profiles of nitrate are shown in Fig.3.13. At PP1 the water column was devoid of nitrate up to a depth of 57 m. Its concentration started increasing downwards. At PP 2 nitrate was not present up to 17 m. Downwards it increased slightly to 2.17 μ M at 45 m but again decreased further below. PP3, 4 and 5 had similar characteristics as PP1. The nitrate concentration in the surface layer was near zero but increased downwards from depths of 27, 50 and 55m respectively. Though PP6 was a shallow station it showed heterogeneity in terms of nitrate concentration. The surface water at this station had nitrate concentration 0.47 μ M which decreased to near zero between 2-5 m but increased again to 0.50 μ M at 11 m.

PP7 was a bloom station with high chlorophyll in its surface waters but very little nitrate (\sim 0.01-0.07 μ M) in the surface waters. It increased slightly to 0.47 μ M

at ~5 m. There was again a decrease in nitrate at around 18 m. Downwards it increased to a maximum of 10.65 μM at 130 m. Though station PP8 was in a general area dominated by *Noctiluca* bloom, this station was out side the actual *Noctiluca* patch and this is reflected on the nitrate concentration here as well.

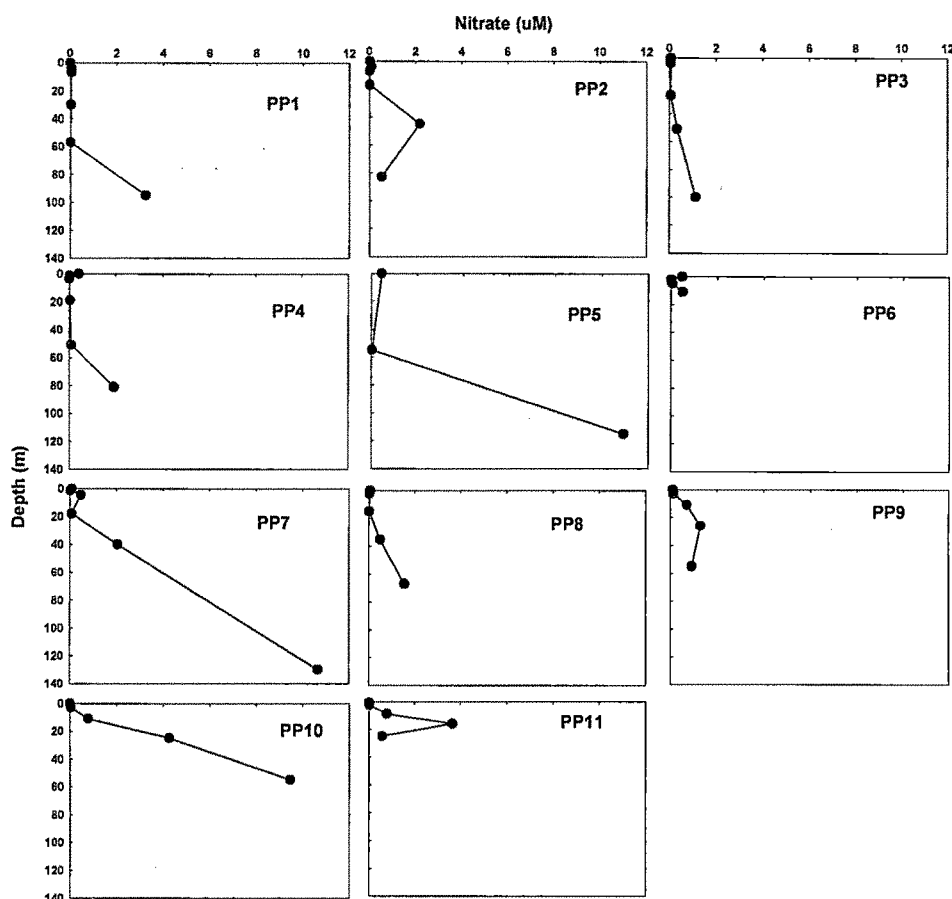


Fig 3.13 Vertical profiles of nutrients at different stations during the present study (cruise SS#222)

The nitrate concentration was low throughout the photic zone with almost no nitrate in the surface layer. Its concentration started increasing below 27 m but this increase was less compared to the other bloom stations. These three stations had high concentrations of Chl-*a* and were characterized by the presence of bloom dominated by green *Noctiluca scintillans*. During this period of the year these areas are influenced by convective mixing which brings ample nutrients, mainly nitrate, to the

surface triggering high primary production often resulting in blooms. Though the bloom was present, high nitrate concentrations in surface waters were not observed. An earlier study in this area (Sanjeev Kumar 2004) had reported a large concentration of nitrate ($\sim 100 \text{ mmolm}^{-2}$) in the surface waters. The lesser concentration of nitrate suggests that most of the upwelled nitrate was utilized efficiently to trigger the high production and hence the bloom.

3.3.3 Hydrographic conditions

The present study was carried out during the months of February-March when this part of the world is under influence of the winter monsoon. During this period the Sea Surface Temperature (SST) of the Arabian Sea decreases upto $5\text{-}6^\circ\text{C}$ on a south-north transect. Madhupratap et al., (1996) has reported a northward decrease in SST at a rate of 0.5°C per degree latitude during the winter in the Arabian Sea. During the present study the maximum SST of 28.9°C was recorded at one of the southernmost station (PP2) and a minimum of 25.2°C was recorded at PP10, a station in the north. The rate of decrease was low in the south i.e., from 10°N to 17°N , where SST decreased from 28.8°C to 28.2°C but in the north the rate of decrease was high; it decreased from 28.2°C to 25.2°C between 17°N to 22°N (Fig 3.14). The rate of decrease was more ($\sim 0.65^\circ\text{C}$ per latitude) than that reported by Madhupratap et al., (1996). The lowering of sea surface temperature was associated with the increase in salinity of the surface waters. Salinity was low in the south and increased gradually towards the north. The minimum salinity of 33.8 psu was recorded at the southernmost station PP1 and a maximum of 36.6 psu was recorded at PP10, a station in the north. Unlike SST which showed a rapid decrease over a comparatively small area in the north, salinity showed a gradual increase over the whole study region.

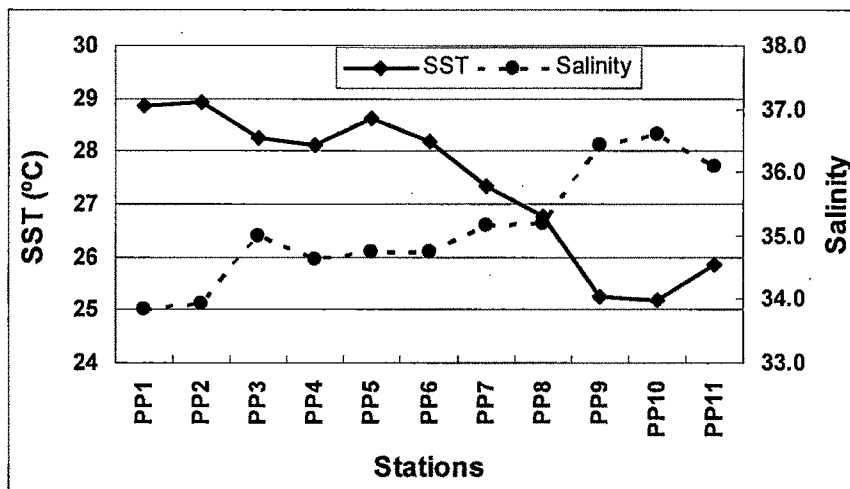


Fig 3.14 SST and salinity at different stations in the eastern Arabian Sea during Feb-March 2004.

During the winter land loses temperature much faster than the ocean. This results in wind from the land towards the ocean. As this wind is cool and dry, it absorbs moisture and in this process it causes evaporation of the surface water in the northern Arabian Sea. Excess evaporation over precipitation causes an increase in salinity of the surface waters. This dense surface water tends to sink and causes convective mixing. This transports nutrient rich deeper cold water to the surface and lowers SST. Figure 3.14 shows anti-correlation between SST and salinity: decrease in SST is associated with an increase in salinity. Higher rate of decrease in SST suggests more intense winter cooling and this has also been reflected in the column N-uptake rates and f -ratios, which will be discussed later in this chapter. Though the effect of winter cooling could be observed in SST and salinity, the same could not be observed in temperature based mixed layer depth or MLD (Fig 3.15). The deepest MLD was at PP1, a station in the south. MLD at this station was 37m. Rest of the stations did not show a well defined MLD. Temperature profiles of all other stations showed lots of undulation. As the sampling was done towards the end of the winter monsoon, undulations in temperature profiles suggest the dying phase of the winter cooling phenomenon.

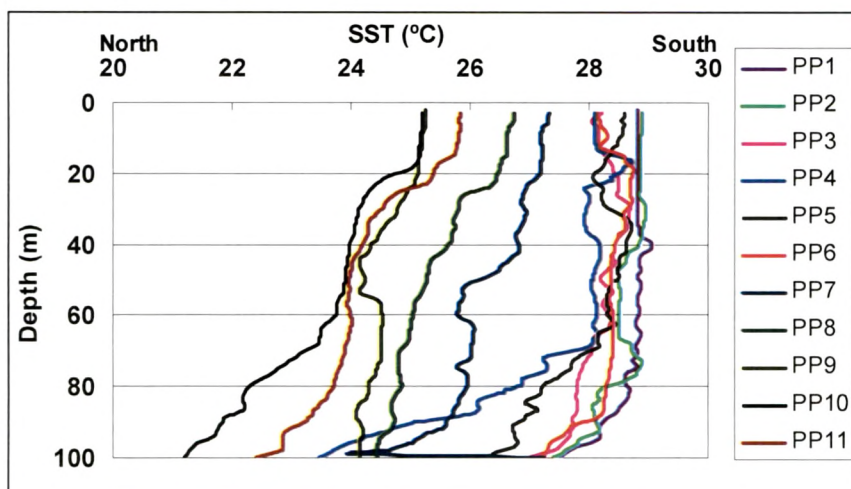


Fig 3.15 Temperature-depth profiles at different stations obtained using CTD data during Feb.-March 2004

3.4 ¹⁵N based Productivity in the late winter monsoon (Feb.-March 2004)

3.4.1 Total Production

The rates of nitrogen uptake, integrated over euphotic zone, varied from 2.7 mmolNm⁻²d⁻¹ to 23.4 mmolNm⁻²d⁻¹ over the study area. The higher rates were measured at the stations in the north (PP9, 10 and 11), whilst the lower rates were associated with the southern stations (Fig.3.16). The same spatial variability in the nitrogen uptake was also reported by Owens et al., (1993) i.e., the lower uptake in the south and the higher in the north with an overall increasing trend from south to north, in the north-western Arabian Sea.

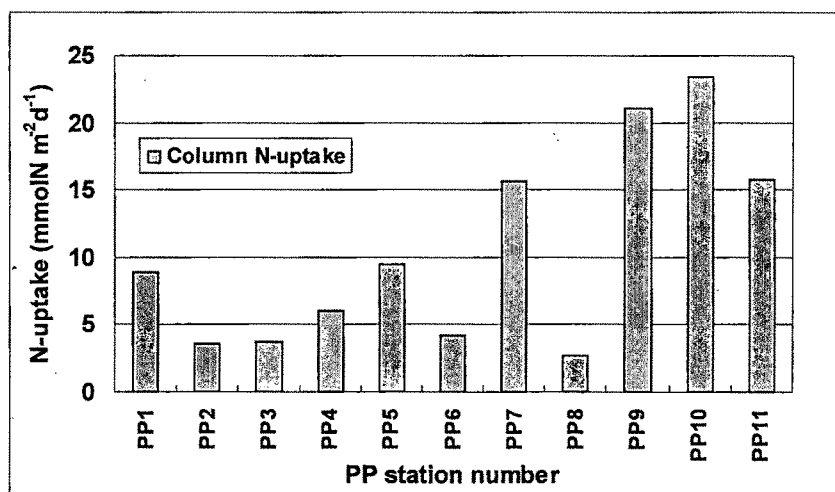


Fig. 3.16. Station-wise column-integrated total N-uptake for eastern Arabian Sea during the present study (total N-uptake rate is a sum of nitrate, ammonium and urea uptake rates)

At the southern stations (PP1 to PP 4 i.e., 10°N to 14°N) the mean depth of the euphotic zone was more, ~95 m. Column-integrated total N-uptake varied from 3.6 to 8.8 mmolNm⁻²d⁻¹. At PP5 samples were collected from only three depths, from 100%, 5% and 1% light levels. Therefore the column production could have been somewhat underestimated. PP6 was a shallow station (<20 m) because of the presence of a sub-surface bank, sea bed was visible at this station, only 4 depths could be sampled here. The column production (integrated only up to 20% light level) is relatively high, 4.2 mmolNm⁻²d⁻¹. We have sampled 4 stations (PP7, and PP9 to PP11) in the northeastern part of Arabian Sea during a phytoplankton bloom (defined as surface Chl-*a* ≥ 1 mg Chl m⁻³) dominated by *Noctiluca scintillans* (green autotrophic variety). At PP7 the concentration of *Noctiluca scintillans* was less despite having relatively high nitrate in the surface waters. As this station was the southernmost among other bloom stations we suspect that the bloom had not yet initiated at the time of sampling. The column integrated total N-uptake rate of 15.6 mmolNm⁻²d⁻¹ was the lowest compared to other bloom stations, of which the nitrate uptake rate was 3-fold higher than the combined ammonium and urea uptake rates. Though PP8 was located north of PP7, it was outside the bloom patch and therefore was not considered as a bloom station for the present analysis. Here the column N-

uptake was $2.7 \text{ mmolNm}^{-2}\text{d}^{-1}$. From PP9 to PP11, the concentration of *Noctiluca* ($1.2\text{-}2.7 \text{ mgm}^{-3}$) was so high that a significant amount of light ($\sim 22 \%$) got absorbed near the surface. The depth of photic zone also decreased (mean photic depth $\sim 50 \text{ m}$). Though the mean column N-uptake was very high ($\sim 19 \text{ mmolNm}^{-2}\text{d}^{-1}$) it was comparable to those reported by Owens et al., (1993) ($23.1 \text{ mmolNm}^{-2}\text{d}^{-1}$) from the central Arabian Sea during the late summer monsoon. McCarthy et al., (1999) has also reported N-uptake rates varying from $9.2 \text{ mmolNm}^{-2}\text{d}^{-1}$ to $40 \text{ mmolNm}^{-2}\text{d}^{-1}$ during winter monsoon for the central Arabian Sea. Watts and Owens (1999) reported N-uptake rates varying from $1.1 \text{ mmolNm}^{-2}\text{d}^{-1}$ to $23.6 \text{ mmolNm}^{-2}\text{d}^{-1}$ for the northwestern Arabian Sea during an intermonsoon period. A large variation in the N-uptake rate, ranging from $0.1 \text{ mmolNm}^{-2}\text{d}^{-1}$ to $13 \text{ mmolNm}^{-2}\text{d}^{-1}$ had also been reported by Sambrotto (2001) during the spring intermonsoon and the summer monsoon for the northern Arabian Sea.

3.4.2 New Production

For the present study, as mentioned in earlier chapter, nitrate uptake is considered as new production. Euphotic zone integrated nitrate uptake rate or new production during the late winter monsoon in the eastern Arabian Sea showed significant variation in new production; it varied from $0.63 \text{ mmolNm}^{-2}\text{d}^{-1}$ to $20.91 \text{ mmolNm}^{-2}\text{d}^{-1}$. It was low in the southern sector of the sampling area but was significantly higher in the northern sector. The mean new production in the southern sector or the non bloom area was $2.1 \text{ mmolNm}^{-2}\text{d}^{-1}$ whereas in the bloom area it was $15.7 \text{ mmolNm}^{-2}\text{d}^{-1}$, almost eight fold higher. Station-wise nitrate uptake rate is shown in figure (3.17). Lowest new production of $0.63 \text{ mmolNm}^{-2}\text{d}^{-1}$ ($\sim 50.4 \text{ mgCm}^{-2}\text{d}^{-1}$) was measured at PP2, located in the southern part. Nitrate uptake rate increased northward, from $0.63 \text{ mmolNm}^{-2}\text{d}^{-1}$ at a station in the southernmost part to $20.91 \text{ mmolNm}^{-2}\text{d}^{-1}$ at one of the northernmost station. This is due to the unavailability of nitrate in the surface layer of the southern stations. At these stations plankton depended on other sources for their nitrogen needs.

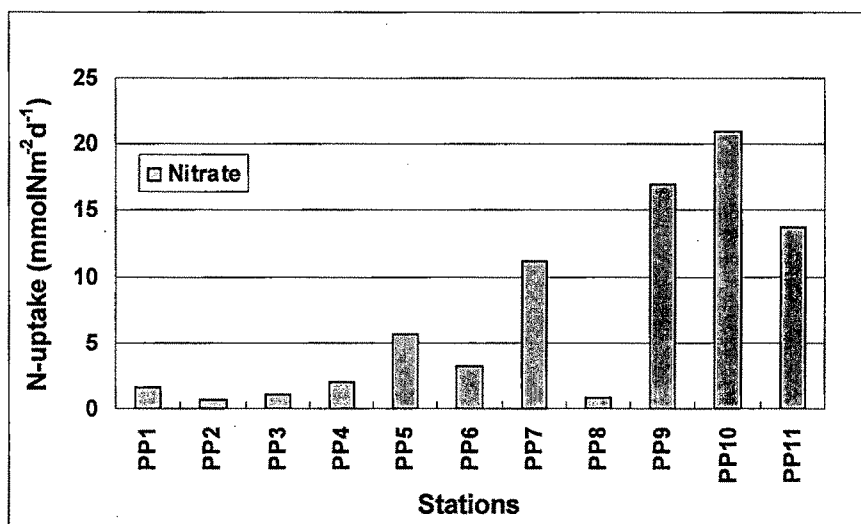


Fig 3.17 New production at different stations in the eastern Arabian Sea during the late winter monsoon.

At the northern stations where the winter cooling is more effective and bring ample nitrate in the surface layer due to convective mixing and thus the deepening of the mixed layer, nitrate uptake by the plankton increases. The average new production measured during the present study in the non-bloom area is less by ~ 1 $\text{mmolNm}^{-2}\text{d}^{-1}$ from the average value reported by McCarthy et al., (1999) for January-February ($3.21 \text{ mmolNm}^{-2}\text{d}^{-1}$) during the winter monsoon for the central Arabian Sea but is less than those for the month of October ($1.54 \text{ mmolNm}^{-2}\text{d}^{-1}$). Watts and Owens (1999) have reported mean nitrate uptake rates of $2.38 \text{ mmolNm}^{-2}\text{d}^{-1}$ for the northwestern Arabian Sea during an intermonsoon period. New production estimates reported by Watts and Owens (1999) are comparable with those of the present study.

The present study indicates the presence of two different biogeochemical provinces in the eastern Arabian Sea during the late winter monsoon: less productive southern and more productive northern regions. The southern sector was characterized by low column N-uptake and thus low new production. The column integrated total N-uptake rates, although low, increased progressively towards north. This increase may be the effect of more intense winter cooling towards the north. The northern part was a highly productive zone, with very high N-uptake and new

production. The process of convective mixing is also seen in the temperate and polar areas but increase in productivity or development of bloom has not been reported. In the northeastern Arabian Sea, the presence of ample light, coupled with nitrate input triggers the bloom. Nitrate based phytoplankton community during development of bloom (Bienfang et. al., 1990) and ammonium based community during later periods (Rees et. al. 2002) have been reported. The column integrated total production (x) and new production (y), show a significant correlation (Fig.3.18): for non-bloom stations: $y = (0.44 \pm 0.23)x - (0.30 \pm 1.38)$; (coefficient of determination, $r^2 = 0.43$) and for bloom stations, $y = (1.08 \pm 0.23)x - (4.68 \pm 4.46)$; ($r^2 = 0.91$).

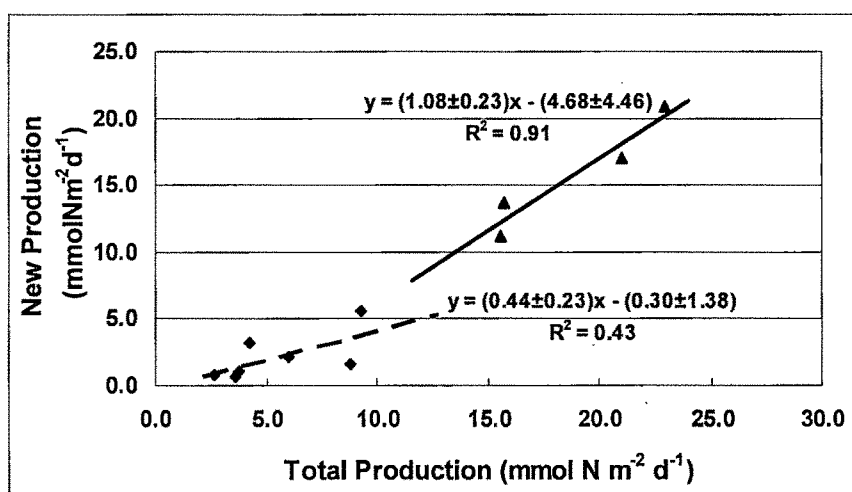


Fig 3.18 Relationship between total N uptake rate and nitrate uptake rate in the eastern Arabian Sea during the late winter monsoon.

The slope of regression (i.e., 0.44 and 1.0 for non-bloom and bloom stations respectively) is the maximum possible value of the f -ratio and can be used to estimate new production over a large area using ocean color remotely-sensed data. The present study suggests that though there is significant variation in the total N-uptake in the eastern Arabian Sea, the new production can be more than 90% of the total production, particularly in the northern part during *Noctiluca* bloom. Thus this area plays a significant role in the atmospheric carbon sequestration and hence in the global carbon cycle.

3.4.3 Regenerated Production

The sum of ammonium and urea uptake rates is considered as regenerated production for the present study. The ammonium uptake rates varied from a low of 0.36 $\text{mmolNm}^{-2}\text{d}^{-1}$ to a high of 3.28 $\text{mmolNm}^{-2}\text{d}^{-1}$, the highest was at the southern most station *i.e.*, PP1 (Fig 3.19). The ammonium uptake decreased northward to a low of 0.36 $\text{mmolNm}^{-2}\text{d}^{-1}$ at station PP6. At PP7 it again increased to 1.89 $\text{mmolNm}^{-2}\text{d}^{-1}$. This may be because of the increase in the depth of photic zone at this column; the photic zone depth of 130 m was the maximum at PP7.

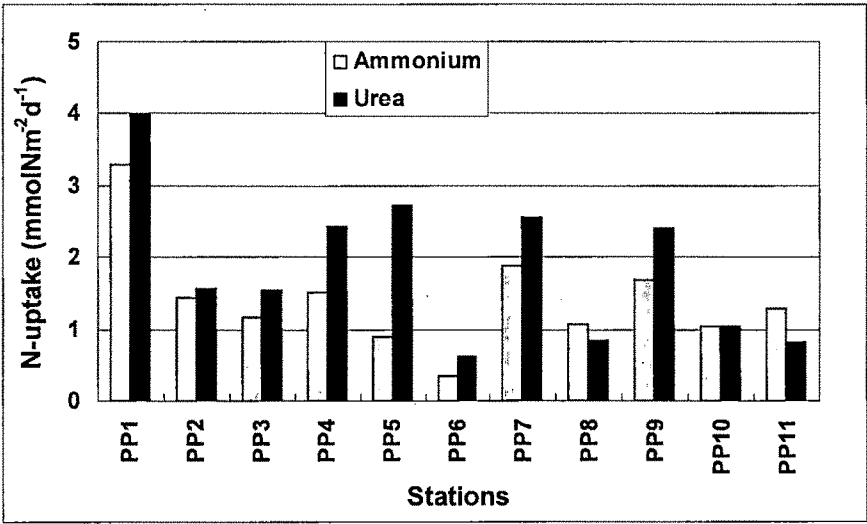


Fig 3.19 Ammonium and urea uptake rates at different stations in the eastern Arabian Sea during the late winter monsoon.

The ammonium uptake rates at bloom and non-bloom stations varied between 1.03 $\text{mmolNm}^{-2}\text{d}^{-1}$ to 1.89 $\text{mmolNm}^{-2}\text{d}^{-1}$ and 0.36 $\text{mmolNm}^{-2}\text{d}^{-1}$ to 3.28 $\text{mmolNm}^{-2}\text{d}^{-1}$ respectively. The mean ammonium uptake rates at the non-bloom and bloom stations were 1.39 $\text{mmolNm}^{-2}\text{d}^{-1}$ and 1.47 $\text{mmolNm}^{-2}\text{d}^{-1}$ respectively. Urea uptake rates were more than ammonium uptake rates at almost all the stations except at PP8, PP10 and PP11. At PP10 both ammonium and urea uptakes rates were almost equal and at PP8 and PP11 ammonium uptake rates were more than urea uptake rates. These three station lie in the *Noctiluca* bloom patch and thus they suggest that ammonium was preferred more than urea during the *Noctiluca* bloom. Urea uptake rates varied from 0.36 $\text{mmolNm}^{-2}\text{d}^{-1}$ to 3.99 $\text{mmolNm}^{-2}\text{d}^{-1}$ over the study area. At the

bloom and non-bloom stations it varied between 0.82 $\text{mmolNm}^{-2}\text{d}^{-1}$ to 2.55 $\text{mmolNm}^{-2}\text{d}^{-1}$ and 0.63 $\text{mmolNm}^{-2}\text{d}^{-1}$ to 3.99 $\text{mmolNm}^{-2}\text{d}^{-1}$ respectively. The mean urea uptake rates at bloom and non-bloom stations were 1.70 $\text{mmolNm}^{-2}\text{d}^{-1}$ and 1.96 $\text{mmolNm}^{-2}\text{d}^{-1}$ respectively.

3.4.4 *f*-ratios in the eastern Arabian Sea during Feb.-March 2004

The *f*-ratios also showed significant spatial variation in the eastern Arabian Sea during the late winter monsoon (Fig 3.20); it was low in the southern sector (0.17 at PP2) whereas was very high in the north (0.91 at PP10) where the *Noctiluca* bloom was present (Table 3.1). In the south (non-bloom area) the *f*-ratio was in general low; it varied from 0.18 to 0.34. Also, the *f*-ratio increased progressively towards the north, 0.18 at PP1 to 0.34 at PP4. Similar trend in *f*-ratio were also reported by Sanjeev Kumar et al. (2008) for the eastern Arabian Sea during Feb.-March 2003. At the incomplete station *i.e.*, PP5 and PP6 the *f*-ratio was 0.61 and 0.77 respectively. Since at PP5 samples were collected from only three depths, the *f*-ratio could have been somewhat overestimated. At PP6, being a shallow station (<20 m) because of the presence of a sub-surface bank, only 4 depths could be sampled. The *f*-ratio is also high here, 0.77, suggesting presence of nitrate based phytoplankton community.

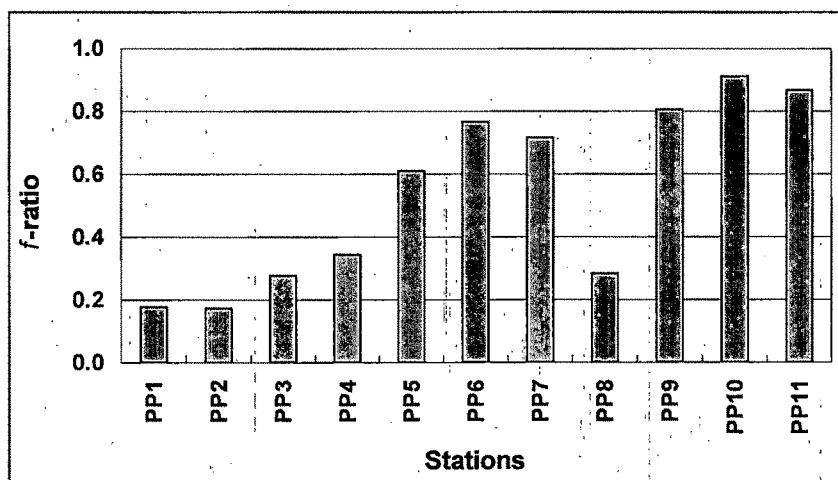


Fig. 3.20 *f*-ratios at different stations in the Eastern Arabian Sea during the late winter monsoon.

Stations	New Production	Regenerated Production		Total*	<i>f</i> -ratio
	ρNO_3^*	ρNH_4^*	ρNH_2^*	Production	
PP 1	1.56	3.28	3.99	8.8	0.18
PP 2	0.63	1.43	1.56	3.6	0.17
PP 3	1.04	1.16	1.55	3.7	0.28
PP 4	2.06	1.52	2.43	6.0	0.34
PP 5	5.64	0.89	2.73	9.3	0.61
PP 6	3.25	0.36	0.63	4.2	0.77
PP 7	11.19	1.89	2.55	15.6	0.72
PP 8	0.75	1.07	0.85	2.7	0.28
PP 9	16.97	1.67	2.40	21.0	0.81
PP 10	20.91	1.03	1.04	23.0	0.91
PP 11	13.66	1.27	0.82	15.8	0.87

* all uptake rates are in $\text{mmolNm}^{-2}\text{d}^{-1}$

Table 3.1 ^{15}N based productivity and *f*-ratios during Feb.-March 2004 (late winter monsoon) in the eastern Arabian Sea

3.5 Chlorophyll-*a*, nutrients and physical parameters during December-2004 in the northwestern Arabian Sea

3.5.1 Chlorophyll-*a*

Chlorophyll concentrations were measured at all the 11 stations during the early winter monsoon cruise as well. As almost all the stations were in the northern Arabian Sea, zonation in south-north transect could not be seen. Chlorophyll concentration was, in general, low at all the stations. The mean surface chlorophyll concentration over the study area during the present season was 0.33 mgChlm^{-3} but varied significantly over the study area; it varied from a low of 0.19 mgChlm^{-3} to 0.51 mgChlm^{-3} , the maximum was at PP3 and the minimum was at PP8. The mean column integrated Chl-*a* was $22.42 \text{ mgChlm}^{-2}$. It varied from $18.38 \text{ mgChlm}^{-2}$ to $27.26 \text{ mgChlm}^{-2}$, the maximum was at PP10 and the minimum was at PP5. Station-wise integrated chlorophyll values and chlorophyll-depth profiles are shown in Fig 3.21 and Fig 3.22.

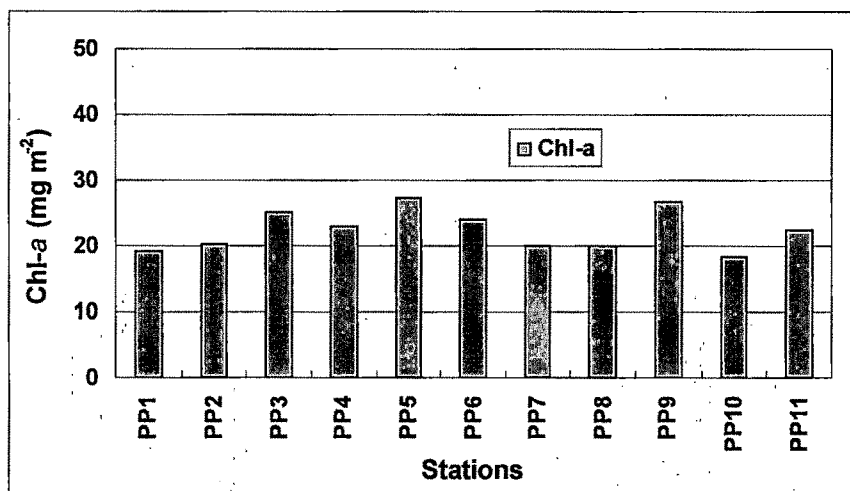
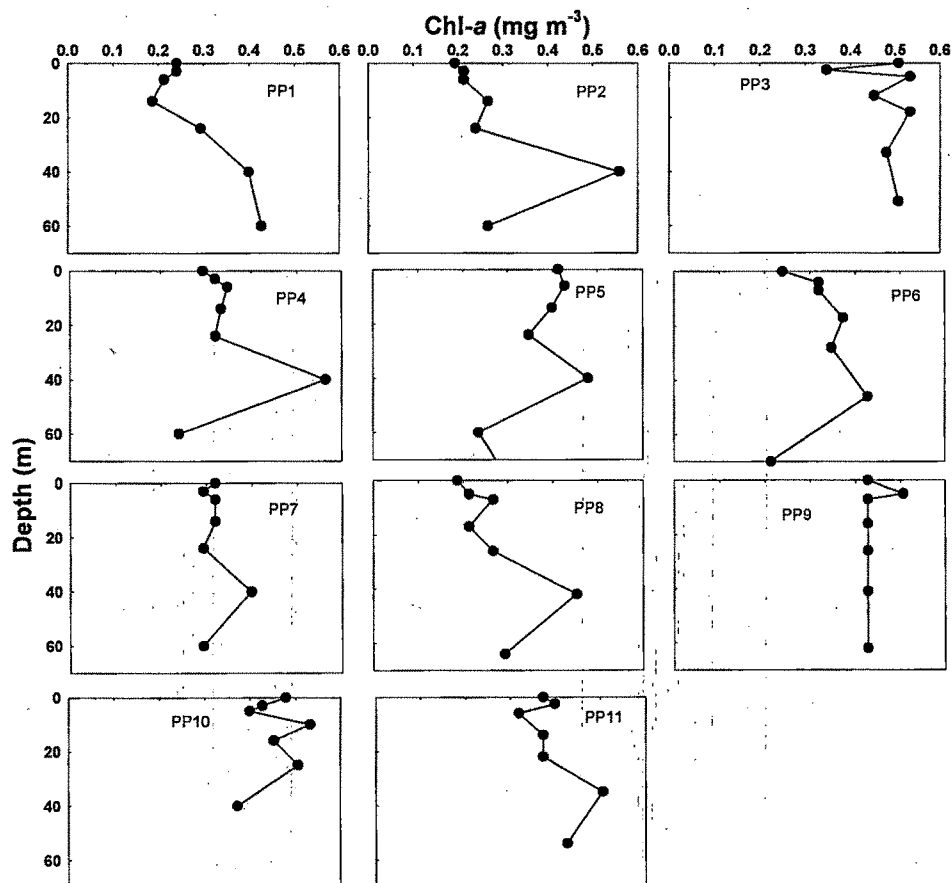


Fig 3.21 Station-wise column integrated chlorophyll concentration during Dec-2004

During the early winter monsoon most of the stations had irregular chlorophyll-depth profiles with more than one deep chlorophyll maximum (DCM), one immediately below the surface and other at a depth of 40-50 m; the deeper peak being more prominent than the upper ones. At PP1, the chlorophyll concentration decreased at 14 m depth as compared to the surface but again increased gradually to reach a maximum of 0.42 mgChlm^{-3} at a depth of 60 m. PP2, PP4, PP8 and PP11 had similar profiles with prominent DCM at around 40m. PP3 has very irregular profiles as compared to the other stations; chlorophyll varied between 0.3 to 0.5 mgChlm^{-3} in the upper layer. PP5 and PP7 had two chlorophyll peaks, one at 6 m and another at 40 m but the peak at 40 m was more prominent than that at 6 m depth. Chlorophyll decreased below 40 m. At PP6 chlorophyll increased downwards to reach a maximum of 0.42 mgChlm^{-3} at a depth of 46 m which again decreased with increasing depth. At PP9 chlorophyll was the same throughout the column except one undulation in the upper 7 m; chlorophyll value increased to 0.51 mgChlm^{-3} at a depth of 5 m but again decreased to 0.43 mgChlm^{-3} at 7m and remained almost the same in the column. At PP10 chlorophyll varied between 0.39 mgChlm^{-3} to 0.53 mgChlm^{-3} in the upper water column. Though the chlorophyll-depth profiles at different stations showed some undulations at most of the stations, the variation was very small and varied between 0.1 - 0.2 mgChlm^{-3} .



3.22 Vertical profiles of Chl-*a* at different stations in the eastern Arabian Sea during the early winter monsoon (Dec - 2004)

3.5.2 Nutrients

Samples were collected from different depths for ambient nitrate measurement. The vertical profiles of nitrate at different stations are shown in Fig. 3.23. PP1 and PP3 have almost similar vertical profiles; nitrate concentration was very low ($<0.2 \mu\text{M}$) throughout the column. At PP2 and PP4 the ambient nitrate concentration was below $0.5 \mu\text{M}$ at the surface but increased to $6.2 \mu\text{M}$ at a depth of 60 m at PP2 and to $6.3 \mu\text{M}$ at 40 m which further increased to $8.4 \mu\text{M}$ at 80 m at station PP4. PP5 had no nitrate (nitrate concentration below detection limit i.e., $0.01 \mu\text{M}$) in the column. PP6, PP7 and PP8 had similar profiles with very less nitrate

concentration in the upper 40m but increased suddenly to 5.4 μM and 2.6 μM at depths of 70 m and 60 m depths at PP6 and PP7 respectively and to 1.5 μM at a depth of 64 m at PP8. Unlike other stations PP9 and PP10 had nitrate present in the water column but the concentration was not high, it varied from 0.24 μM to 0.56 μM at PP9 and from 0.31 μM to 0.75 μM at PP10. Surface water was again devoid of nitrate at PP11; it was below detection limit upto a depth of 35 m but increased thereafter to 0.46 μM at 54 m.

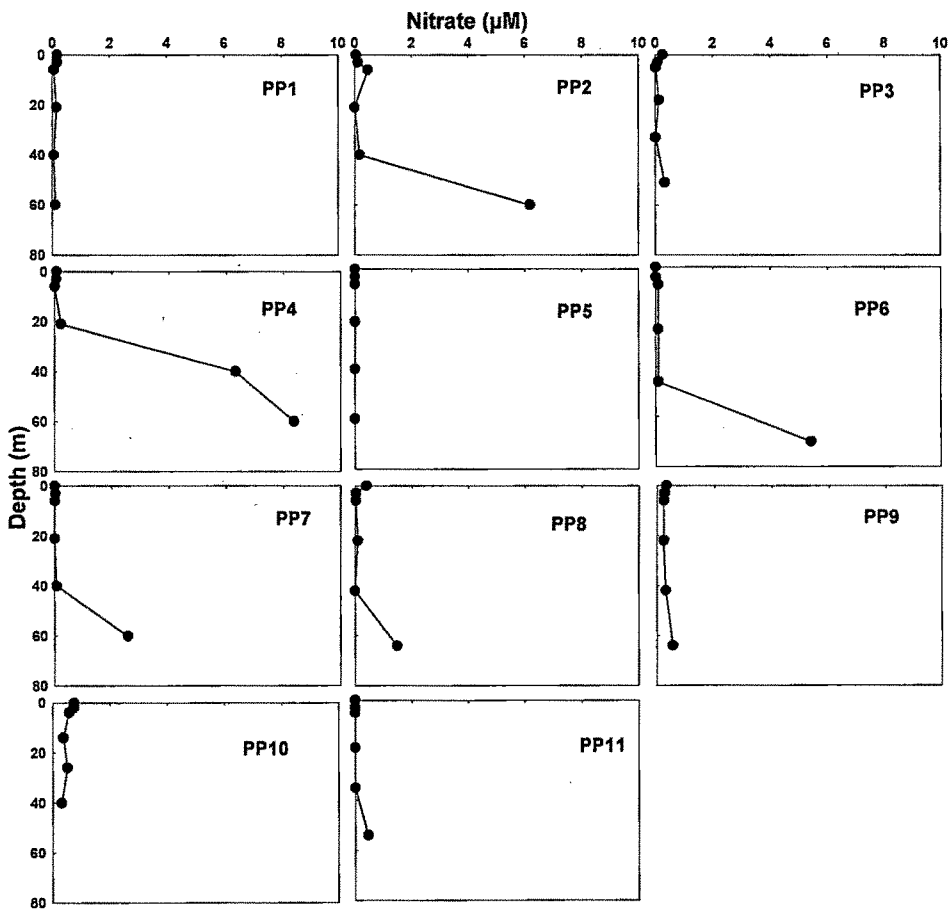


Fig 3.23 Vertical profiles of nitrate at different stations during December-2004

Integrated nitrate concentration during this period varied from a low of 4.4 mmol m^{-2} to a high of 210.7 mmol m^{-2} . The highest nitrate was at PP4 because of

high nitrate concentration in the deeper waters ($>6 \mu\text{M}$). If PP4 is excluded then integrated nitrate varied from $4.4 \mu\text{M}$ to $70.1 \mu\text{M}$ which is significantly less than the integrated nitrate concentration ($\sim 100 \text{ mmol m}^{-2}$) reported by Sanjeev Kumar et al., (2008) for January 2003.

3.5.3 Hydrographic conditions

The eastern Arabian Sea was again studied during the month of December. This period of the year is characterized by the reversal of wind, from Himalaya to the ocean, and onset of winter monsoon. During this period also SST decreases on from south to north but the magnitude of the decrease is less as compared to that in the months of Feb.-March. SST decreased from 28.6°C to 26.3°C at an interval of 7° latitude, between 14°N to 21°N , during the present study (Fig 3.24). The maximum SST of 28.6°C was recorded at the southernmost station PP1 and a minimum of 26.3°C was recorded at a northernmost station PP9. The rate of SST decrease per latitude was $\sim 0.3^\circ\text{C}$ which is significantly less, almost half, than those during Feb.-March 2004.

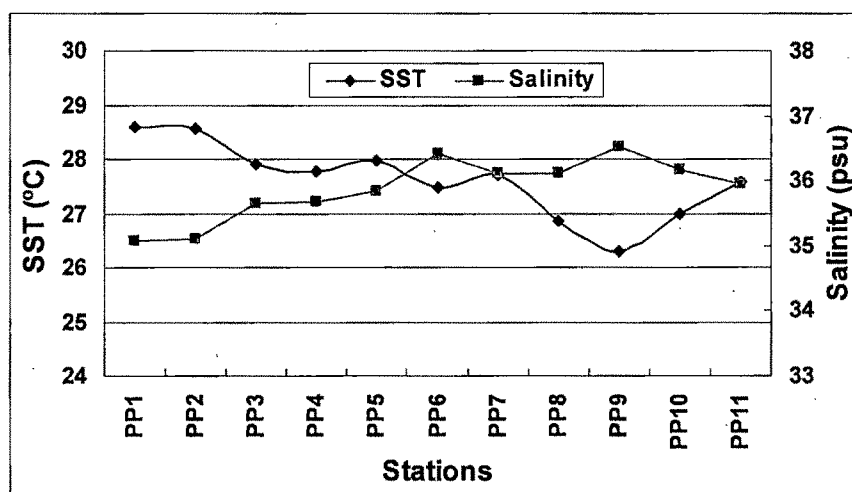


Fig 3.24 SST and salinity at different stations in the eastern Arabian Sea during early winter monsoon (Dec-2004)

Similar to the late winter monsoon, during the month of December also the decrease in SST was associated with an increase in salinity of the surface waters.

Salinity increased from 35.08 in the south at PP1 to 36.52 in the north at PP9. Though increase in salinity and decrease in SST was observed during present study also, its magnitude was less as compared to that observed during the late winter monsoon (Feb.-March 2004). Salinity increased by 2.8 during the late winter monsoon whereas during the early winter it increased by only 1.4. SST decreased by 2.32°C during the present study whereas the same had decreased by 3.6°C during the late winter monsoon. This suggests that the winter cooling effect was not much pronounced during the present study (December 2004) as it was during the late winter monsoon (Feb.-March 2004). Even though winter cooling was not much intense during the present study, the temperature based mixed layer depth was more than those during the late winter monsoon (Fig 3.25).

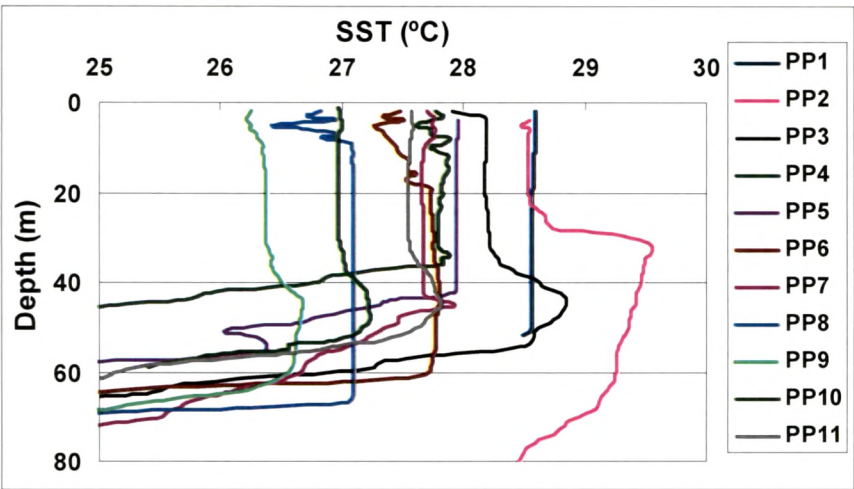


Fig 3.25 Temperature-depth profiles at different stations obtained using CTD data during December 2004

The mean MLD during the present study was found to be ~40 m; the maximum MLD (66 m) was observed PP8 (21.3°N) and a minimum (24 m) was observed at PP2 16°N. A clear trend in MLD from south to north could not be observed. At PP1 the mixed layer depth was almost 50 m which decreased to 24 m at a latitudinal interval of 1.5°. From PP2 northwards upto PP6 i.e., from 16°N to 19°N a general increase in MLD could be seen. MLD increased from 24 m at PP2 to 55 m at PP6.

PP7 and PP8 had mixed layer depths of 43 and 66 m respectively. PP9, 10 and 11 had almost the same mixed layer depth of 31 m. The presence of deep mixed layer during December may be due to the effect of winter cooling which starts in December and continues till the end of February (Madhupratap et al., 1996).

3.6 ¹⁵N based Productivity study during the early winter monsoon (December 2004)

3.6.1 Total production

Total productivity for the present study has been calculated as a sum of nitrate uptake rates and conservative estimates of ammonium and urea uptake rates. The rates of nitrogen uptake, integrated over the photic zone, varied from 4.07 mmolNm⁻²d⁻¹ to 23.31 mmolNm⁻²d⁻¹ (Fig 3.26). Unlike the late winter monsoon when higher uptake rates were measured at stations in the southern part of the eastern Arabian Sea, during the early winter monsoon no such pattern was seen in the N-uptake rates at different stations in the same region (these PP stations are not the same stations described earlier). At PP1 total N-uptake rate was 10.51 mmolNm⁻²d⁻¹ which increased anomalously to 23.31 mmolNm⁻²d⁻¹ at PP2, 1°N of PP1.

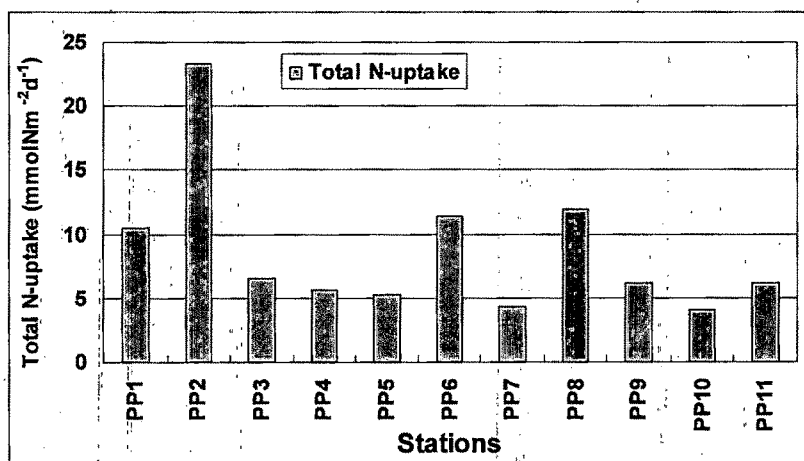


Fig. 3.26 Total N-uptake rate (new production) at different stations in the eastern Arabian Sea during December 2004.

N-uptake rate again decreased to $6.51 \text{ mmolNm}^{-2}\text{d}^{-1}$ at PP3. This station had also been sampled during the late winter monsoon (PP7 of SS222); column N-uptake was more than twice ($15.6 \text{ mmolNm}^{-2}\text{d}^{-1}$) that of the early winter monsoon. PP4 and PP5 had almost the same column N-uptake rates, $5.68 \text{ mmolNm}^{-2}\text{d}^{-1}$ and $5.21 \text{ mmolNm}^{-2}\text{d}^{-1}$ respectively. PP6 and PP8 had higher N-uptake rates, $11.40 \text{ mmolNm}^{-2}\text{d}^{-1}$ and $11.95 \text{ mmolNm}^{-2}\text{d}^{-1}$ respectively, compared to other stations sampled during the present study. The sudden increase in the nitrogen uptake was mainly due to an increase in the nitrate uptake rates. PP9 to PP11 had column N-uptake rates varying between $4.07 \text{ mmolNm}^{-2}\text{d}^{-1}$ to $6.15 \text{ mmolNm}^{-2}\text{d}^{-1}$. The mean N-uptake rate during the present study was $8.65 \pm 5.61 \text{ mmolNm}^{-2}\text{d}^{-1}$. It was significantly lower, almost one-fourth, than the mean N-uptake rate reported for the month of Jan.-Feb. and similar to the N-uptake rates during the month of October by McCarthy et al., (1999) from the central Arabian Sea. Though the column N-uptake rate measured during the present study is on the higher side, a similar variation had also been reported by Watts and Owens (1999) for the northwestern Arabian Sea during an intermonsoon period. The uptake rates reported by Watts and Owens (1999) varied between $1.1 \text{ mmolNm}^{-2}\text{d}^{-1}$ to $23.6 \text{ mmolNm}^{-2}\text{d}^{-1}$. Sambrotto (2001) has also reported N-uptake rates varying from $0.1 \text{ mmolNm}^{-2}\text{d}^{-1}$ to $13 \text{ mmolNm}^{-2}\text{d}^{-1}$ for the spring intermonsoon and summer monsoon from the northern Arabian Sea.

3.6.2 New Production

Photic zone integrated nitrate uptake rate or new production during early winter monsoon 2004 varied from $1.95 \text{ mmolNm}^{-2}\text{d}^{-1}$ to $19.70 \text{ mmolNm}^{-2}\text{d}^{-1}$ (Fig 3.27) over the study area. New production was more at stations PP2, PP6 and PP7; nitrate uptake rates at these stations were 19.7 , 9.02 and $8.69 \text{ mmolNm}^{-2}\text{d}^{-1}$ respectively. Excluding these three stations, the nitrate uptake varied from $1.95 \text{ mmolNm}^{-2}\text{d}^{-1}$ to $5.70 \text{ mmolNm}^{-2}\text{d}^{-1}$ at rest of the stations. At stations PP9, 10 and 11 also had moderately high new production; nitrate uptake rates at these stations were 4.70 , 3.52 and $4.91 \text{ mmolNm}^{-2}\text{d}^{-1}$ respectively. Like total production, any significant spatial pattern in new production also could not be observed as was the case during the late winter monsoon 2004. The mean column new production over the study area

was $6.12 \text{ mmolNm}^{-2}\text{d}^{-1}$, which reduced to $3.74 \text{ mmolNm}^{-2}\text{d}^{-1}$ when three highly productive stations were excluded. The mean nitrate uptake rate was twice of the mean nitrate uptake ($3.24 \text{ mmolNm}^{-2}\text{d}^{-1}$) reported by McCarthy et al., (1999) for the month of Jan-Feb and four-times of that in the month of October ($1.54 \text{ mmolNm}^{-2}\text{d}^{-1}$).

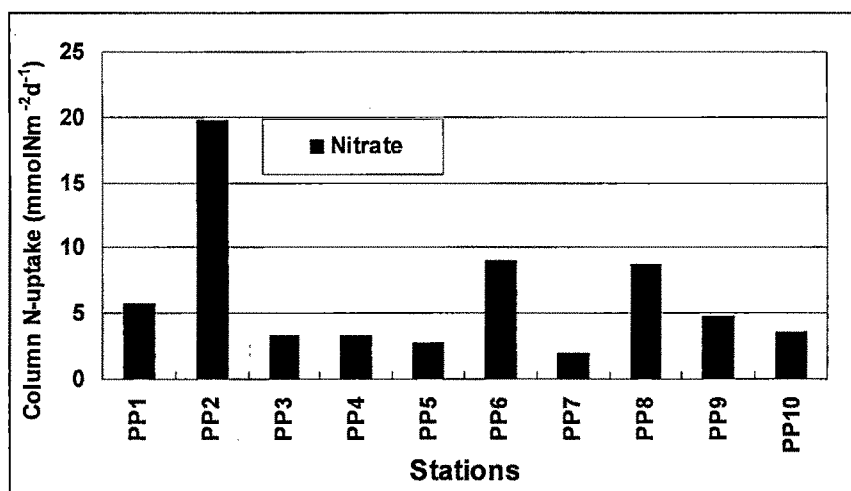


Fig. 3.27 Nitrate uptake rate (new production) at different stations in the eastern Arabian Sea during December 2004.

The nitrate uptake rate measured during the present study is almost half of the rate reported by Sanjeev Kumar et al., (2008) for the months of Feb.-March 2003 ($12.7 \text{ mmolNm}^{-2}\text{d}^{-1}$) but is almost thrice of that reported for the month of January 2003 ($2.3 \text{ mmolNm}^{-2}\text{d}^{-1}$). In comparison to the rates of nitrate uptake measured during the late winter monsoon, new production during December is thrice that of a non-bloom ($2.1 \text{ mmolNm}^{-2}\text{d}^{-1}$) region but is less than half of that ($15.7 \text{ mmolNm}^{-2}\text{d}^{-1}$) in the bloom area. Station PP7 and PP8 of SS-222 (late winter monsoon) were repeated during the present study as PP3 and PP6. Nitrate uptake increased almost five-fold, from $3.25 \text{ mmolNm}^{-2}\text{d}^{-1}$ during early winter to $15.6 \text{ mmolNm}^{-2}\text{d}^{-1}$ during the late winter monsoon in the presence of the *Noctiluca* bloom at station PP3 of the present study. At PP6 nitrate uptake decreased from $9.02 \text{ mmolNm}^{-2}\text{d}^{-1}$ to $2.7 \text{ mmolNm}^{-2}\text{d}^{-1}$, again from the early winter monsoon to the late winter monsoon. These clearly suggests that the productivity pattern has significant heterogeneity over

space and time in the eastern Arabian Sea but still this part of the world ocean has a potential of high new productivity. The strong correlation ($r^2 = 0.96$) between the column integrated nitrate uptake and total N-uptake (Fig 3.28) also supports this argument. The slope of the regression (0.88) gives the fraction of the total production that can be exported out of the photic zone. High slope suggests higher ability of this part of the ocean to produce which can be exported to the deep. High slope (>0.9) was also evident in this part during the late winter monsoon during the bloom, though it was low (0.44) during the same season in the southern part where the winter cooling was not that effective.

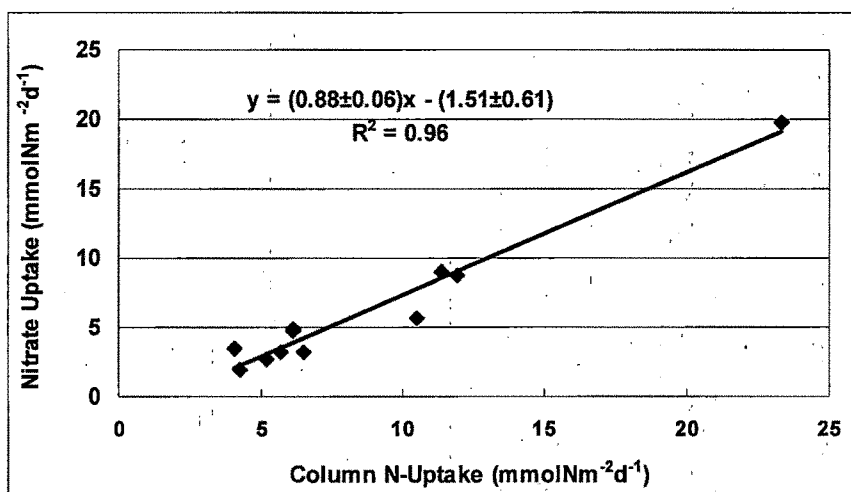


Fig 3.28 Relationship between total N-uptake during the early winter monsoon (December) in the eastern Arabian Sea.

3.6.3 Regenerated production

Ambient ammonium and urea concentration could not be measured during the present study and hence a conservative estimate of their uptake rates was made. Ammonium uptake rate varied from $0.47 \text{ mmolNm}^{-2}\text{d}^{-1}$ to $2.79 \text{ mmolNm}^{-2}\text{d}^{-1}$ (Fig 3.29) and urea uptake rates varied from $0.08 \text{ mmolNm}^{-2}\text{d}^{-1}$ to $2.02 \text{ mmolNm}^{-2}\text{d}^{-1}$. The mean ammonium and urea uptake rates were $1.81 \text{ mmolNm}^{-2}\text{d}^{-1}$ and $0.79 \text{ mmolNm}^{-2}\text{d}^{-1}$ respectively. The mean ammonium uptake rate during December was more than that during the Feb.-March but urea uptake was almost half. An interesting

observation is that while urea uptake was more than ammonium at most stations during the late winter monsoon, during the present study ammonium uptake was more than urea uptake rate at all the stations. Also, urea uptake decreased from south to north while no such trend could be seen in the ammonium uptake. During the late winter monsoon also no such trend was observed.

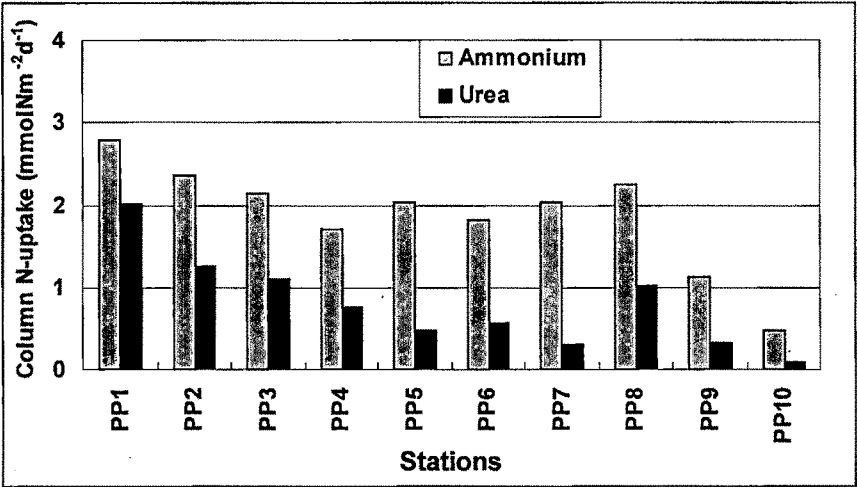


Fig 3.29 Ammonium and urea uptake rates at different stations in the Eastern Arabian Sea during early winter monsoon.

3.6.4 *f*-ratio during December-2004

The *f*-ratio was calculated as a ratio of nitrate uptake to total N-uptake (a sum of nitrate, ammonium and urea uptakes). As the ammonium and urea uptake rates are conservative estimates, here a ratio of new to total production represents the upper bound of the *f*-ratio. Figure 3.30 shows the station-wise *f*-ratio measured during this study. Estimated *f*-ratio during early winter monsoon varied from a minimum of 0.46 at PP7 to a maximum of 0.87 at PP10 (Table 3.2). This suggests that at most 46 to 87% of the total production can be exported to the deep under steady state. The mean *f*-ratio during the present study was estimated to be 0.67; significantly higher than the average *f*-ratio estimated in the non-bloom region (0.38) during the late winter monsoon and slightly less than the same in the *Noctiluca* bloom (0.82) region. The *f*-ratio estimated here is so far the highest observed in this region for the early winter monsoon period. Sanjeev Kumar et al., (2008) have reported *f*-ratio varying from

0.11 to 0.53 (mean = 0.24) for January-2003 and from 0.45 to 0.61 (mean = 0.46) for Feb-March 2003 from the eastern Arabian Sea.

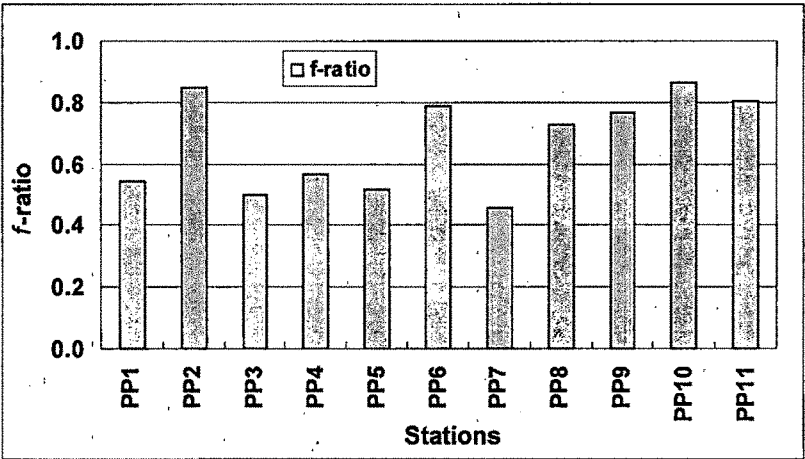


Fig 3.30 *f*-ratio at different stations in the eastern Arabian Sea during the early winter monsoon.

Stations	New	Regenerated		Total*	f-ratio
	Production	Production		Production	
	ρNO ₃ *	ρNH ₄ *	ρNH ₂ *		
PP 1	5.70	2.79	2.02	10.51	0.54
PP 2	19.70	2.36	1.25	23.31	0.85
PP 3	3.25	2.14	1.11	6.51	0.50
PP 4	3.21	1.70	0.76	5.68	0.57
PP 5	2.68	2.04	0.49	5.21	0.51
PP 6	9.02	1.82	0.57	11.40	0.79
PP 7	1.95	2.03	0.29	4.27	0.46
PP 8	8.69	2.25	1.01	11.95	0.73
PP 9	4.70	1.13	0.32	6.15	0.76
PP 10	3.52	0.47	0.08	4.07	0.87
PP 11	4.91	1.18	ND	6.09	0.81

* all uptake rates are in mmolNm⁻²d⁻¹

Table 3.2 ¹⁵N based productivity and *f*-ratios during December 2004 (early winter monsoon) in the eastern Arabian Sea

3.7 Effect of winter cooling on the f -ratio

Madhupratap et al., (1996) suggested that northeast trade wind, which is dry and has low temperature, causes increase in evaporation over precipitation in the northern Arabian Sea. Increase in evaporation leads to cooling of the surface layer which makes the surface water denser. Increase in evaporation over precipitation also causes densification of the surface water which sinks resulting in convective mixing. This causes deepening of the mixed layer and consequent transport of nutrient rich deeper water to the surface. During the present study also decrease in sea surface temperature (SST) and an increase in the salinity is observed on a south-north transect. SST decreased from 28.8°C in the south to 25.2°C in the north during Feb-March 2004 and from 28.6 to 26.3 during Dec-2004 (Table 3.3). Salinity increased from 33.8 in the south to 36.1 in the north and from 35.1 to 36.2 during Feb-March and Dec-2004 respectively. This significant change in SST and salinity is due to the winter cooling effect. The phenomenon of winter cooling was more intense in the Feb-March than Dec and the same was more intense in the north as compared to the South; SST decreased from 28.2°C at PP6 to 25.2°C at PP10. It decreased by more than 3°C over 4.5° latitudinal difference. Salinity also showed a sudden increase from 34.8 at PP6 to 36.6 at PP10 during the late winter.

a).

Stations	SST (°C)	Salinity
PP 1	28.8	33.8
PP 2	28.9	33.9
PP 3	28.2	35.0
PP 4	28.1	34.6
PP 5	28.6	34.7
PP 6	28.2	34.8
PP 7	27.3	35.2
PP 8	26.8	35.2
PP 9	25.2	36.4
PP 10	25.2	36.6
PP 11	25.9	36.1

b).

Stations	SST (°C)	Salinity
PP' 1	28.6	35.1
PP' 2	28.5	35.1
PP' 3	27.9	35.6
PP' 4	27.8	35.7
PP' 5	27.9	35.8
PP' 6	27.5	36.4
PP' 7	27.7	36.1
PP' 8	26.8	36.1
PP' 9	26.3	36.5
PP' 10	26.9	36.2
PP' 11	27.6	35.9

Table 3.3 Sea Surface Temperature (SST) and salinity a) during Feb.-March 2004 (late winter monsoon) b) during Dec-2004 (early winter monsoon) in the eastern Arabian Sea. PP1 to PP 11 represent stations during the late winter monsoon and PP'1 to PP'11 represent station during the early winter monsoon. PP is different from PP'.

The rate of decrease in the SST was more than 0.6°C per degree during Feb-March. Madhupratap et al., (1996) has reported SST decrease at a rate of 0.5°C per degree latitude during winter in this region. This higher rate of decrease in SST per degree latitude suggests more intense winter cooling effect in this region in 2004. Intense cooling effect resulted in transport of nutrients from the deeper layer to the surface and consequently this triggered a bloom, dominated by *Noctiluca scintillans*, in the north. The increase in nitrate uptake, total N-uptake and *f*-ratio over a south-north transect also suggests the influence of more intense winter cooling. The *f*-ratio in the north, *Noctiluca* dominated area, was significantly high; the mean *f*-ratio was 0.86. The *f*-ratio during the present study is significantly higher than those reported by Sanjeev Kumar et al., (2008). They reported an increase from a low of 0.11 in the south to a high of 0.27 in the north. McCarthy et al., (1999) has also reported *f*-ratio varying from 0.03 to 0.31 during winter monsoon for the central Arabian Sea. Bienfang et al., 1990 has suggested nitrate based phytoplankton community during the initial phase of the bloom. High *f*-ratio measured during this study, in accordance with Bienfang et al., 1990, suggests the developing phase of the bloom where nitrate uptake dominates the total nitrogen uptake. Nitrate required by phytoplankton is brought to the photic zone, from the deeper layer, through the convective mixing caused by cool dry air from the Himalaya.

3.8 Export flux in the Arabian Sea during the winter monsoon

Export production in the Arabian Sea also oscillates with the changing atmospheric forcing; export of carbon out of the euphotic zone is usually less than 10% of the primary production during the non-bloom season (Buesseler et al., 1998) but exception to this it increases to more than 75% of the total primary production during the bloom (Ramaswamy et al, 2005). The present study shows that during the late winter monsoon in the southern part of the eastern Arabian Sea the export production is 38% of the total production. The mean export production in this region was 168 mgCm⁻²d⁻¹ which increased to 1256 mgCm⁻²d⁻¹, more than 82% of the total primary production, during the *Noctiluca Scintillans* bloom in the northern part of the eastern Arabian Sea. Average POC (Particulate Organic Carbon) flux of 332

mgCm⁻²d⁻¹, representing 36% of the primary production, has been reported by Ramaswamy et al., (2005) from the eastern Arabian Sea during northeast monsoon (February-2007) using ²³⁴Th deficit technique. The amount of carbon export reported by Ramaswamy et al., (2005) is twice of the export estimated using ¹⁵N during the present study but the fraction of total primary production getting exported is the same. This difference may be due to the difference in the primary production; Ramaswamy et al., (2005) have reported column daily primary production of ~900 mgCm⁻²d⁻¹ whereas the mean column production during the present study was ~450 mgCm⁻²d⁻¹. Though the present data is in good agreement with those reported by Ramaswamy et al., (2005), discrepancy in the ²³⁴Th and sediment trap data has been reported by Sarin et al., 1996 where he found that ²³⁴Th derived export flux is higher than those measured using the sediment trap; export flux measured using ²³⁴Th was 290 and 251 mgCm⁻²d⁻¹ during Feb-March 1994 and 1995 whereas the same measured using the sediment trap was 371 and 986 mgCm⁻²d⁻¹ for the top 100 m. During the early winter monsoon (Dec-2004) the mean export production was ~490 mgCm⁻²d⁻¹ which is 67% of the total production. ²¹⁰Pb scavenging technique also does not give accurate estimation of C_{org} flux (Borole 2002).

3.9 Conclusions

The results from the new productivity measurements during the late winter monsoon are:

1. The Arabian Sea was characterized by the presence of two different biogeochemical provinces during the late winter monsoon: low productive southern province and highly productive northern province with an overall increasing trend from the south to the north.
2. Total productivity in the southern region averaged around 5.5 mmolNm⁻²d⁻¹ (440 mgCm⁻²d⁻¹) whereas in the north it was 19 mmolNm⁻²d⁻¹ (1520 mgCm⁻²d⁻¹); increase in productivity from the south to north was more than three fold.

3. New productivity also increased on south-north transect, from $2.1 \text{ mmolNm}^{-2}\text{d}^{-1}$ ($168 \text{ mgCm}^{-2}\text{d}^{-1}$) in the south to $15.7 \text{ mmolNm}^{-2}\text{d}^{-1}$ ($1256 \text{ mgCm}^{-2}\text{d}^{-1}$) in the north. Increase in new productivity was more than 7-fold.
4. High nitrate uptake during the *Noctiluca* bloom at the northern stations measured during the present study, in accordance with Bienfang et al., (1990), suggests the developing phase of the bloom where nitrate contributed most to the total N-uptake.
5. Urea uptake rate was higher than the ammonium uptake rate at all the non-bloom stations but during the *Noctiluca* bloom in the northern stations, ammonium was preferred to urea by the plankton.
6. The column integrated total production (x) and new production (y), show a significant correlation (Fig.2): for non-bloom stations: $y = (0.44 \pm 0.23) x - (0.30 \pm 1.38)$; (coefficient of determination, $r^2 = 0.43$) and for bloom stations, $y = (1.08 \pm 0.23) x - (4.68 \pm 4.46)$; ($r^2 = 0.91$). The slopes of regression (i.e., 0.44 and 1.0 for non-bloom and bloom stations respectively) are the maximum possible values of the *f*-ratio, in the respective seasons.

The results from productivity measurements during early winter monsoon are:

1. During the early winter monsoon total productivity varied from $4.07 \text{ mmolNm}^{-2}\text{d}^{-1}$ ($326 \text{ mgCm}^{-2}\text{d}^{-1}$) to $23.31 \text{ mmolNm}^{-2}\text{d}^{-1}$ ($1865 \text{ mgCm}^{-2}\text{d}^{-1}$) with a mean of $8.65 \text{ mmolNm}^{-2}\text{d}^{-1}$ ($692 \text{ mgCm}^{-2}\text{d}^{-1}$). Productivity during this season was almost half of that during the bloom but was more than the productivity in the south during the late winter monsoon.
2. New productivity showed a large variation; it varied from a low of $1.95 \text{ mmolNm}^{-2}\text{d}^{-1}$ ($156 \text{ mgCm}^{-2}\text{d}^{-1}$) to a high of $19.70 \text{ mmolNm}^{-2}\text{d}^{-1}$ ($1576 \text{ mgCm}^{-2}\text{d}^{-1}$).
3. Ammonium uptake was more than urea uptake at all the stations unlike those during the late winter monsoon. Also the mean ammonium uptake rate was more than that during the late winter but urea uptake was almost half.
4. The *f*-ratio varied from 0.46 to 0.87. This suggests that 46-87% of the total productivity can be exported to the deep under a steady state condition.

Relation between total and new productivity yielded a slope of 0.88 which suggests that at most 88% of the total productivity can be exported.

These results indicate almost three fold increase in the total productivity during the developing phase of the *Noctiluca* bloom. This increase was more than seven fold in new productivity. During early winter monsoon total and new productivity was less than those during the bloom but was more compared to non-bloom, southern, regions. Above results from the two seasons suggests that productivity in the Arabian Sea is heterogeneous in space and time but still this basin is capable of high export production during blooms and thus plays a significant role in global carbon cycle.

Chapter Four

The Equatorial and Southern Indian Ocean

4.1 Introduction

The equatorial region of the Indian Ocean is distinctly different from the other two major oceans in the sense that it lacks equatorial upwelling unlike the Pacific and Atlantic. This is because the driving wind field is different in the Indian Ocean: in the Pacific and Atlantic oceans the southeast trades do not cross the equator and hence causes an equatorial divergence whereas in the Indian Ocean the annual-mean wind on the equator is eastwards causing convergence on the equator. The near-equatorial winds in the Indian Ocean are weak throughout the year and change directions four times a year (Fig. 4.1). Consequently the associated surface currents also change direction four times a year; it flows westward during the winter, weakly westward during the summer and strongly eastward during the spring and fall inter-monsoons. In the north, along Somalia and Oman coasts and also along the western Indian coast upwelling takes place only during the summer monsoon.

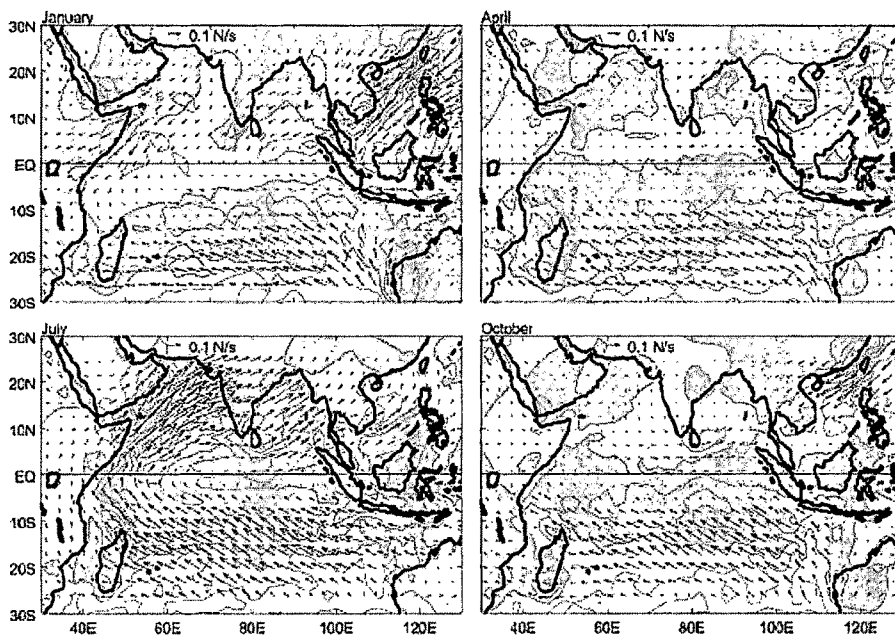


Fig. 4.1 Figure showing wind stress field for the Indian Ocean during January, April, July and October (Source: Miyama et al., 2003). The contour interval for wind curl is 10^7 Nm^{-3} , and negative values are shaded. After Hellerman and Rosenstein (1983).

The upwelled water can come from depths of 200–300 m, occasionally with temperatures colder than 15°C and densities in excess of 26.5 kgm⁻³ (Schott and McCreary, 2001). These temperatures and densities correspond to those in southern mid-latitudes near 40°S. Waters upwelled off Somalia, having low salinities, also clearly suggest southern-hemispheric origin (Fischer et al., 1996). All these suggest that the Indian Ocean meridional circulation has a shallow overturning cell where a northward subsurface branch supplies water for the northern hemisphere upwelling and a southward branch returns the same to the southern Indian Ocean (Miyama et al., 2003). There is also a net heat transport towards the south associated with this flow since the subsurface branch imports cooler water into the northern hemisphere and the surface branch exports warmer water to the south. This circulation is referred as the cross-equatorial cell (CEC). Two other cells, namely sub tropical cell (STC) and the eastern limb of sub tropical cell (Eastern STC), are also found in the equatorial region of the Indian Ocean. These are shallow overturning cells causing upwelling in the southern region of the Indian Ocean. The subtropical cell causes upwelling in a band of 5°S to 10°S in the central and western Indian Ocean and is driven by negative wind stress curl in this region associated with equatorward weakening of the southeast trades. Observational evidences, such as rise in pycnocline to the surface, are well documented but the same has not been recorded in terms of SST (Wyrki 1988; Levitus et al., 1994). Ocean colour satellite data also indicates presence of phytoplankton bloom (Murtugudde et al., 1999) in this band attributable to the upwelling caused by overturning cells. The other cell, known as eastern limb of subtropical cell, causes upwelling in the eastern equatorial Indian Ocean *i.e.*, along Java and Sumatra coast, occasionally it also causes upwelling along the equator. It is now reasonably established, though dependent on season and direction of trade winds, that equatorial upwelling does take place in the Indian Ocean, no data exists on the phytoplankton productivity. The equatorial Indian Ocean is still a virgin area and the present data set is the first of its kind from this important basin.

4.2 Physical parameters, chlorophyll-*a* and nutrients in the equatorial Indian Ocean during pre-monsoon season 2005

4.2.1 Hydrographic conditions:

During the present study sampling was done along two different transects, namely along 77°E and 83°E. Five stations were taken along each transect at every 2.5° latitude starting from 5°N to 5°S: PP1 to PP5 along 77°E and PP6 to PP10 along 83°E. Latitude-wise variation in sea surface temperature (Fig 4.2) along 77°E and 83°E transects are shown in Fig 4.2. SST at 5°N (PP1) was 30.2°C which decreased towards the equator to 29.7°C and 29.4°C respectively at 2.5°N (PP2) and equator (PP3). It again increased slightly to the south of equator, from 29.4 to 29.7°C at 2.5°S (PP4) and remained the same at 5°S (PP5). The minimum SST was recorded at the equator and the maximum was at 5°N.

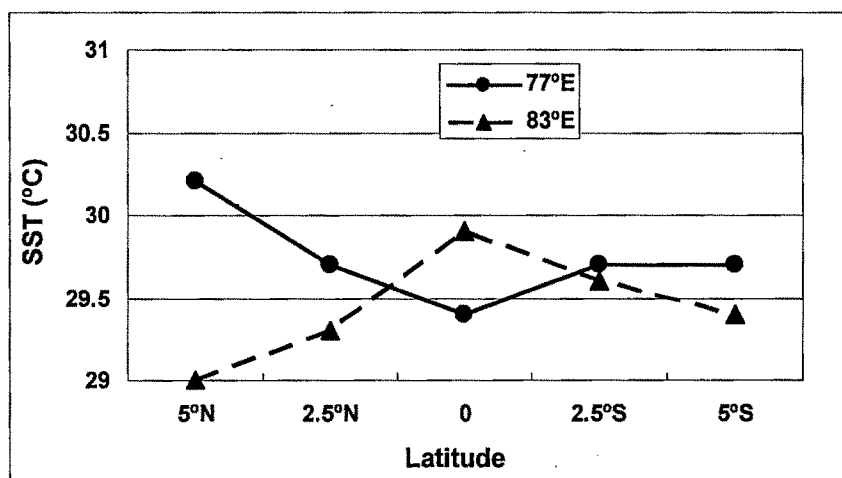


Fig 4.2 SST (°C) at all stations along 77°E and 83°E transects

Along 83°E transect SST increased towards the equator, from 29.0°C at 5°N (PP6) to 29.9°C at equator but again decreased south of equator to 29.4°C at 5°S (PP10). Unlike 77°E transect where a general decrease in SST was observed from 5°N to equator, an increase was observed between the same latitude along 83°E.

Sea Surface salinity increased from 5°N to the equator along 77°E (Fig 4.3), from 33.3 to 35.2 but decreased south of equator to 33.8 at 5°S; surface water at

equator had the maximum salinity. Along 83°E, though a similar increasing trend in salinity was there from 5°N to the equator (Fig 4.3), the magnitude of change was relatively smaller; it increased from 34.0 at 5°N to 34.7 at equator. Also unlike at 77°E where it decreased south of equator, salinity increased till 2.5°S and started decreasing only after that.

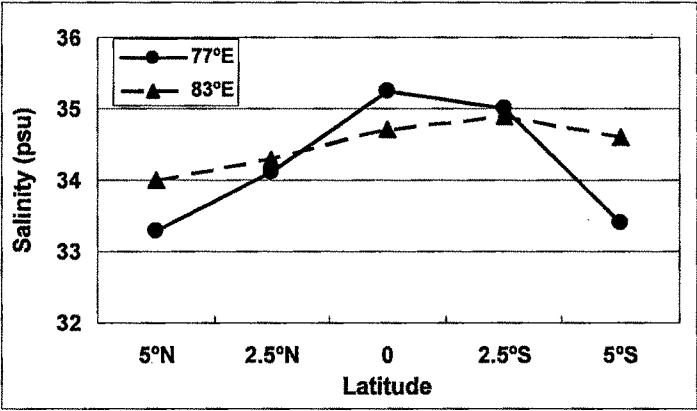


Fig 4.3 Salinity at all stations along 77°E and 83°E transects

4.2.2 Nutrients

Among nutrients only nitrate could be measured during the present study in the equatorial Indian Ocean during the pre-monsoon season. Photic zone integrated nitrate concentration varied from 370.7 mmol m⁻² to 1665.4 mmol m⁻² over the study region (Fig 4.4); it varied from 397.8 mmol m⁻² to 1665.4 mmol m⁻² along 77°E transect and 370.7 mmol m⁻² to 1294.1 mmol m⁻² along 83°E transect. A comparison of the integrated nitrate concentrations at stations along the two transect suggests that at stations north of the equator nitrate concentration was more at stations along 77°E as compared to those along 83°E. Among equatorial stations, station along 77°E had nitrate one fourth of those along 83°E. Among the stations south of equator, stations along 83°E again had more nitrate compared to the stations along 83°E at 2.5°S whereas at 5°S nitrate concentration was almost the same at both the stations.

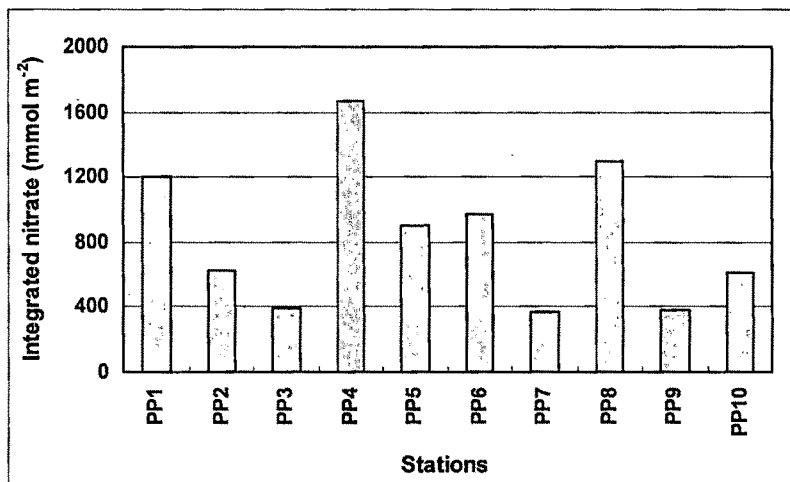


Fig 4.4 Photic zone integrated nitrate at different stations in the equatorial Indian Ocean. The maximum nitrate was measured at PP3 and a minimum was measured at PP7.

PP1 and PP9, the surface nitrate concentrations were 0.3 and 0.85 μM and at rest of the stations nitrate concentration was below the detection limit in the surface waters. Depth profiles of the nitrate at different stations are shown in Fig 4.5. At most of the PP stations, surface waters till a depth of 30-40 m the nitrate concentration was below the detection limit. Nitrate concentration increased dramatically to higher concentration at relatively deeper depths at most of the stations of the equatorial Indian Ocean. At most of the stations it increased to more than 5 μM at a depth of 40-60 m and was more in the range of 10-15 μM below 80 m depth. Higher concentrations at the deeper layers coupled with photic depth in this region during the sampling season resulted in higher values of photic zone integrated column nitrate values.

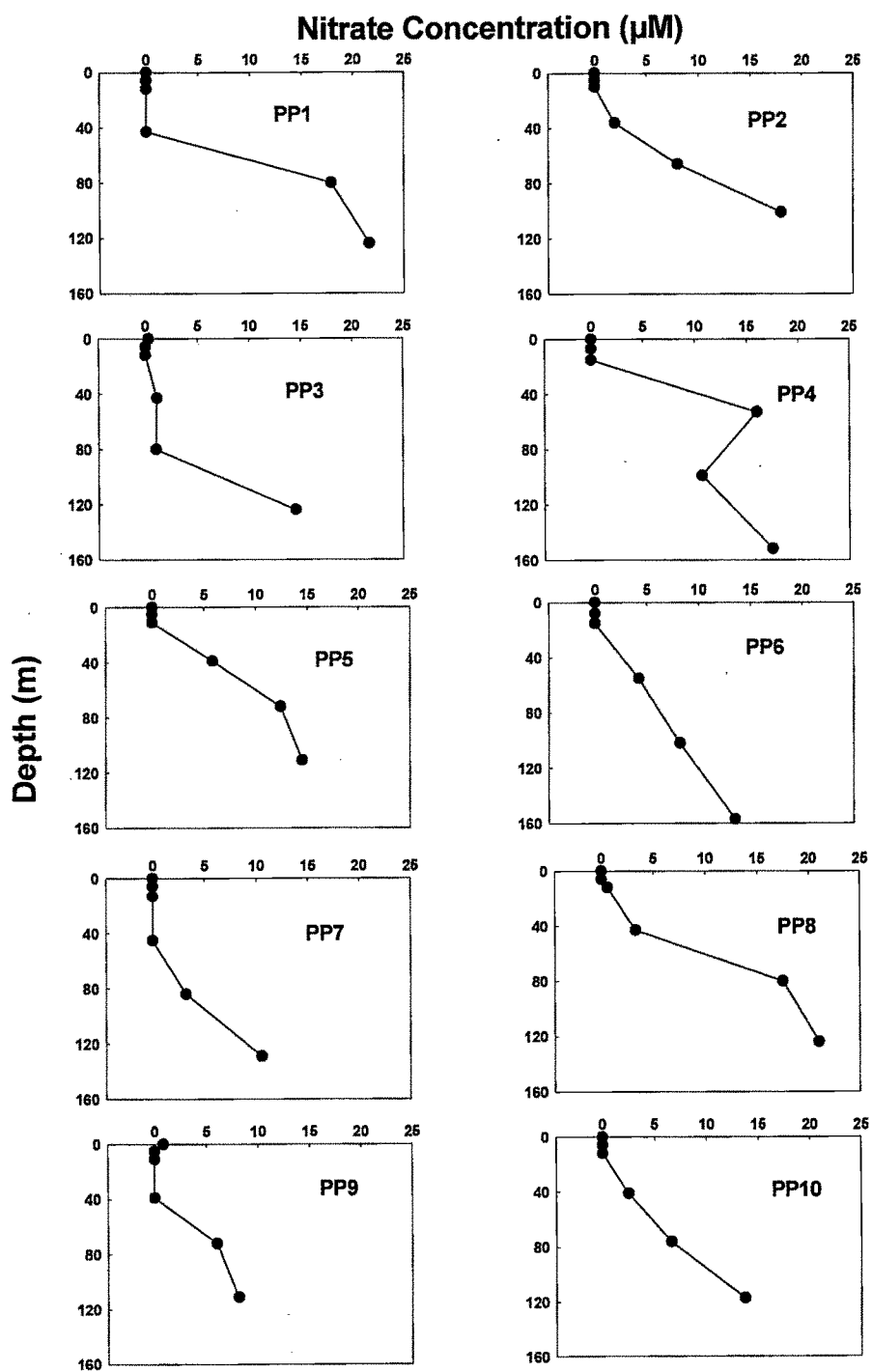


Fig 4.5 Depth profiles of nitrate at different stations in the equatorial Indian Ocean during pre-monsoon 2005

4.3 ¹⁵N based productivity studies in the equatorial Indian Ocean during pre-monsoon 2005

4.3.1 Total Production

The rates of nitrogen uptake, integrated over the photic zone, span more than an order of magnitude over the study area and it varied from 19.1 mmolNm⁻²d⁻¹ to 171.1 mmolNm⁻²d⁻¹ (Fig 4.6). N-uptake rates were abnormally high at PP5 (5°S; 77°E) and PP8 (0°; 83°E). Excluding these two stations, N-uptake rates varied from 19.1 mmolNm⁻²d⁻¹ to 78.3 mmolNm⁻²d⁻¹. Though higher uptake rates were measured at almost all the stations, the N-uptake rates were low in the upper mixed layer and increased tremendously below mixed layer. Most of the productivity was confined below the mixed layer. This was mainly because nitrate concentration was below detection limit in the mixed layer, and in the absence of nitrate ammonium and urea were the preferred nutrients. But below the mixed layer, where the concentration of ambient nitrate increased dramatically, nitrate uptake also increased.

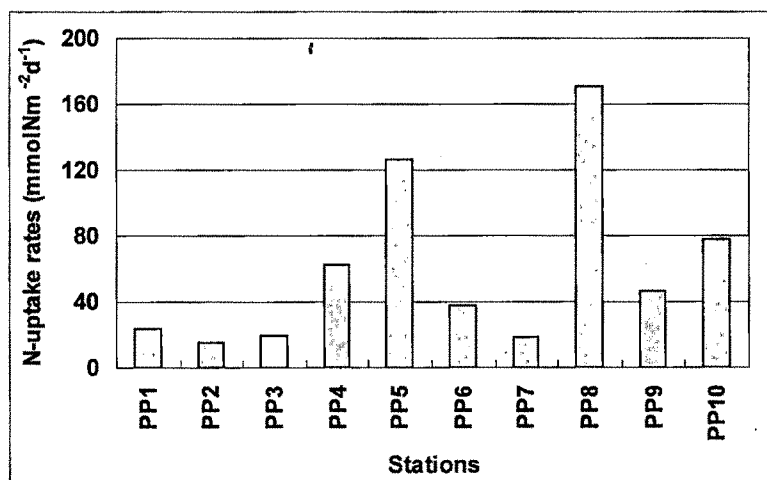


Fig 4.6 Total N-uptake rates at different stations in the equatorial Indian Ocean during pre-monsoon 2005

The mixed layer integrated N-uptake rates were very low and were similar to the rates reported from the other oligotrophic regions around the world ocean. It varied from 0.81 mmolNm⁻²d⁻¹ to 2.23 mmolNm⁻²d⁻¹ over the study area (Fig 4.7). The mean N-uptake rate over the study area was 1.32 mmolNm⁻²d⁻¹ and along 77°E and 83°E it was 1.22 mmolNm⁻²d⁻¹ and 1.43 mmolNm⁻²d⁻¹ respectively. N-uptake

rates were higher along 83°E transect compared to 77°E transect at all the stations except at the equator where rate was higher at 77°E than 83°E. No meridional difference could be seen in total N uptake rates at 5°N and 5°S; it was almost the same at both the stations ($1.17 \text{ mmolNm}^{-2}\text{d}^{-1}$ and $1.40 \text{ mmolNm}^{-2}\text{d}^{-1}$ respectively). At 2.5°N there was a two-fold increase in total N-uptake rate at 83°E compared to 77°E whereas at 2.5°S this increase was more than two-fold. Among the stations at the equator total N-uptake rate was almost 4-fold higher at 77°E compared to 83°E. This difference at the equator is because of the difference in the mixed layer depth at 77°E and 83°E; at 77°E the mixed layer depth was 35 m whereas at 83°E it was only 15 m. The change in MLD may be because of the presence of high wind speed ($>15 \text{ m/s}$) at equator at 83°E during sampling and may be just a transient event and may not be generalized. Excluding this extreme equatorial event, at all the other stations productivity along 83°E was more than the productivity along 77°E.

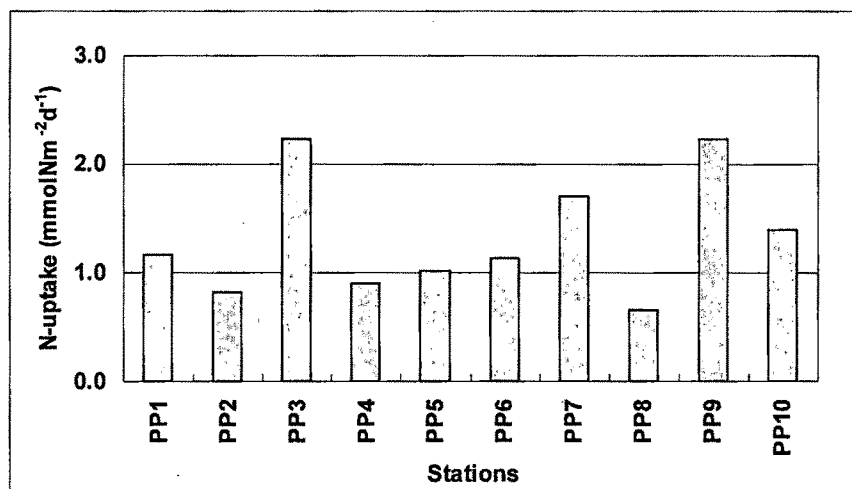


Fig 4.7 Mixed layer depth integrated total N-uptake rates at different stations in the equatorial Indian Ocean during pre-monsoon 2005

One of the main reasons may be the influx of pacific water through the Indonesian throughflow (Gordon and Fine 1996). Though it is well established that it plays a major role in ocean circulation and heat exchange (Godfrey 1996), its effect on the productivity is still not known. It is still not known that whether it carries only heat or it carries nutrients as well and hence more such studies in this region are

required to ascertain the effect of the Indonesian throughflow on the biogeochemistry of the Indian Ocean and on the biological productivity of this basin.

4.3.2 New Production:

In the equatorial Indian Ocean photic zone integrated column nitrate uptake rates were significantly high and showed lots of heterogeneity in space during the pre-monsoon season; it varied from 12.84 $\text{mmolNm}^{-2}\text{d}^{-1}$ to 167.17 $\text{mmolNm}^{-2}\text{d}^{-1}$ over the study region. It varied from 12.84 $\text{mmolNm}^{-2}\text{d}^{-1}$ to 123.71 $\text{mmolNm}^{-2}\text{d}^{-1}$ with a mean of 45.85 $\text{mmolNm}^{-2}\text{d}^{-1}$ along 77°E transect and from 14.90 $\text{mmolNm}^{-2}\text{d}^{-1}$ to 167.17 $\text{mmolNm}^{-2}\text{d}^{-1}$ with a mean of 66.65 $\text{mmolNm}^{-2}\text{d}^{-1}$ along 83°E transect (Fig 4.8). In general nitrate uptake rates were higher along 83°E transect at the stations north of the equator but were higher along 77°E transect at stations south of the equator. The most dramatic increase was observed at the equator where column integrated nitrate uptake rates increased more than order of magnitude at 83°E as compared to the same on 77°E. A significant part of nitrate uptake rate was confined in layers below the photic zone. This, again, may be because of the presence of high ambient nitrate concentrations below the mixed layer.

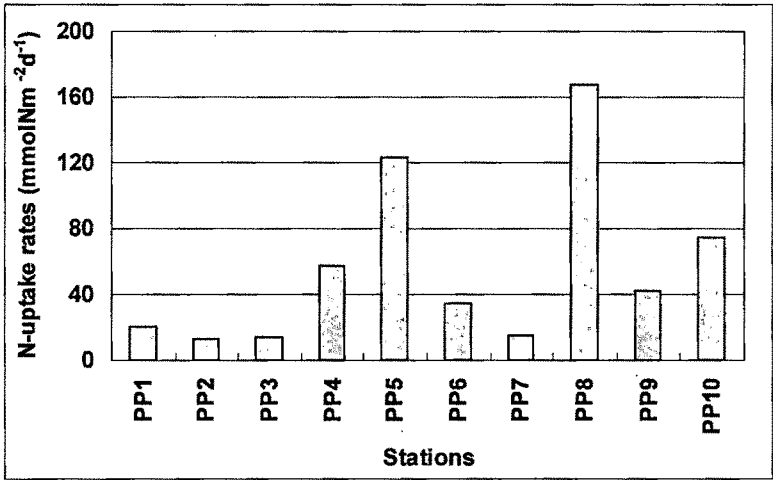


Fig 4.8 Photic zone integrated total nitrate uptake rates (new production) at different stations in the equatorial Indian Ocean during pre-monsoon 2005

The mixed layer integrated nitrate uptake rates were very low during the pre-monsoon 2005. It varied from a minimum of $0.12 \text{ mmolNm}^{-2}\text{d}^{-1}$ to a maximum of $0.84 \text{ mmolNm}^{-2}\text{d}^{-1}$. The mean new production over the study area was $0.32 \text{ mmolNm}^{-2}\text{d}^{-1}$. It was very low ($0.20 \text{ mmolNm}^{-2}\text{d}^{-1}$) along 77°E transect but was more the twice ($0.43 \text{ mmolNm}^{-2}\text{d}^{-1}$) along 83°E transect. New production varied over a small range along 77°E ; it varied from a low of $0.12 \text{ mmolNm}^{-2}\text{d}^{-1}$ to a high of $0.30 \text{ mmolNm}^{-2}\text{d}^{-1}$ and along 83°E transect the variation was quite large, from a low of $0.21 \text{ mmolNm}^{-2}\text{d}^{-1}$ to a high of $0.84 \text{ mmolNm}^{-2}\text{d}^{-1}$. New production or nitrate uptake rate was low at station along 77°E transect than those along 83°E at all the stations except the equator where new production was higher at 83°E compared to 77°E (Fig 4.9). There was a significant variation in the nitrate uptake rates at stations south of the equator. It was $0.18 \text{ mmolNm}^{-2}\text{d}^{-1}$ at 5°N , 77°E which increased 3-fold to $0.55 \text{ mmolNm}^{-2}\text{d}^{-1}$ at 5°N , 83°E . At 2.5°N 7-fold increased was observed in the nitrate uptake rate from 77°E to 83°E ; it increased from $0.12 \text{ mmolNm}^{-2}\text{d}^{-1}$ to $0.84 \text{ mmolNm}^{-2}\text{d}^{-1}$ (Fig 4.9). At the stations south of the equator i.e., at 2.5°S and 5°S nitrate uptake rates were almost similar at 77°E and 83°E .

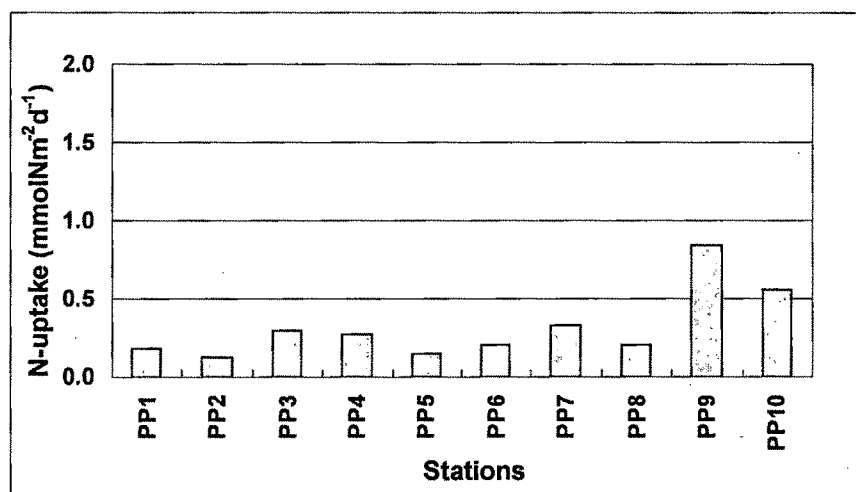
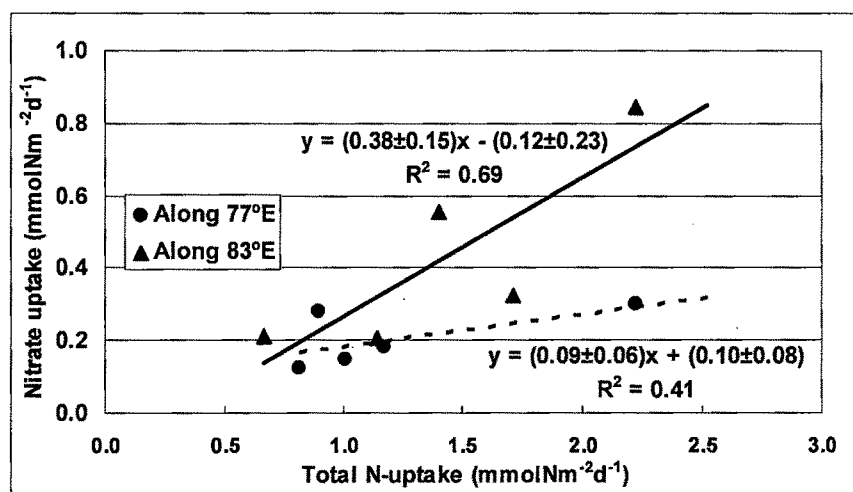


Fig 4.9 Station-wise mixed layer depth integrated nitrate uptake rates (new production) at different stations in the equatorial Indian Ocean during pre-monsoon 2005

Relation between mixed layer integrated nitrate uptake rates (new production) and total uptake rates (total production) suggests two different slopes for

the two transects (Fig 4.10). Along 77°E the correlation was weak (correlation coefficient = 0.41) with a lower slope {New Production = (0.09 ± 0.06) Total production + (0.10 ± 0.08) } where as along 83°E correlation was more significant (correlation coefficient = 0.69) with relatively higher slope {New Production = (0.38 ± 0.15) Total production - (0.12 ± 0.23) }. Different slopes along different transects suggests presence of two different biogeochemical provinces in the equatorial Indian Ocean with significantly different potential of export production. Capability of the equatorial ocean for export production is low as compared to that of the Arabian Sea (present study), Bay of Bengal (Sanjeev Kumar et al., 2004) and the Southern Ocean (present study). The slope of the regression equation between new and total production suggests that along 77°E transect only 9% of the total mixed layer production can be exported to the deep where the export production along 83°E transect may be as high as 38%, almost 4-fold higher, of the mixed layer integrated total production.



4.10 Relation between mixed layer integrated total N-uptake rate and nitrate uptake rate in the equatorial Indian Ocean during pre-monsoon 2005

4.3.3 Regenerated production

Ambient ammonium and urea concentrations could not be measured during the present study. For the calculation of regenerated production it was assumed that the tracer added was the only source of nutrient for the plankton and the uptake rates



given here are potential uptake rates for ammonium and urea. Ammonium uptake rate varied from $1.14 \text{ mmolNm}^{-2}\text{d}^{-1}$ to $2.17 \text{ mmolNm}^{-2}\text{d}^{-1}$ along 77°E transect in the equatorial Indian Ocean. At 5°N (PP1) ammonium uptake rate was $2.17 \text{ mmolNm}^{-2}\text{d}^{-1}$ which decreased to $1.15 \text{ mmolNm}^{-2}\text{d}^{-1}$ at 2.5°N (PP2). At the equatorial station (PP3) it again increased to $1.44 \text{ mmolNm}^{-2}\text{d}^{-1}$. At a station south of the equator, i.e., 2.5°S (PP4) it further increased to $2.17 \text{ mmolNm}^{-2}\text{d}^{-1}$ but again decreased to $1.14 \text{ mmolNm}^{-2}\text{d}^{-1}$ at 5°S (PP5). Along 83°E transect ammonium uptake rate varied from $1.26 \text{ mmolNm}^{-2}\text{d}^{-1}$ to $2.44 \text{ mmolNm}^{-2}\text{d}^{-1}$. Stations south of equator had more ammonium uptake rates as compared to stations north of the equator. At 5°N (PP10), along 83°E transect, ammonium uptake rate was $2.35 \text{ mmolNm}^{-2}\text{d}^{-1}$. It increased slightly to reach a maximum of $2.44 \text{ mmolNm}^{-2}\text{d}^{-1}$ at 2.5°N (PP9) but again decreased to $2.13 \text{ mmolNm}^{-2}\text{d}^{-1}$ at a station at equator (PP8). At stations south of equator ammonium uptake rate was comparatively less; it was $1.26 \text{ mmolNm}^{-2}\text{d}^{-1}$ and $1.33 \text{ mmolNm}^{-2}\text{d}^{-1}$ at 2.5°S (PP7) and 5°S (PP6) respectively. The mean ammonium uptake rate along 77°E transect was less than those along 83°E transect: it was $1.61 \text{ mmolNm}^{-2}\text{d}^{-1}$ and $1.90 \text{ mmolNm}^{-2}\text{d}^{-1}$ along 77°E and 83°E transect respectively.

Ammonium uptake rates at different stations are shown in Fig 4.11. At 5°N ammonium uptake rate was slightly more at 83°E but at 2.5°N it was more than twice compared to that at 77°E . Ammonium uptake was also more at 83°E than at 77°E at the equator. At 2.5°S it was more at 77°E than 83°E and at 5°S it was almost the same at both the longitudes. Urea uptake rates varied from $1.19 \text{ mmolNm}^{-2}\text{d}^{-1}$ to $2.53 \text{ mmolNm}^{-2}\text{d}^{-1}$ along 77°E transect and from $1.14 \text{ mmolNm}^{-2}\text{d}^{-1}$ to $2.52 \text{ mmolNm}^{-2}\text{d}^{-1}$ along the 83°E transect (Fig 4.12). Along the 77°E , urea uptake rate was $1.56 \text{ mmolNm}^{-2}\text{d}^{-1}$ at 5°N . It decreased to $1.19 \text{ mmolNm}^{-2}\text{d}^{-1}$ at 2.5°N but increased more than twice to reach a maximum of $3.13 \text{ mmolNm}^{-2}\text{d}^{-1}$ at a station at the equator. The equatorial station at 77°E had maximum urea uptake rate measured during the present study. At a station south of the equator i.e. at 2.5°S , urea uptake rate again decreased to $2.59 \text{ mmolNm}^{-2}\text{d}^{-1}$. It further decreased to $1.67 \text{ mmolNm}^{-2}\text{d}^{-1}$ at 5°S . Along 83°E urea uptake rate was $1.55 \text{ mmolNm}^{-2}\text{d}^{-1}$ at 5°N . At 2.5°N and the equator it was $1.14 \text{ mmolNm}^{-2}\text{d}^{-1}$ and $1.77 \text{ mmolNm}^{-2}\text{d}^{-1}$ respectively. Urea uptake rate

again increased south of the equator, i.e., at 2.5°S to 2.52 mmolNm⁻²d⁻¹ but decreased to 1.96 mmolNm⁻²d⁻¹ at 5°S. In contrast to ammonium uptake rate, the mean urea uptake rate was more along the 77°E transect than the 83°E transect: it was 2.03 mmolNm⁻²d⁻¹ along 77°E and 1.79 mmolNm⁻²d⁻¹ along 83°E transects respectively. A comparison of urea uptake rates at stations having different longitudes but same latitude is shown in Fig 4.12. At 5°N, 2.5°N and 2.5°S urea uptake rate remained almost the same at both 77°E and 83°E, but at 0° latitude, urea uptake at 77°E was almost twice that at 83°E. Along both transects ammonium uptake was more than the urea uptake at stations north of the equator and the equator, and was less than urea uptake at stations south of the equator.

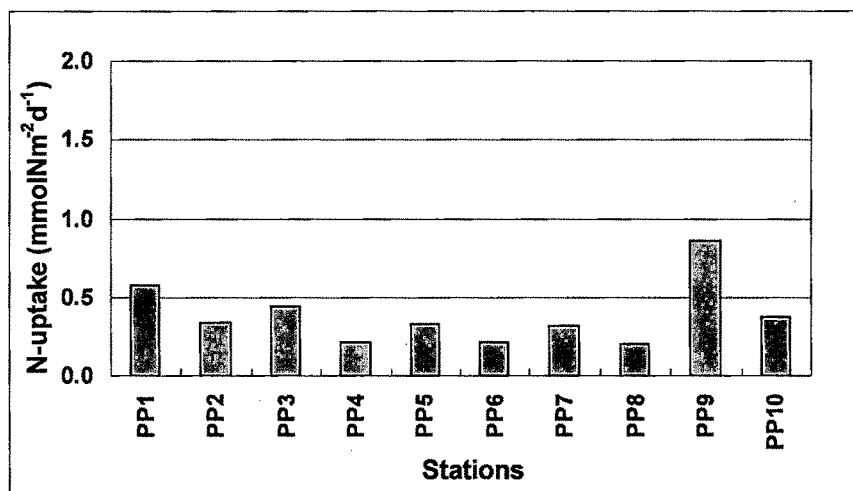


Fig. 4.11 Mixed layer depth integrated ammonium uptake rates at different stations in the equatorial Indian Ocean during pre-monsoon 2005

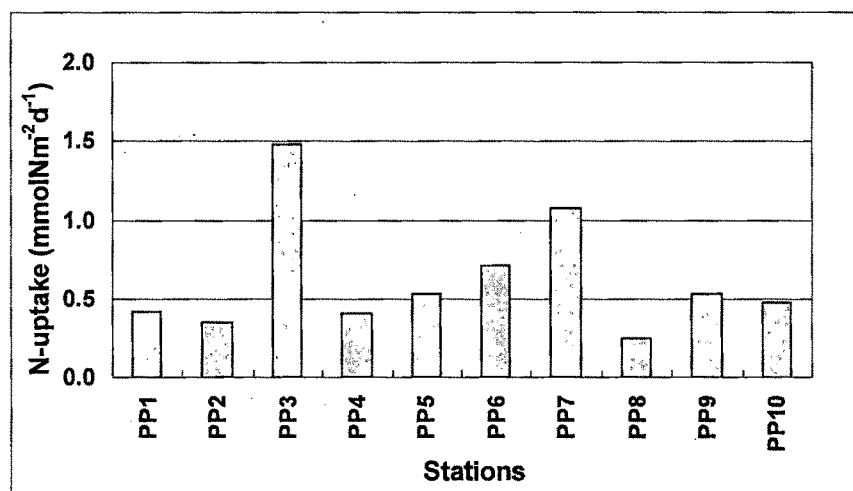


Fig. 4.12 Mixed layer depth integrated urea uptake rates at different stations in the equatorial Indian Ocean during pre-monsoon 2005

4.3.4 *f*-ratios in the equatorial Indian Ocean

The column integrated *f*-ratio was very high in the equatorial Indian Ocean; it varied from 0.85 to 0.98 over the entire region (Fig 4.13). Along 77°E transect *f*-ratio varied from 0.85 to 0.98 whereas along 83°E transect it varied from 0.80 to 0.98. The mean *f*-ratio along 77°E and 83°E were 0.87 and 0.91 respectively. These values are comparable to *f*-ratios reported from upwelling regions of the northwestern Arabian Sea during the summer monsoon; Watts and Owens (1999) has reported *f*-ratios as high as 0.92 from the upwelling regions of the Arabian Sea. The *f*-ratio found during the present study in the equatorial region of the Indian Ocean is significantly higher than that at the other parts of the Indian Ocean. This is again due to availability of huge amount of nitrate in the water column below the mixed layer and thus may have been somewhat overestimated. Mixed layer integrated *f*-ratio were very low compared to the column integrated *f*-ratios; they varied from 0.16 to 0.40 over the entire region. The *f*-ratios were low along 77°E transect; it varied from 0.16 to 0.31 with a mean of 0.18. The maximum *f*-ratio of 0.31 along this transect was found at PP4. Excluding PP4 the *f*-ratio varied from a low of 0.13 to a high of 0.18. Along 83°E, the *f*-ratio varied from 0.18 to 0.40 with a progressively increasing trend. The mean along this transect was 0.29.

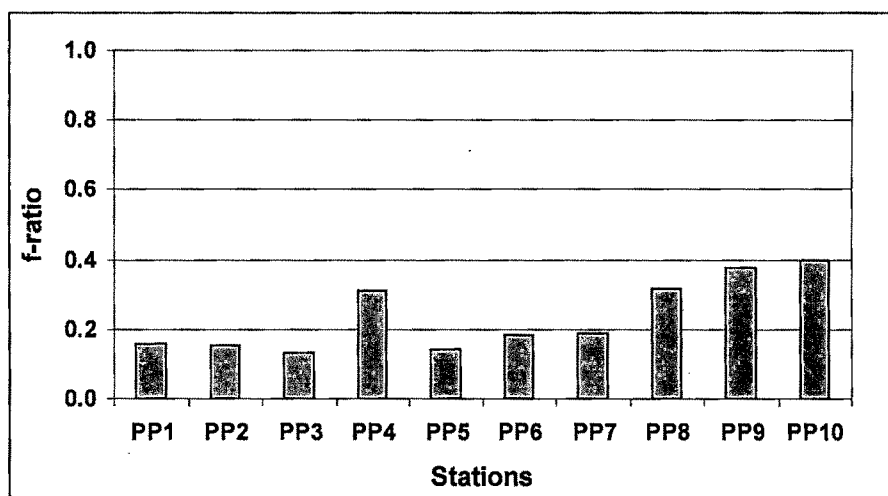


Fig. 4.13 *f*-ratios at different stations in the equatorial Indian Ocean.

4.4 SOUTHERN OCEAN

The Southern Ocean is now delimited as the world's fifth ocean by the International Hydrographic Organization (IHO). It comprises of the southern portions of the Pacific, Atlantic and the Indian Oceans (Fig.4.14) and it constitutes approximately 10% of the world's oceans. The Southern Ocean plays an important role in the global carbon cycle and climate regulation by acting as a net sink, *via* solubility and biological pumps, for the atmospheric CO₂ (Chisholm et al., 2001). The biogeochemistry of the Southern Ocean is controlled by two major current systems: the eastward flowing Antarctic Circumpolar Current (ACC) and the westward flowing Antarctic Coastal Current (Constable and Nicol 2003). The Antarctic Circumpolar Current (ACC), the only current that flows completely around the globe, is the strongest current in the world ocean and the most important current in the Southern Ocean. The ACC, as it encircles the Antarctic continent, flows eastward through the southern portions of the Atlantic, Indian, and Pacific Oceans. The strong westerly wind generates upwelling of nutrient rich deep water in this region. According to an estimate (Anderson, 2003) only half of the upwelled nutrients are consumed by phytoplankton present here and the rest are carried back into the deep sea via formation of Antarctic intermediate water (AAIW) and

Antarctic bottom water (AABW). Global and low latitude export production is controlled by the amount of intermediate and deep water formed at subantarctics (Sarmiento et al, 2003; Marinov et al, 2006). Some of the areas of the world’s ocean such as the Southern Ocean, the equatorial and the North Pacific Ocean contain huge amounts of unused macro-nutrients such as nitrate in their surface waters. Despite this, the productivity in these areas is low (column integrated primary productivity varies between 130-220 mgCm⁻²d⁻¹; Gervais and Reibesell 2002). The growth of phytoplankton and uptake of nutrients, during their growth, causes depletion of major nutrients in the surface layer. The persistence of these nutrients in the surface waters of the Southern Ocean suggests retardation of plankton growth due to some reason. Because of this property these regions are described as “High Nutrient Low Chlorophyll” or HNLC regions (Minas et. al., 1986; Dugdale and Wilkerson, 1986; Martin et. al., 1991; Mitchell et. al., 1991). The Southern Ocean is unique in the sense that it is the largest HNLC region in the world oceans; its surface water also contains significant amounts of macronutrients such as nitrate, silicate and phosphate to support high primary production and yet the productivity in this region is quite low.

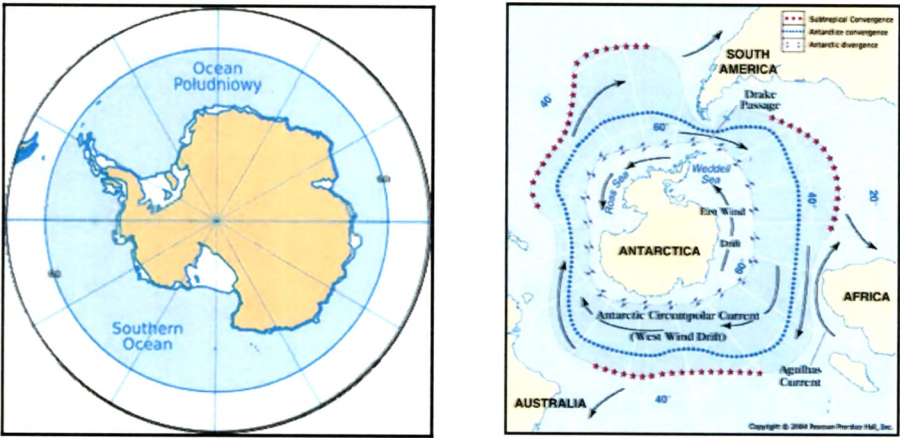


Fig 4.14. The aerial extent of the Southern Ocean (left) and the cartoon of the Antarctic Circumpolar Current (ACC; right).

Several causes have been proposed in the past to explain the existence of the HNLC condition particularly in the Southern Ocean. The important ones are: presence of deep mixed layer, low sea surface temperature, low specific growth rate,

grazing control, sun-light limitation, trace metal toxicity and Fe-limitation. The insufficient availability of micronutrients such as iron (Fe) ($<10^{-12}$ M in the open ocean) appears to be the main cause for observed low productivity in such regions (Martin et al., 1991). The role of iron in controlling the productivity in the open ocean and, consequently the climate is called the “Iron Hypothesis”.

Martin and his colleagues (Martin and Fitzwater 1988) were the first to measure the concentration of iron in the waters of the Gerlache strait (Antarctic coast) and the Drake Passage (offshore). They concluded that the offshore locations were less productive ($\sim 100 \text{ mgCm}^{-2}\text{d}^{-1}$) because of lack of iron ($<0.16 \text{ nM}$). They also proposed that the coastal stations received iron ($\sim 7.4 \text{ nM}$) from the continental margins and so the productivity was very high ($3 \text{ gCm}^{-2}\text{d}^{-1}$) and therefore the supplied iron did not get transported to the open ocean (Martin et al., 1990). Iron can limit productivity in the open ocean because (i) it is required for the synthesis of chlorophyll and it helps in plant metabolism (Geider and LaRoche 1994) and (ii) lack of iron may also cause decline in the photosynthetic electron transfer (Geider and LaRoche 1994; Hutchins 1995) which in turn may lead to low photosynthetic efficiency (*i.e.*, production per unit chlorophyll). The idea of iron limitation got momentum when it was shown, through bottle scale experiments carried out for the first time at station PAPA (50°N , 145°W) in the sub-arctic north Pacific by Martin and his colleagues, that there is a rapid increase in the chlorophyll concentration and nitrate was totally consumed after 4 days since the iron enrichment (Martin and Fitzwater 1988). This was followed by a number of large-scale Fe-enrichment experiments carried out to test the hypothesis of Fe-limitation in different HNLC regions (Hutchins 1995).

In the Southern Ocean four large scale iron enrichment experiments have been done, two each in the Pacific sector (SOIREE and SOFeX) and the Atlantic (EisenEx and EiFex) (Martin et al. 1991; Coale et. al., 1996; Gervais and Riebesell 2002; Coale et. al., 2004); the Indian sector of the Southern Ocean still remains unexplored. The first large scale iron enrichment experiment in the Southern Ocean was done in February 1999 in the Australian (Pacific) sector (Boyd and Law, 2001). The iron enrichment site was observed for 13 days on-board and an increase of more

than 10-fold was measured in column primary production ($\sim 1.3 \text{ gCm}^{-2}\text{d}^{-1}$) (Gall et al., 2001). Chlorophyll increased markedly ($\sim 2 \text{ }\mu\text{g l}^{-1}$), nitrate and silicate concentration in the surface waters decreased during these 13 days but export flux measured for “IN” and “OUT” patches were not significantly different.

SOIREE was followed by EisenEx, another large scale iron fertilization experiment, in Atlantic during austral spring, 2000. Primary production during EisenEx increased from $130\text{--}220 \text{ mgCm}^{-2}\text{d}^{-1}$ at an “OUT” patch station to $\sim 800 \text{ mgCm}^{-2}\text{d}^{-1}$ after 16 days. Chl-a increased from $48\text{--}56 \text{ mgm}^{-2}$ to 231 mgm^{-2} after 21 days of enrichment. Another enrichment experiment SOFeX was carried out in the Pacific sector of the southern Ocean. During this experiment two patches were fertilized, each having different silica concentration; the northern and southern patches had Si concentrations of $<5 \text{ }\mu\text{M}$ and $>60 \text{ }\mu\text{M}$ respectively. The northern patch witnessed almost a 10-fold increase in Chl-a and a 4-fold increase in the carbon biomass, whereas in the southern patch Chl-a increased almost 8-fold and productivity increased from $\sim 3.5 \text{ mgCm}^{-3}\text{d}^{-1}$ to $\sim 55 \text{ mgCm}^{-3}\text{d}^{-1}$ (Coale et al., 2004). Absolute nitrate uptake rate also increased by factors of 15 and 25 respectively in the northern and southern patches compared to control regions (Coale et al., 2004). *f*-ratio increased from 0.1–0.2 to 0.5–0.6 in the southern patch (silica rich) and from 0.3 to 0.4 in the northern patch (silica depleted) which suggested that availability of iron increases nitrate uptake by marine plankton (Coale et al., 1996).

More recently it has been proposed that natural iron fertilization due to upwelling of nutrient rich water from deep leads to development of bloom in the Kerguelen plateau sector of the Southern Indian Ocean (Blain et al., 2007). As a consequence of these experiments now it is well established that iron addition could cause increased carbon sequestration. Even though most the Fe-enrichment experiments have seen a significant increase in the chlorophyll, studies pertaining to the nitrogen biogeochemistry are limited. The Indian Sector of the Southern Ocean constitutes $\sim 39\%$ ($13.1 \times 10^6 \text{ sq. km}$) by area (deBaar et al., 2005) and is the least explored area (Slawyk 1979; Probyn and Painting 1985; Collos and Slawyk 1986; Mengesha et. al., 1998; Semeneh et al., 1998; Savoye et. al., 2004), compared to the Pacific and Atlantic oceans, in terms of N-uptake studies. Our knowledge about the

N uptake and the f -ratio characteristics of this region is rather limited. The present study highlights new results of N-uptake and f -ratios from the Indian sector of the Southern Ocean, though only based on bottle-scale experiments.

4.5 Summary of the earlier work

Slawyk (1979) was the first to study nitrate uptake rates from the Kerguelen Island area of the Southern Ocean. He described the Southern Ocean water as transparent water with relatively high photic depth, varying between 50 to 100 m. He reported very low nitrate uptake rates, varying from $0.03 \text{ mmolNm}^{-2}\text{d}^{-1}$ to $0.12 \text{ mmolNm}^{-2}\text{d}^{-1}$ with a mean of $0.06 \text{ mmolNm}^{-2}\text{d}^{-1}$. Probyn and Painting (1985) reported N-uptake rates for the surface waters of the coastal regions between Cape Ann and Mawson in the Southern Indian Ocean. The N-uptake rate reported by them was significantly high; it varied from $2.16 \text{ mmolNm}^{-3}\text{hr}^{-1}$ to $5.41 \text{ mmolNm}^{-3}\text{hr}^{-1}$ with a mean of $4.47 \text{ mmolNm}^{-3}\text{hr}^{-1}$. They reported a preference for reduced nitrogen (ammonium and urea) over nitrate by the phytoplankton of the Antarctic coastal waters; the mean f -ratio was 0.42. They also studied the nitrate uptake according to the size class and found that the phytoplankton of size $<200 \mu\text{m}$ contributed the maximum to nitrate uptake; nanoplankton (size $< 15 \mu\text{m}$) and picoplankton (size $< 1 \mu\text{m}$) contributed mostly to regenerated production. Mengesha et al., (1998) studied N-uptake characteristics of the Southern Ocean waters over two different seasons, austral spring and summer 1994, for a small area near Kerguelen Island. They found a pronounced seasonal variation in the nitrogen uptake in the Indian sector of the Southern Ocean. During spring the specific and absolute nitrate uptake dominated over ammonium and urea uptakes whereas during summer ammonium uptake was more than nitrate uptake. The specific nitrate uptake during spring was 0.0048 hr^{-1} which reduced to 0.0011 hr^{-1} in the summer. Ammonium uptake increased slightly, from 0.0015 hr^{-1} in spring to 0.0018 hr^{-1} in the summer. The f -ratio also decreased in the summer but showed considerable variation; it varied from 0.68 to 0.85 in spring and from 0.17 to 0.63 in summer. They observed a transition from nitrate based autotrophic community in spring to regenerated nitrogen based community in summer. Specific nitrate and ammonium uptake rates reported for the surface waters

by Semeneh et al., (1998) were lower than the earlier reported rates; specific nitrate and ammonium uptake rates were 0.001 hr^{-1} and 0.0004 hr^{-1} respectively in the Prydz Bay area in 1991. Though the specific nitrate uptake rate was more in the open ocean zone relative to coastal zone (the mean specific uptake rate in coastal zone was 0.5 hr^{-1} whereas in the open ocean zone it was 1.0 hr^{-1}), specific total N-uptake rate (a sum of specific nitrate and ammonium uptake rates) was almost the same. The same trend was seen in the f -ratio as well; the mean f -ratio in coastal zone was 0.42 whereas in the open ocean zone it was 0.68. The absolute total N-uptake rate in the coastal zone was more than three fold higher than the rate in the open ocean zone; the absolute N-uptake rate was $147.2 \pm 71.9 \mu\text{molNm}^{-3}\text{d}^{-1}$ in the coastal zone and was $38.9 \pm 24.7 \mu\text{molNm}^{-3}\text{d}^{-1}$ in the open ocean zone. They also reported N-uptake rates from a longitudinal transect along 62°E . The specific nitrate uptake rates from this region was also (0.001 hr^{-1}) low but ammonium uptake rate was high (0.0019 hr^{-1}). The absolute total N-uptake rate was almost double that at the open ocean zone of the Prydz Bay but the f -ratio was low (0.034).

Savoye et al., (2004) studied N-uptake and f -ratio characteristics of the Australian sector of the Southern Ocean. They reported a continuous increase in total N-uptake and nitrate uptake rates on a north-south transect. Nitrate uptake rate increased from a low of $1.4 \text{ mmolN/m}^2/\text{d}$ at 48.8°S to a high of $8.8 \text{ mmolNm}^{-2}\text{d}^{-1}$ at 64.9°S , total N-uptake rate increased from 4.9 ± 0.7 to $9.2 \pm 2.2 \text{ mmolNm}^{-2}\text{d}^{-1}$. Ammonium and urea uptake rates remained almost constant ($2.3 \pm 0.5 \text{ mmolNm}^{-2}\text{d}^{-1}$ and $0.5 \pm 0.1 \text{ mmolNm}^{-2}\text{d}^{-1}$ respectively). The f -ratio also increased southwards, from 0.33 in the north to 0.69 in the south.

Sambrotto and Mace (2000) reported N-uptake rates and f -ratios from the western Pacific sector of the Southern Ocean along 170°W . Like Semeneh et al., (1998), they also reported high N-uptake rates for the late austral spring/ early summer (December); the column integrated nitrate and total N-uptake rates were as high as $10 \text{ mmolNm}^{-2}\text{d}^{-1}$ and $30 \text{ mmolNm}^{-2}\text{d}^{-1}$. He also found that a significant part of the N-uptake was from the surface waters and subsurface contribution was very less. During summer, new production reduced by an order of magnitude in the same

area. The f -ratio varied from 0.04 to 0.5; high f -ratios were measured at the ice edge during spring and lower f -ratios were measured during summer.

4.6 Chlorophyll a, nutrients and physical parameters during Feb-March 2006 in the Southern Indian Ocean

4.6.1 Chlorophyll-a

Chlorophyll was measured at all the stations in the Southern Ocean using a submersible fluorescence probe. The Southern Ocean showed significant variations in chlorophyll concentration. During the study period the maximum column integrated (integrated up to photic zone) chlorophyll concentration of 155 mgm^{-2} was found at the Antarctic coastal station. Integrated chlorophyll concentration decreased significantly towards the north and varied between 46 to 99 mgm^{-2} (Fig. 4.15 left panel), except at station PP4 where it was 144 mgm^{-2} . Chlorophyll profiles at different stations are shown in Fig 4.15-right panel.

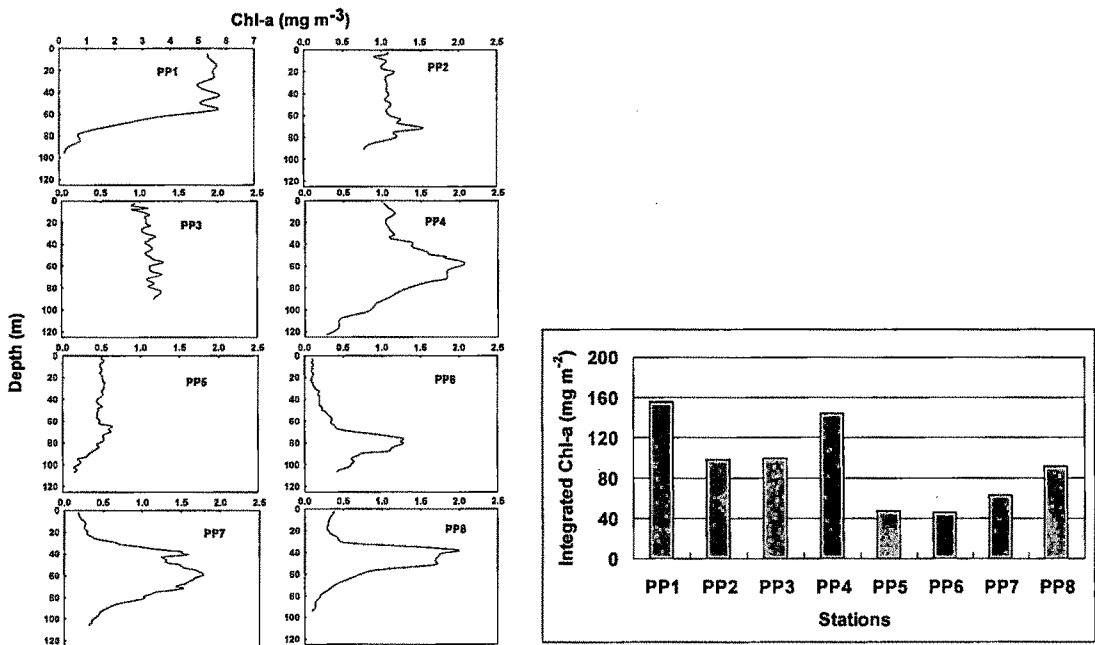


Fig. 4.15 Vertical profiles of Chl-a (left panel) and column integrated Chl-a (right panel) at different stations in the Southern Indian Ocean

In the Coastal zone of Antarctica (PP1) the chlorophyll was high; it varied between 2-6 mgm^{-3} in the adjoining areas. Though both green algae and diatoms were present, the latter dominated as they contributed to more than 65% of the total Chl-*a*. Though Chl varied between 4.97 to 5.74 mgm^{-3} in the upper layer, it was almost constant up to 55m. It decreased below, to a minimum of 0.2 at 96 m. Away from the coast, at PP2, surface Chl-*a* decreased significantly to 1.09 mgm^{-3} . Here also it was almost constant up to 60m, increased downward to reach a maximum of 1.55 mgm^{-3} at a depth of 71 m but again decreased downwards. Green algae dominated over diatoms at this station; green algae contributed more than 70% to the total Chl-*a*.

At PP3, Chl-*a* varied between 0.94 to 1.27 mgm^{-3} throughout the photic zone; green algae and diatoms contributed 60 and 40% of the total Chl concentration. Surface Chl at PP4 was similar to PP3 i.e, 1.02 mgm^{-3} but unlike PP3 it had a marked deep chlorophyll maximum (2.04 mgm^{-3}) at 56 m. Chlorophyll decreased to 0.28 mgm^{-3} at 123 m. Here also the green algae (>70%) dominated over the diatoms. Chlorophyll concentration decreased significantly to 0.49 mgm^{-3} in the surface waters of station PP5 and remained almost the same up to a depth of 63 m. It increased slightly to 0.63 mgm^{-3} at a depth of 65 m but again decreased to 0.15 mgm^{-3} at 107 m. A marked deep chlorophyll maximum was not present at this station. The concentration of diatoms reduced significantly at this station, green algae contributed more than 85% to the total Chl. Chlorophyll further decreased to 0.1 mgm^{-3} at PP6. A marked deep chlorophyll maximum was at a depth of 76 m where the chlorophyll concentration was 1.28 mgm^{-3} . Only green algae were present in upper water column; diatoms were not there in the water column up to a depth of 70 m.

The equatorial station (PP7 and PP8) exhibited similar characteristics in terms of chlorophyll in the water column. Both the stations had marked deep chlorophyll maximum at depths of 62 and 41 m respectively. Surface waters were devoid of diatoms, though they were present in the deeper waters.

4.6.2 Nutrients

Samples from all the stations and all corresponding depths were analysed for ambient nitrate concentrations. During the present study the nitrate concentrations found for the surface waters of the Southern Ocean were typical of that area. Vertical profiles of ambient nitrate at different stations in the Southern Ocean are shown in Fig 4.16. All stations had high nitrate concentrations ($\sim 20 \mu\text{M}$) in the surface and they remained high throughout the column. At PP6, the northernmost station in the Indian sector of the Southern Ocean, the ambient nitrate concentration was significantly less compared to other southern Ocean stations, $5.65 \mu\text{M}$.

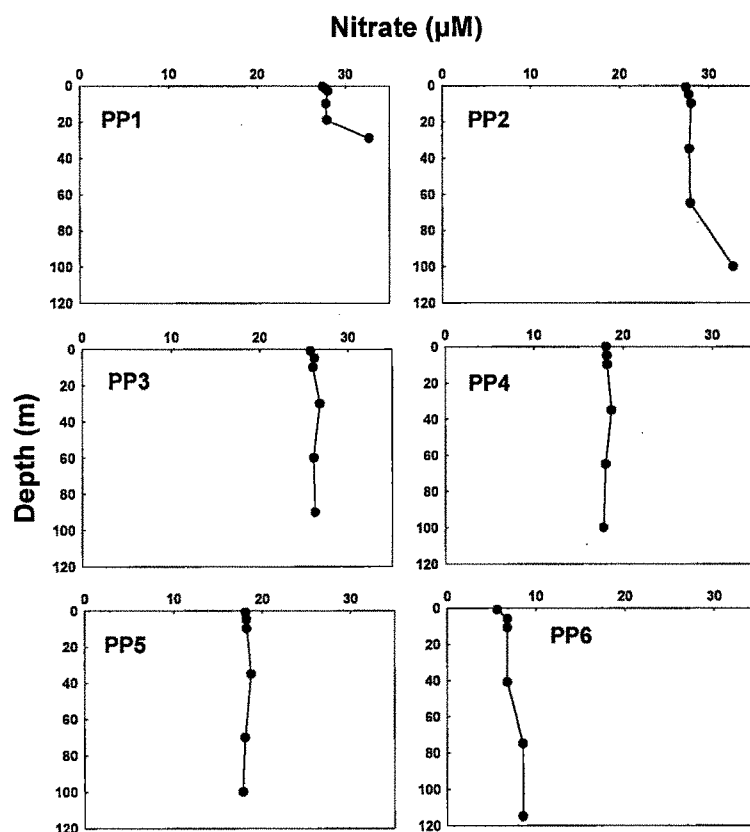


Fig. 4.16 Vertical profiles of ambient nitrate concentrations at different stations in the Southern Indian Ocean.

4.6.3 Hydrographic Conditions

The physical conditions encountered during the present study were typical of that area i.e., low sea surface temperature and deeper mixed layer in the south close to Antarctica and relatively shallow mixed layer in the north. Meridional variation in SST is shown in Fig. 4.17 where PP1 is the southern most station and PP8, a station in the equatorial Indian Ocean. In the areas adjoining Antarctic coast the SST was very low, lowest SST was -1.7°C . Though it increased slightly to -0.9°C at 65°S the low temperature zone continued up to 58°S where SST was 0.9°C . SST increased northwards to 11°C at PP4, a station south of subtropical front (STF). There was sharp rise in SST from 43°S to 40°S . 40°S marks the presence of STF in the Indian Ocean where the cold sub-antarctic water meets warm subtropical waters. In the equatorial region SST was almost the same. Southern Ocean close to the Antarctic coast is characterized by the presence of deep mixed layer. During the present study temperature based mixed layer depth (MLD) was more than 90 m at the station in the Antarctic waters, i.e., at PP1, PP2 and PP3 (Fig 4.18).

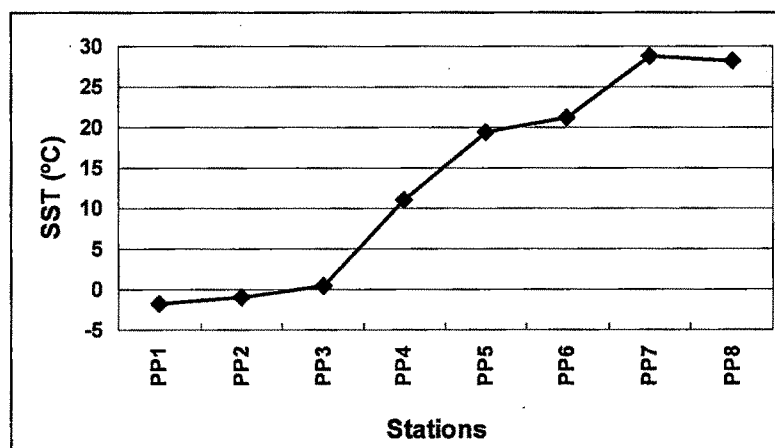


Fig. 4.17 SST (in $^{\circ}\text{C}$) at different stations in the Southern Indian Ocean

The presence of deep MLD in the Southern Indian Ocean causes entrainment of nutrients, mainly nitrate into the upper layer. Since these newly entrained nitrates are not utilized efficiently by the plankton present there, the upper layer water of this area rich in nutrients (nitrate) throughout a year. Absence of micro-nutrient iron is believed to be responsible for underutilization of these nitrates.

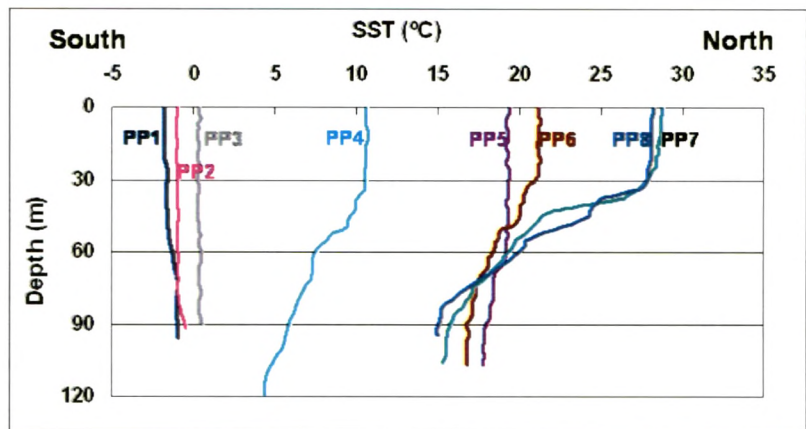


Fig. 4.18 Temperature-depth profiles at different stations in the Southern Indian Ocean. The stations in the south had deeper mixed layers compared to those in the north.

At PP4 at 43°S MLD decreased to 45 m. MLD again deepened to ~72 m at 40°S at STF. Temperature-depth profile of station PP6 (north of STF) was similar to that of PP4 (south of STF) but MLD at PP6 of 39 m was less than that at PP4. The equatorial Indian Ocean had almost similar temperature depth profiles; MLD at both the stations was 30 m.

4.7 ¹⁵N based productivity during late austral summer 2006

4.7.1 Total Production

The main aim of the present study was to characterize the Indian sector of the Southern Ocean on the basis of N-uptake rates and *f*-ratios. For the present study ¹⁵N measurements were done at six different stations in the Southern Ocean and at two different stations at the equatorial Indian Ocean. The rates of total N-uptake, integrated over the photic zone showed a significant variation in the Southern Indian Ocean. Euphotic zone integrated total N-uptake rate varied from 1.73 mmolNm⁻²d⁻¹ to 12.26 mmolNm⁻²d⁻¹ in the Southern Indian Ocean (Fig. 4.19).

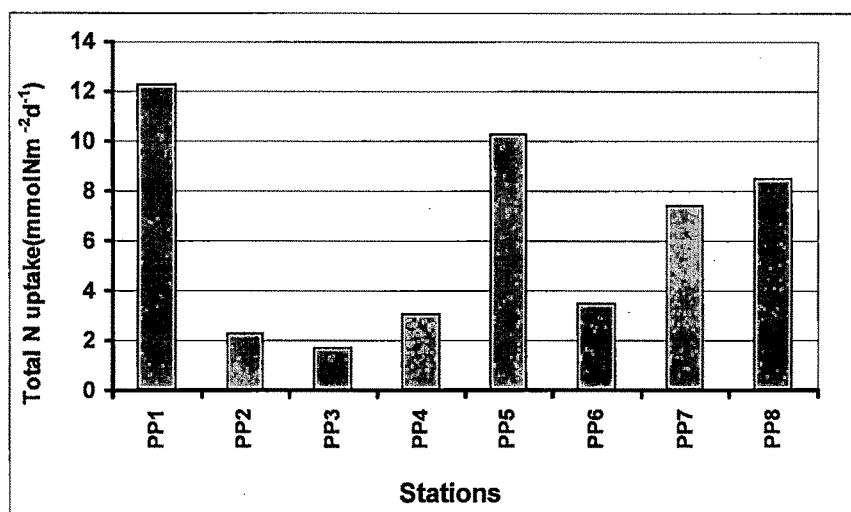


Fig 4.19 Total N-uptake rates at different stations in the Southern Indian Ocean

At station PP 1, which lies in coastal zone of Antarctica (69.18°S, 76°E), the total N uptake rate is very high ($\sim 12.3 \text{ mmolNm}^{-2}\text{d}^{-1}$), the highest observed during the present study. In terms of carbon, the total carbon uptake during late austral summer in the Antarctic coastal zone is $981.5 \text{ mgCm}^{-2}\text{d}^{-1}$. High carbon uptake rate in coastal regions of Antarctica was also reported by other authors (Treguer and Jacques, 1992). Probyn and Painting (1985) reported N-uptake as high as $5.91 \text{ mmolNm}^{-2}\text{hr}^{-1}$ (mean = $4.74 \text{ mmolNm}^{-2}\text{hr}^{-1}$) for a coastal station between the Cape Ann and Mawson. High production in this zone has also been reported by pCO_2 measurements by Poisson et al., (1994). The production here is high, because the coastal region receives ample nutrients from the Antarctic continent. These nutrients are derived through the coastal continental erosion and the run off contains significant amount of iron along with other major nutrients. At PP2, located to the north of PP1, N-uptake decreased drastically to $2.3 \text{ mmolNm}^{-2}\text{d}^{-1}$ ($\sim 183.8 \text{ mgCm}^{-2}\text{d}^{-1}$). Though ambient iron measurements were not done, we suspect that iron is not transported up to this station. This is because of the formation of Antarctic bottom water (AABW). During late summer, water near the Antarctic coast starts freezing (Vyas et al., 2004), leaving all the salts behind. This extra input of salt to the remaining water makes it very dense and it sinks to form AABW. The formation of

AABW takes place near the coast and during this process it carries unused nutrients, also the nutrients supplied through coastal erosion, along with it. This results in the absence of iron in the surface waters of the regions to the north of the Antarctic coast and limits the production farther from the coast. Productivity further decreased northwards and this low productivity zone extended up to the Sub-tropical front (STF) i.e., 40°S. The mean column N-uptake rate in this zone ($1.17 \pm 0.36 \text{ mmolNm}^{-2}\text{d}^{-1}$) is significantly less than those reported by Savoye et al., (2004) (mean = $5 \text{ mmolNm}^{-2}\text{d}^{-1}$) for the Australian sector of the Southern Ocean at similar latitudes. The decrease in productivity in this zone has been attributed to the strong stratification due to the melting of sea ice in summer by Treguer and Jacques, (1992). Also, silicon is considered as one of the limiting nutrients in this zone. Since the major species here are diatoms, because of the lack of silicon they are not able to proliferate. We have taken two stations, PP 3 and PP 4, in two different regimes: PP 3 in the zone of high Si concentration ($>30 \mu\text{M}$) and PP 4 in the zone of low Si concentration ($1\text{--}3 \mu\text{M}$). At PP 3, though the silicon concentration is more than that at PP 4, the productivity is less. Column N-uptake rates at PP 3 and PP 4 are $1.73 \text{ mmolNm}^{-2}\text{d}^{-1}$ ($\sim 138.2 \text{ mgCm}^{-2}\text{d}^{-1}$) and $3.05 \text{ mmolNm}^{-2}\text{d}^{-1}$ ($\sim 244 \text{ mgCm}^{-2}\text{d}^{-1}$) respectively. This variation in column production suggests that silicon is not the ultimate limiting nutrient in this area; rather, iron likely acts as a limiting nutrient. This is reflected in the photosynthetic efficiency (mgC/mgChl/hr) of phytoplankton present here. The photosynthetic efficiency of phytoplankton at PP 3 and PP 4 is very low ($\sim 0.08 \text{ mgC/mgChl/hr}$ and $0.26 \text{ mgC/mgChl/hr}$ respectively). This occurs due to the lack of micro nutrient, iron (Coale et. al., 2004; Martin et. al., 1991; Gervais and Riebesill 2002). Iron helps in the plant metabolism (Geider and La Roche 1994), and lack of iron may cause a decline in the photosynthetic electron transfer (Geider and La Roche 1994; Hutchins 1995) and this may decrease the photosynthetic efficiency of phytoplankton present there. There was a sudden increase in productivity at PP5 (40°S). Column N-uptake increased to $10.26 \text{ mmolNm}^{-2}\text{d}^{-1}$ ($\sim 821 \text{ mgCm}^{-2}\text{d}^{-1}$) but again decreased to $3.49 \text{ mmolNm}^{-2}\text{d}^{-1}$ ($\sim 279 \text{ mgCm}^{-2}\text{d}^{-1}$) at 35°S. The 40°S marks the presence of STF (sub-tropical front) which defines the northern boundary of the Antarctic Circumpolar Current (ACC) and it

separates the subtropical warm waters from sub-Antarctic cold waters (Sparrow and Heywood, 1996). This is marked by the sudden change of surface temperature (upto 4°C) and salinity (Stramma, 1992). Upwelling of the Antarctic intermediate water (AAIW) takes place at STF which triggers high carbon fixation. The upwelled water is carried northward as surface advection (Marinov et al., 2006) but its effect is not reflected on production at station north of STF *i.e.* PP 6 (35°S).

Two stations were sampled at the equatorial region of the Indian Ocean, an oligotrophic region with almost no nitrate in the surface. The equatorial Indian Ocean differs from the other two major oceans as it does not possess a mean equatorial upwelling regime, rather it is characterized by the seasonally reversing circulation pattern, similar to the Arabian Sea: Summer monsoon (Jul/Aug) and winter monsoon (Jan/Feb) (Schott et. al., 2002). Mean Column N-uptake rate at equatorial region was $\sim 8 \text{ mmolNm}^{-2}\text{d}^{-1}$ ($640 \text{ mgCm}^{-2}\text{d}^{-1}$). Despite being oligotrophic with almost no nutrient in the surface layer the productivity of this region was quite high, in fact higher than most of the stations in the Southern Ocean where the nutrients were present in plenty. This may be because it receives sufficient amount of atmospheric dust, rich in iron, from the Asian and the African continents.

4.7.2 New Production

In late austral summer the whole Southern Indian Ocean is characterized by high nitrate uptake and hence high new production. Euphotic zone integrated nitrate uptake rates or new production during late austral summer in the Indian sector of the Southern Ocean (Fig. 4.20) varied from $0.92 \text{ mmolNm}^{-2}\text{d}^{-1}$ to $7.7 \text{ mmolNm}^{-2}\text{d}^{-1}$. The highest new production of $616 \text{ mgCm}^{-2}\text{d}^{-1}$ was observed at the Antarctic coast and lowest of $73.6 \text{ mgCm}^{-2}\text{d}^{-1}$ (the lowest observed during the present study), at a station at 58°S. Nitrate was the main form of nitrogen preferred by plankton at all the stations in the Southern Indian Ocean except at a station north of STF at 35°S where reduced form of nitrogen was preferred. Over a large part of the Southern Ocean *i.e.* from north of Antarctic coastal zone to STF at 40°S, the nitrate uptake was low and varied from 0.92 to $1.58 \text{ mmolNm}^{-2}\text{d}^{-1}$ with a mean of $1.67 \pm 0.36 \text{ mmolNm}^{-2}\text{d}^{-1}$.

Though low new production ($0.64 \pm 0.36 \text{ mmolNm}^{-2}\text{d}^{-1}$) in this region has also been reported earlier (Slawyk 1979), new production during the present study is higher.

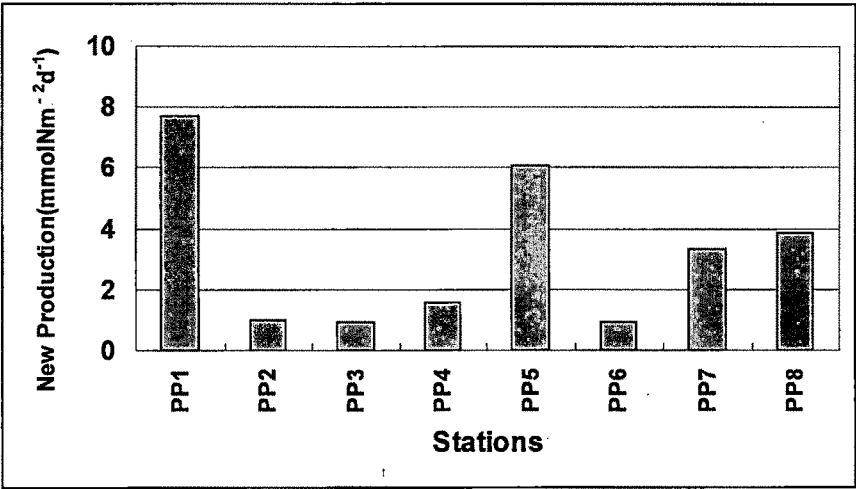


Fig. 4.20 New production at different stations in the Southern Indian Ocean

New production increased at PP5 to $6.05 \text{ mmolNm}^{-2}\text{d}^{-1}$; it was more than four times the new production at the previous stations but decreased again to $0.96 \text{ mmolNm}^{-2}\text{d}^{-1}$ at PP6. At the equatorial region new production remained almost the same; mean new production was $3.62 \text{ mmolNm}^{-2}\text{d}^{-1}$.

The plot of total N-uptake (on x-axis) and nitrate uptake (on y-axis) shows very significant correlation between the two: $y = (0.63 \pm 0.06) x - (0.66 \pm 0.42)$ (coefficient of determination, $r^2 = 0.95$; Fig. 4.21.). The slope of line of regression suggests the maximum possible value of f -ratio (0.63) for this zone. The plot also suggests that the minimum regenerated production for this region is $\sim 1 \text{ mmolNm}^{-2}\text{d}^{-1}$. This large area is traditionally regarded as a low productive area where the surface nutrients are not utilized fully. Our measurements show that even though the productivity over a large area of the Southern Ocean is low, the f -ratio is moderately high. This signifies that a large part of production could get transported to deeper ocean and thus this area has the potential to play a significant role in atmospheric carbon sequestration.

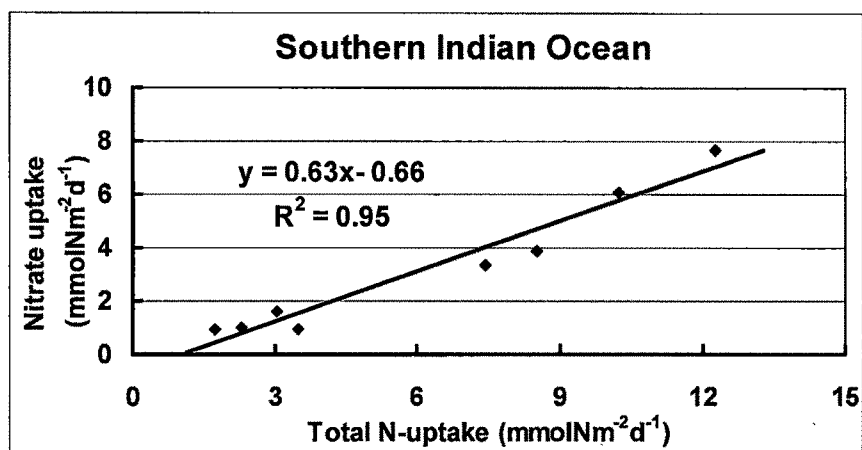


Fig 4.21 Relationship between total N uptake and nitrate uptake in the Southern Indian Ocean

4.7.3 Regenerated production

Ambient ammonium and urea measurements could be done during the present study and hence a conservative estimate of ammonia and urea uptake rates, their sum is regenerated production, was made assuming that water column was devoid of ammonium and urea (Fig 4.22). Ammonium uptake rates varied from 0.54 $\text{mmolNm}^{-2}\text{d}^{-1}$ at PP2 north of Antarctic Coastal zone to 3.30 $\text{mmolNm}^{-2}\text{d}^{-1}$ over the study area in the coastal region of Antarctica. At PP1 ammonium uptake rate was almost half of the nitrate uptake rate. Away from the coastal zone ammonium uptake decreased drastically; the mean ammonium uptake rate in the Southern ocean, between north of Antarctic coast up to south of STF (40°S), was 0.70 ± 0.25 $\text{mmolNm}^{-2}\text{d}^{-1}$. Ammonium uptake increased significantly at STF to 2.53 $\text{mmolNm}^{-2}\text{d}^{-1}$.

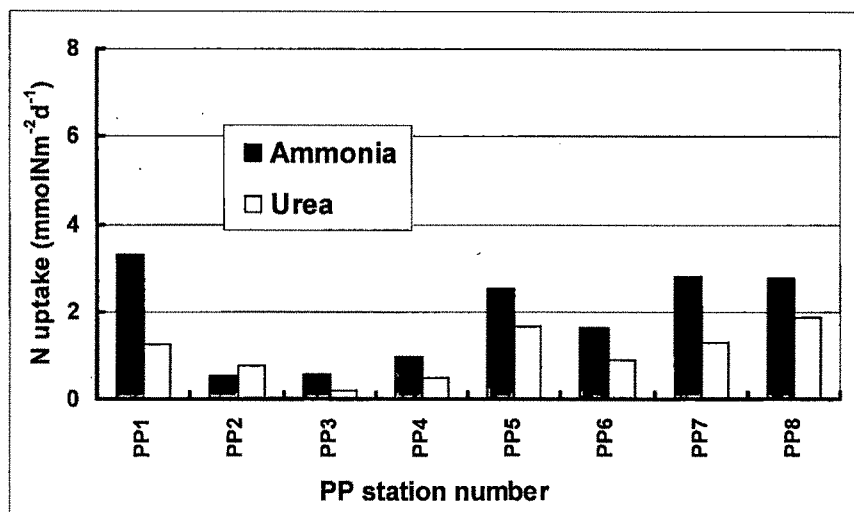


Fig. 4.22 Ammonium and urea uptake rates at different stations in the Southern Indian Ocean. Both the estimates are conservative.

North of STF at PP6 ammonium uptake decreased slightly to $1.61 \text{ mmolNm}^{-2}\text{d}^{-1}$. This may be the effect of very high production at PP 5, resulting in high regeneration there and some portion of this regenerated nutrients get transported to the north by the northward moving Antarctic intermediate water. The presence of regenerated nutrients such as ammonium inhibits the nitrate uptake (Mengesha et al. 1998). The same seems to hold true at PP 6. In the equatorial region of the Indian Ocean the ammonium uptake at both the stations was almost the same, $\sim 2.78 \text{ mmolNm}^{-2}\text{d}^{-1}$.

Conservative estimate of ammonium varied from 0.22 to $1.86 \text{ mmolNm}^{-2}\text{d}^{-1}$ over the study area. At PP1, the coastal station, urea uptake rate was almost one third of the ammonium uptake rate and one sixth of the nitrate uptake rate. Mean urea uptake rate in the Southern Ocean between 65°S to 40°S was $0.49 \text{ mmolNm}^{-2}\text{d}^{-1}$. At STF i.e., at 40°S (PP5) urea uptake rate was thrice and at 35°S (PP6) it was almost double of that at Southern Ocean. The equatorial Indian Ocean did not show significant variation in the urea uptake rate; it was $1.30 \text{ mmolNm}^{-2}\text{d}^{-1}$ and $1.86 \text{ mmolNm}^{-2}\text{d}^{-1}$ at PP7 and PP8 respectively.

4.7.4 *f*-ratios in the Southern Ocean

The *f*-ratios presented here for the Southern Indian Ocean represent the upper bound since they were calculated using the conservative estimates of ammonium and urea uptake rates. The *f*-ratio in the Southern Ocean was moderately high (Fig 4.23); the mean *f*-ratio for the southern ocean stations, i.e., from PP1 to PP6, was 0.50. This was significantly lower than the values reported by Collos and Slawyk (1986) for the Indian Sector waters along 66.5°E transect. They reported *f*-ratios as high as 0.98 from a station at 43°S on the same longitudinal transect. The present study also had a station PP4 on the same latitude but at 48°E. The *f*-ratio here was 0.52, almost half of the value reported by Collos and Slawyk. Savoye et al., 2004 has also reported high *f*-ratio (0.55) from the Australian sector of the Southern Ocean on similar latitudes. Mengesha et al., 1998 has reported *f*-ratio varying from 0.17 to 0.63 with the mean of 0.39 from Kerguelen area in the Indian Ocean. The *f*-ratio of 0.50 indicates that the autotrophic community was based equally on nitrate as well as regenerated nutrients where ammonium and urea contributed to 50% of the total productivity. Mean *f*-ratio of 0.50 has also been reported by others for different sectors of the Southern Ocean; Smith and Nelson (1990) reported mean *f*-ratio of 0.53 during spring for the Weddell Sea. Goeyens et al., (1991) reported a mean *f*-ratio of 0.58 for the same region and the same season. During the present study the highest *f*-ratio was observed at the Antarctic Coast and the lowest at PP6, a station north of STF. The *f*-ratio of 0.63 for the Antarctic coastal water is one and half times of the value (0.42) reported by Probyn and Painting (1985) for the coastal waters. The *f*-ratio was low (0.27) at PP6 a consequence of high production at PP5 which resulted in high regeneration, some portion of which could have been transported to the north by the northward moving Antarctic intermediate water.

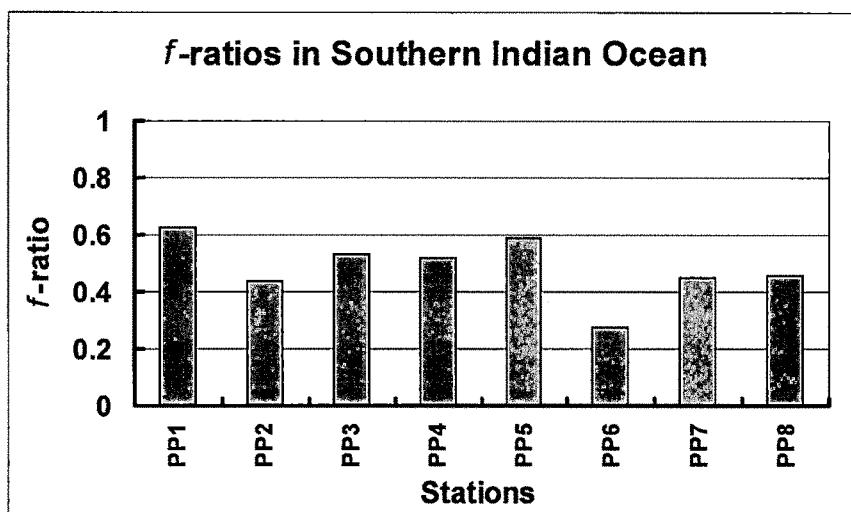


Fig. 4.23 f -ratios at different stations in the Southern Indian Ocean.

Previous studies from the Pacific and Atlantic sectors of the Southern Ocean (Probyn and Painting 1985; Smith and Nelson 1990; Smith 1991; Treguer and Jacques 1992) showed that phytoplankton growth in open ocean areas of the Southern Ocean largely depended upon ammonium for its nitrogen need and hence the f -ratio was relatively low. Mengesha et al. (1998) reported low mean specific nitrate and ammonium uptake rates during summer (0.0011 hr^{-1} and 0.0018 hr^{-1} respectively; urea was not measured) from transect along 62°E for the austral summer, 1994. The f -ratio varied from 0.17 to 0.63 with the mean of 0.39. We observed consistently higher nitrate uptake rates (0.0052 hr^{-1}) during summer 2006, but ammonium specific uptake rate (0.0013 hr^{-1}) was comparable with value reported by Mengesha et al. (1998). Specific urea uptake rate during our study was 0.0011 hr^{-1} . High specific nitrate uptake rate and increased f -ratio indicate a probable shift in the regime, from regenerated to new production in the last 12 years but more data are required, on larger temporal and spatial scales, to substantiate this preliminary observation. This signifies also that a large part of surface production could get transported to the deep and thus this area has the potential role in atmospheric carbon sequestration, under a favorable micronutrient regimes.

4.8 Iron experiment

All iron experiments have proved beyond doubt that the Southern Ocean is iron limited and addition of iron enhances productivity. However, the effect of iron on uptake of different N-substrates is still poorly known. Only a few studies (Van Leeuwe et al., 1997; Reay et al., 2001) determined the effect of iron enrichment on the uptake of different substrates such as nitrate, ammonium and urea. The present work is the first such study in the Indian sector of the Southern Ocean. We carried out bottle scale ^{15}N tracer-iron enrichment experiment in the Indian Sector of the Southern Ocean at two different stations to get a preliminary estimate of the role of iron on productivity and on individual nutrient uptake rates and f -ratios.

Station IEE1 lay in typical Southern Ocean waters, i.e., south of sub-tropical front, and IEE2 lie north of STF. The 40° - 41°S latitude marks the presence of STF (sub-tropical front) in the Indian Ocean which defines the northern boundary of the Antarctic Circumpolar Current (ACC) and it separates the subtropical warm waters from sub-Antarctic cold waters (Sparrow and Heywood 1996). This is marked by the sudden change of surface temperature (upto 9°C) and salinity (Stramma 1992). Upwelling of the Antarctic intermediate water (AAIW) takes place at STF which triggers high carbon uptake. The upwelled water is carried northward as surface advection (Marinov et al., 2006). During the present study STF was located at 41°S and was marked by large temperature gradient (Srivastava et al., 2007). The same is reflected in SST at IEE1 and IEE2 as well; SST at IEE1 & 2 was 11.3°C and 20.3°C respectively. Euphotic zone depth was 100 m and 115 m and temperature-based mixed layer depth was 45 m and 39 m at IEE1 and 2 respectively. The nitrate concentration was 18.1 and $8.6\ \mu\text{M}$ and silicate concentration was $1.66\ \mu\text{M}$ and $0.3\ \mu\text{M}$ respectively at both the stations. The concentration of nitrate and silicate both decreased significantly at IEE2 compared to IEE1. Both these stations lay in a low silicate zone (Coale et al., 1996) where silica concentration in the surface waters is not enough to support large population of diatoms. This was reflected in surface chlorophyll and species composition as well: at IEE1 surface chlorophyll was $\sim 1\ \mu\text{g l}^{-1}$ where green algae were the dominant species contributing more than 65% of the total Chl a . Euphotic zone integrated Chl a was significantly high $\sim 134\ \text{mg m}^{-2}$. At

IEE2 surface chlorophyll was significantly less ($0.1 \mu\text{g l}^{-1}$) and euphotic zone integrated chlorophyll was $\sim 49 \text{ mgm}^{-2}$, significantly less compared to IEE1. Diatoms were absent at this station and only green algae contributed to the total chlorophyll.

The results of nitrate, ammonium and urea uptake and the f -ratios, from both the stations, under controlled and enriched iron conditions are shown in Table 4.1 and 4.2 respectively.

Duration of Incubation (in hrs)	Nitrate uptake (nM N)		Ammonium uptake (nM N)		Urea uptake (nM N)		Total N- uptake (nM N)		f -ratio	
	No Iron	With Iron	No Iron	With Iron	No Iron	With Iron	No Iron	With Iron	No Iron	With Iron
24	29	19	11	6	17	17	58	42	0.50	0.44
48	24	73	12	21	14	41	50	134	0.47	0.54
72	12	36	10	24	11	47	33	107	0.38	0.34

Table 4.1. Nitrate, ammonium and urea uptake and the f -ratios at station IEE 1 under controlled and enriched iron conditions

Duration of Incubation (in hrs)	Nitrate uptake (nM N)		Ammonium uptake (nM N)		Urea uptake (nM N)		Total N- uptake (nM N)		f -ratio	
	No Iron	With Iron	No Iron	With Iron	No Iron	With Iron	No Iron	With Iron	No Iron	With Iron
24	28	30	39	74	36	31	103	136	0.27	0.22
48	31	31	48	53	72	52	151	135	0.20	0.23
72	37	23	70	5	71	63	178	91	0.21	0.26

Table 4.2. Nitrate, ammonium and urea uptake and the f -ratios at station IEE 2 under controlled and enriched iron conditions

At IEE1 the total N-uptake did not show any significant change (within the uncertainty limit) in the 1st 24 hrs. This clearly suggests that even a sudden supply of a large amount of dissolved iron was not able to simulate nitrogen uptake. In other words, usually Fe-starved phytoplankton were not able to respond immediately to this Fe-feast but were responding to the same as the time progressed. This is why N-uptake increased almost thrice under Fe enrichment compared to the control case at the end of 48 hours; nitrate and urea uptake increased more than

three-fold and ammonium uptake increased two-fold. An increase in the absolute nitrate uptake by a factor of 15 in another silicon-poor zones in the Pacific sector of the Southern Ocean has been reported earlier (Coale et al., 2004). In HLNC area of the equatorial Pacific Ocean iron enrichment caused 14-fold increase in the nitrate uptake on 6th day (Coale et al., 1996); it increased from $<10 \text{ nMhr}^{-1}$ to 133 nMhr^{-1} ; the effect of iron enrichment on ammonium and urea uptake were not studied earlier. An increase in specific nitrate uptake rate, under iron enrichment, has also been reported from the Southern Ocean sector of the Atlantic Ocean (Coale et al., 1996). The same effect of iron enrichment could not be seen at IEE2 on the total N-uptake; within the limit of uncertainty, it remained almost the same in “control” and “enriched” condition. This may be because the water here is not Fe-starved. Station IEE2 lay north of STF, in a zone where upwelled Antarctic intermediate water (AAIW) is getting advected. This water may be transporting macro-nutrients iron with it. As plankton of this station is not Fe-starved, they are not responding to iron enrichment.

The f -ratio did not show any significant change due to iron enrichment at IEE1 during the 1st and the 2nd day but it reduced slightly on the 3rd day in both the, “control” as well as “enriched”, sets. The f -ratio has reported to increase from 0.1-0.2 to 0.3-0.4 on Fe-enrichment in silica depleted zone of the Southern Pacific (Coale et al., 2004). This result was based on nitrate uptake and carbon uptake measurements; ammonium and urea uptake rates were not measured. During the present study Fe-enrichment not only enhanced nitrate uptake but they increased ammonium and urea uptake as well and this is the reason their net effect on f -ratio could not be observed at IEE1. The f -ratio showed considerable variation; it varied from 0.68 to 0.85 in spring and from 0.17 to 0.63 in summer in Indian sector Southern Ocean waters near Kerguelen Island (Mengesha et al., 1998). A mean f -ratio of 0.42 in coastal zone and 0.68 in the open ocean zone has also been reported for the Prydz Bay area (Semeneh et al., 1998). The f -ratio from the western Pacific sector of the Southern Ocean along 170°W has been reported to vary from 0.04 to 0.5; high f -ratios were measured at the ice edge during spring and lower f -ratios were measured during summer (Sambrotto and Mace 2000). At IEE2 also no significant change was observed in the f -ratio

because of iron enrichment; it remained almost the same in both, “control” and “enriched”, conditions.

In summary, preliminary results of ^{15}N tracer-Fe enrichment experiment from IEE1 suggests that addition of iron does not enhance primary productivity during the initial stage of the enrichment but takes some time to increase the uptake. The availability of iron increases uptake of all substrates of nitrogen *i.e.*, nitrate, ammonium and urea. This was clearly reflected in enhancement in uptake rates of all substrates at station IEE1 under “enriched condition”. This is in contrast to the earlier belief that availability of iron enhances uptake of nitrates only and not of ammonium and urea. As it enhanced uptake of all forms of nitrogen at IEE1, the *f*-ratio remained almost the same under both, “control” and “enriched” conditions. One of the major limitations of the present study is unavailability of ambient iron concentration in the surface waters of the Indian sector of the Southern Ocean and this needs to be incorporated in future investigations to understand the effect of iron on N-uptake rates in a better way.

4.9 Conclusions

The results from the equatorial Indian Ocean are:

1. Total N-uptake was low: it varied from $0.66 \text{ mmolNm}^{-2}\text{d}^{-1}$ to $2.23 \text{ mmolNm}^{-2}\text{d}^{-1}$. Mean N-uptake was $1.32 \text{ mmolNm}^{-2}\text{d}^{-1}$ ($105.6 \text{ mgCm}^{-2}\text{d}^{-1}$)
2. New production along the 77°E transect was $0.20 \text{ mmolNm}^{-2}\text{d}^{-1}$ ($16 \text{ mgCm}^{-2}\text{d}^{-1}$), almost half of that $0.43 \text{ mmolNm}^{-2}\text{d}^{-1}$ ($34.4 \text{ mgCm}^{-2}\text{d}^{-1}$) along the 83°E transect.
3. The *f*-ratio was low though it showed considerable spatial variation: it varied from 0.14 to 0.40. The *f*-ratio was low along 77°E (mean = 0.18) transect but was relatively high along 83°E (mean = 0.29).
4. Urea was the most preferred form of nitrogen for phytoplankton followed by ammonium. Nitrate was the least preferred.
5. Upper mixed had greater control on the productivity of this region. Since this layer was devoid of any nutrients, the productivity was less. Also due to strong stratification the export production was low.

The results from the Southern Indian Ocean are:

1. Euphotic zone integrated total uptake rate varied from $1.73 \text{ mmolNm}^{-2}\text{d}^{-1}$ ($138 \text{ mgCm}^{-2}\text{d}^{-1}$) to $12.26 \text{ mmolNm}^{-2}\text{d}^{-1}$ ($981 \text{ mgCm}^{-2}\text{d}^{-1}$) in the Southern Indian Ocean; the highest rate was measured in the Antarctic coastal zone (69°S).
2. New productivity varied from $0.92 \text{ mmolNm}^{-2}\text{d}^{-1}$ ($73.6 \text{ mgCm}^{-2}\text{d}^{-1}$) to $7.7 \text{ mmolNm}^{-2}\text{d}^{-1}$ ($616 \text{ mgCm}^{-2}\text{d}^{-1}$). The Antarctic coastal zone, equatorial region and STF had more new production compared to other regions of the Southern Ocean.
3. Mean total uptake in a large part of the Southern Ocean was very low. It was $1.73 \text{ mmolNm}^{-2}\text{d}^{-1}$ ($138 \text{ mgCm}^{-2}\text{d}^{-1}$), almost one-seventh of the Antarctic coastal zone.
4. Productivity suddenly increased to $10.26 \text{ mmolNm}^{-2}\text{d}^{-1}$ ($821 \text{ mgCm}^{-2}\text{d}^{-1}$) at sub-tropical front (STF) where Antarctic cold water and subtropical warm water meets.
5. The f -ratio varied from 0.27 to 0.63 in the Southern Ocean with a mean of 0.50 with an upper limit of 0.63.
6. Mean Column N-uptake rate at two equatorial stations sampled during this study was $\sim 8 \text{ mmolNm}^{-2}\text{d}^{-1}$. The f -ratio was almost the same (0.45) at both stations.
7. Preliminary results of ^{15}N tracer-Fe enrichment experiment suggests that addition of iron does not enhance primary productivity during the initial stage of the enrichment but takes some time to increase the uptake.
8. In contrast to the earlier belief that availability of iron enhances uptake of nitrates only and not of ammonium and urea the present study suggest that it enhances uptake of all forms of nitrogen and hence does not appear to affect the f -ratio significantly.

These results are the first comprehensive estimates of nitrogen based productivity in a large area in the Southern Indian Ocean. Relatively higher productivity was measured in Antarctic coastal zone, STF and equatorial Indian

Ocean. A large part of the southern Ocean, HNLC region, is less productive but can have high export production, almost 50% of the total. The f -ratio was moderately high here. Compared to other data from similar regions (Mengesha et al., 1998, Savoye et al., 2004) the present study shows a shift in productivity regime from regenerated nutrient based production to nitrate based production. This means a slightly greater export production in this region than before. Again, a significant correlation between total and new productivity can provide a significant input for the estimation of carbon fluxes over a large region using satellite data.

Chapter Five

Conclusions and Scope for Future Work

Biogeochemical processes including the marine carbon cycle are the key factors in global change. The ocean works as a net sink for CO₂, a potential greenhouse gas, through biological pump. The present study brings new data on oceanic productivity using ¹⁵N tracer technique which not only gives total productivity but also categorise it into new and regenerated productivity; new productivity indirectly gives an estimation of the export production i.e., amount of carbon that is getting removed from the atmosphere for a sufficiently longer time scale through biological activities. For the first time, ¹⁵N based productivity has been measured in the equatorial Indian Ocean. It also provides comprehensive data on new and regenerated productivity and *f*-ratios of the northeastern Arabian Sea and the southern Indian Ocean and has made an effort to assess the role of the Indian Ocean in the Global Carbon Cycle. The important results that have emerged from this study have been summarised below:

5.1 The northeastern Arabian Sea

The results from the new productivity measurements during the late winter monsoon are:

- The Arabian Sea was characterized by the presence of two different biogeochemical provinces during the late winter monsoon: low productive southern province and highly productive northern province with an overall increasing trend from the south to the north.
- Total productivity in the southern region averaged around 5.5 mmolNm⁻²d⁻¹ (440 mgCm⁻²d⁻¹) whereas in the north it was 19 mmolNm⁻²d⁻¹ (1520 mgCm⁻²d⁻¹); increase in productivity from the south to north was more than three fold.
- New productivity also increased on south-north transect, from 2.1mmolNm⁻²d⁻¹ (168 mgCm⁻²d⁻¹) in the south to 15.7 mmolNm⁻²d⁻¹ (1256 mgCm⁻²d⁻¹) in the north. Increase in new productivity was more than 7-fold.
- High nitrate uptake during the *Noctiluca* bloom at the northern stations measured during the present study, in accordance with Bienfang et al.,

(1990), suggests the developing phase of the bloom where nitrate contributed most to the total N-uptake.

- Urea uptake rate was higher than the ammonium uptake rate at all the non-bloom stations but during the *Noctiluca* bloom in the northern stations, ammonium was preferred over urea by the plankton.
- The column integrated total production (x) and new production (y), show a significant correlation (Fig.2): for non-bloom stations: $y = (0.44 \pm 0.23) x - (0.30 \pm 1.38)$; (coefficient of determination, $r^2 = 0.43$) and for bloom stations, $y = (1.08 \pm 0.23) x - (4.68 \pm 4.46)$; ($r^2 = 0.91$). The slope of regression (i.e., 0.44 and 1.0 for non-bloom and bloom stations respectively) is the maximum possible value of the *f*-ratio.

The results from productivity measurements during early winter monsoon:

- During the early winter monsoon total productivity varied from 4.07 mmolNm⁻²d⁻¹ (326 mgCm⁻²d⁻¹) to 23.31 mmolNm⁻²d⁻¹ (1865 mgCm⁻²d⁻¹) with a mean of 8.65 mmolNm⁻²d⁻¹ (692 mgCm⁻²d⁻¹). Productivity during this season was almost half of that during the bloom but was more than the productivity in the south during the late winter monsoon.
- New productivity showed a large variation; it varied from a low of 1.95 mmolNm⁻²d⁻¹ (156 mgCm⁻²d⁻¹) to a high of 19.70 mmolNm⁻²d⁻¹ (1576 mgCm⁻²d⁻¹).
- Ammonium uptake was more than urea uptake at all the stations unlike those during the late winter monsoon. Also the mean ammonium uptake rate was more than that during the late winter but urea uptake was almost half.
- The *f*-ratio varied from 0.46 to 0.87. This suggests that 46-87% of the total productivity can be exported to the deep under a steady state condition. Relation between total and new productivity yielded a slope of 0.88 which suggests that at the most 88% of the total productivity can be exported.

In general, results from the present study suggest almost three fold increase in the total productivity during the developing phase of the *Noctiluca* bloom. This

increase was more than seven fold in new productivity. During early winter monsoon, total and new productivity was less than those during the bloom but was more compared to non-bloom southern regions. The most important finding of the present study for the eastern Arabian Sea is the identification of two different biogeochemical provinces during the late winter monsoon where the northern province was four times more productive than the southern. Above results from the two seasons suggests that productivity in the Arabian Sea is heterogeneous in space and time but still this basin is capable of high export production, with moderately high f -ratio during non-bloom period and very high f -ratio during *Noctiluca* bloom period, and thus plays a significant role in global carbon cycle.

5.2 The equatorial Indian Ocean

The results from the equatorial Indian Ocean are:

- Total N-uptake was very less: it varied from $0.66 \text{ mmolNm}^{-2}\text{d}^{-1}$ to $2.23 \text{ mmolNm}^{-2}\text{d}^{-1}$. Mean N-uptake was $1.32 \text{ mmolNm}^{-2}\text{d}^{-1}$ ($105.6 \text{ mgCm}^{-2}\text{d}^{-1}$)
- New production along 77°E transect was $0.20 \text{ mmolNm}^{-2}\text{d}^{-1}$ ($16 \text{ mgCm}^{-2}\text{d}^{-1}$), almost half of the same $0.43 \text{ mmolNm}^{-2}\text{d}^{-1}$ ($34.4 \text{ mgCm}^{-2}\text{d}^{-1}$) along 83°E transect.
- The f -ratio was low though it showed considerable spatial variation: it varied from 0.14 to 0.40. The f -ratio was low along 77°E (mean = 0.18) transect but was relatively high along 83°E (mean = 0.29).
- Urea was the most preferred form of nitrogen for phytoplankton followed by ammonium. Nitrate was the least preferred.
- Upper mixed had greater control on the productivity of this region. Since this layer was devoid of any nutrients, the productivity was less. Also due to strong stratification the export production was low.

The present study was the first step towards understanding the biogeochemistry of the equatorial Indian Ocean. The results from this region suggest that mixed layer has greater control on the productivity. Total and new production

were very less in this layer and so the f -ratio. Reduced forms of nitrogen were preferred over nitrate.

5.3 The Southern Indian Ocean

The results from the Southern Indian Ocean are:

- Euphotic zone integrated total uptake rate varied from $1.73 \text{ mmolNm}^{-2}\text{d}^{-1}$ ($138 \text{ mgCm}^{-2}\text{d}^{-1}$) to $12.26 \text{ mmolNm}^{-2}\text{d}^{-1}$ ($981 \text{ mgCm}^{-2}\text{d}^{-1}$) in the Southern Indian Ocean; the highest rate was measured in the Antarctic coastal zone (69°S).
- New productivity varied from $0.92 \text{ mmolNm}^{-2}\text{d}^{-1}$ ($73.6 \text{ mgCm}^{-2}\text{d}^{-1}$) to $7.7 \text{ mmolNm}^{-2}\text{d}^{-1}$ ($616 \text{ mgCm}^{-2}\text{d}^{-1}$). The Antarctic coastal zone, equatorial region and STF had more new production compared to other regions of the Southern Ocean.
- Mean total uptake in a large part of the Southern Ocean was very low. It was $1.73 \text{ mmolNm}^{-2}\text{d}^{-1}$ ($138 \text{ mgCm}^{-2}\text{d}^{-1}$), almost one-seventh of the Antarctic coastal zone.
- Productivity suddenly increased to $10.26 \text{ mmolNm}^{-2}\text{d}^{-1}$ ($821 \text{ mgCm}^{-2}\text{d}^{-1}$) at sub-tropical front (STF) where Antarctic cold water and subtropical warm water meet.
- The f -ratio varied from 0.27 to 0.63 in the Southern Ocean with a mean of 0.50 with an upper limit of 0.63.
- Mean Column N-uptake rate at two equatorial stations sampled during this study was $\sim 8 \text{ mmolNm}^{-2}\text{d}^{-1}$. The f -ratio was almost the same (0.45) at both stations.

While a large area of the Southern Indian Ocean is not highly productive, it appears capable of moderate export productivity and thus could be significant in removing atmospheric CO_2 on longer time scales. Relatively high productivity was measured in Antarctic coastal zone, STF and equatorial Indian Ocean. A large part of the Southern Ocean, HNLC region, is less productive but can have high export production, almost 50% of the total. A mean f -ratio of 0.50 in the Southern Ocean

indicates that the autotrophic community uses nitrate as well as regenerated nutrients equally. Compared to other data from similar regions (Mengesha et al., 1998, Savoye et al., 2004) the present study shows a shift in productivity regime from regenerated nutrient based production to nitrate based production, in the last 12 years, possibly due to global warming. This means a slightly greater export production in this region than before. These results are the first comprehensive estimates of nitrogen based productivity in a large area in the Southern Indian Ocean. Again, a significant correlation between total and new productivity can provide a significant input for the estimation of carbon fluxes over a large region using satellite data.

5.4 Scope for future work

Even though some major programmes such as JGOFS and BOBPS have been conducted, a large part of the Indian Ocean still lacks good data coverage, especially the equatorial Indian Ocean and the Southern Ocean. Even though the Arabian Sea has received some attention of oceanographers all over the world for being dynamic in space and time, the major emphasis has been given to the central and western Arabian Sea; the northeastern Arabian Sea is relatively less studied. In order to understand the role of the Indian Ocean, as a whole, in the global carbon cycle we need much more comprehensive understanding of the primary and export productions taking place in this part of the world ocean. For this we need more such observations pertaining to the estimation of new production and the f -ratio. The following issues can be addressed in future research:

- A. The most widely spread form of *Noctiluca scintillans* is completely heterotrophic and is red in colour, survives on a wide range of prey such as phytoplankton and micro-zooplankton [Hansen et al., 2004]. The present study is among the first few works (Sanjeev Kumar et al., 2008) which has highlighted the occurrence of green *Noctiluca* bloom in the northeastern Arabian Sea, enhancing the total as well as new productivity. During this period, the f -ratio may be as high as 0.91. Simultaneous measurement of export flux using other techniques such as sediment trap or ^{234}Th along with ^{15}N tracer technique will also be useful in understanding the role of this basin

in atmospheric carbon sequestration. More studies during the bloom, using nitrogen isotopes, will give a better insight into the biogeochemical properties of this part of the world ocean. More number of studies will also help in establishing whether the biogeochemical divide of northeastern Arabian Sea during bloom was a separate event or was a regular phenomenon.

- B. High productivity events of Arabian Sea is followed by the formation of oxygen minimum zone in sub-surface layer as the concentration of dissolved oxygen with 150-1000 m decreases to less than 0.1 ml/l (Naqvi and Jayakumar 2000). This causes vigorous denitrification, a process through which the ocean loses biologically available nitrogen, where bacteria begin to utilize oxygen derived from NO_3 instead of O_2 for decomposing organic debris. So far, no attempt has been done to study the formation of oxygen minimum zone followed by winter bloom. Quantification of denitrification which follows the bloom of winter monsoon is important to estimate the carbon and nitrogen budget and hence it needs to be incorporated in the future studies.
- C. Planktonic marine cyanobacteria called *Trichodesmium* fixes atmospheric nitrogen during photosynthesis (Capone et al., 1997) and thus they are the source of new nitrogen to the marine cycle (Karl et al., 1997). No direct measurement has been done to quantify N_2 fixation by these cyanobacterium in the Arabian Sea. Direct estimation N_2 fixation in future, using $^{15}\text{N}_2$ tracer, will help understanding the nitrogen cycle of this basin in a better way.
- D. A major limitation of the present study is the unavailability of ambient ammonium and urea concentrations leading to conservative estimate of regenerated production. In the absence of these measurements, regenerated production is often underestimated and thus the f -ratio is overestimated. Even though the Arabian Sea is one of the most studied regions of the world ocean data pertaining to the ambient ammonium and urea measurements are limited.

The same holds true for equatorial Indian Ocean and the southern Indian Ocean. A thorough understanding of the nutrient regimes in these basins will provide immense information about the productivity regimes.

- E. Unavailability of bio-available iron is believed to limit primary production in a large part of the Southern Ocean. A number of large scale iron enrichment experiments have been done in the recent past in different parts of the Southern Ocean to ascertain the role of iron in limiting marine biological productivity but still no such experiment has been carried out in the Indian sector of the Southern Ocean. A study of effect of iron enrichment on the nitrogen uptake rates will give a better insight into the biogeochemistry of the Southern Ocean.
- F. ^{15}N tracer technique can be effectively combined with ^{13}C . A coupled tracer techniques for the estimation of primary and new production may give a better understanding of the productivity regimes and nutrients kinetics and so quantification of new productivity using this technique should be the course of research in the future.

REFERENCES

- Allen C. B. et al. (1996) New production and photosynthetic rates within and outside a cyclonic mesoscale eddy in the north Pacific subtropical gyre, *Deep Sea Research*, **43**, 917-936.
- Anderson F. R., (2003) What regulates the efficiency of the Biological pump in the Southern Ocean, *U.S. JGOFS News*, **12(2)**, 1-4.
- Bange H. W. et. al., (2000) A revised nitrogen budget for the Arabian Sea, *Global Biogeochemical Cycle*, **14**, 1283-1297.
- Bange H.W. et al., (2005) The nitrogen cycle in the Arabian Sea, *Progress in Oceanography*, **65**, 145-158.
- Banase K., (1987) Seasonality of phytoplankton chlorophyll in the central and northern Arabian Sea, *Deep Sea Res I*, **34**, 713-723.
- Barber R.T., (1992) Introduction to the WCE88 cruise: An investigation into why the equator is not greener, *Journal of Geophysical Research*, **97**, 609-610.
- Barber R.T., Murray J.W., and McCarthy J.J., (1994) Biogeochemical interactions in the equatorial Pacific, *Ambio*, **23**, 62-66.
- Bates N. R. et al., (2006a) Ocean carbon cycling in the Indian Ocean: 1. Spatio-temporal variability of inorganic carbon and air-sea CO₂ gas exchange, *Global Biogeochemical Cycles*, **20**, GB3020, doi: 10.1029/2005GB002491
- Bates N. R. et al., (2006b) Ocean carbon cycling in the Indian Ocean: 2. Estimates of net community production, *Global Biogeochemical Cycles*, **20**, GB3021, doi: 10.1029/2005GB002492
- Bender M., Ducklow H., Kiddon J., Marra J. and Martin J. (1992) The carbon balance during the 1989 spring bloom in the North Atlantic Ocean, 47°N, 20°W. *Deep Sea Res.*, **39**, 1707-1725.
- Bianchi, M. et al., (1997) Nitrification rates, ammonium and nitrate distribution in the upper layers of the water column and in sediments of the Indian sector of the Southern Ocean, *Deep-Sea Research II*, **44(5)**, 1017-1032.
- Bienfang P.K. et. al., (1990) Nitrate and ammonium uptake by phytoplankton populations during the spring bloom in Auke Bay, Alaska, Estuarine, *Coastal and shelf sciences*, **30(5)**, 509-524
- Bhattathiri et al., (1996) Phytoplankton production and chlorophyll distribution in the eastern and central Arabian Sea in 1994-1995, *Current Science*, **71(11)**, 857-862

- Blain S. et al., (2007) Effect of natural Iron fertilization on carbon sequestration in the Southern Ocean, *Nature*, **446**, doi:10.1038/nature05700
- Borole D.V., (2002) Analysis of ^{210}Pb in sediment trap samples and sediments from the northern Arabian Sea: evidence for boundary scavenging, *Deep Sea Research I*, **49**(6), 1055-1069.
- Boyd P.W. and Law C.S., (2001) The Southern Ocean Iron Release experiment (SOIREE) – introduction and summary, *Deep Sea Research II*, **48**, 2425-2438
- Broecker W. S., (1982) glacial to interglacial changes in ocean chemistry, *Progress in oceanography*, **11**, 151-197.
- Broecker W.S. and Peng T. H., (1982) Tracers in the Sea, Eldigio, Palisades, New York.
- Bronk D.A., Glibert P.M., and Ward B.B., (1994) Nitrogen uptake, dissolved nitrogen release and new production, *Science*, **265**, 1843-1846.
- Buesseler K. O. et al., (1998) Upper ocean export of particulate organic carbon in the Arabian Sea derived from Thorium-234, *Deep Sea Research II*, **45**, 2461-2487.
- Buesseler K.O., (1991) Do upper-ocean sediment traps provide an accurate record of particle flux?, *Nature*, **353**, 420-423
- Burkill P.H., Mantoura R.F.C. and Owens N.J.P. (1993) Biogeochemical cycling in the northwestern Indian Ocean: a brief overview, *Deep Sea Research II*, **40** (3), 643-649.
- Capone D.G. et al., (1997) *Trichodesmium*, a globally significant marine cyanobacterium, *Science*, **276**, 1221-1229.
- Chisholm W.S., Falkowaski P.G., and Cullen J.J., (2001), Dis-crediting Ocean fertilization, *Science*, **294**, 309-310.
- Coale et al., (1996) A massive phytoplankton bloom induced by an ecosystem-scale iron fertilization experiment in the equatorial Pacific Ocean, *Nature*, **383**, 495-501.
- Coale et al., (2004) Southern Ocean Iron Enrichment Experiment: Carbon cycling in high and low-Si waters, *Science*, **304**, 408-417.
- Collos Y. and Slawyk G., (1986) ^{13}C and ^{15}N uptake by marine phytoplankton IV: Uptake ratios and the contribution of nitrate to the productivity of Antarctic waters (Indian Ocean sector), *Deep-Sea Research*, **33**, 1039-1051.

- Constable A. J., and Nicol S., (2003) Southern Ocean productivity in relation to spatial and temporal variations in the physical environments, *Journal of Geophysical Research*, **108**, C4, doi:10.1029/2001JC001270.
- de Baar J.W.H. et al., (2005) Synthesis of Iron Fertilization experiments: From the iron age in the age of enlightenment, *Journal of Geophysical Research*, **110**, doi:10.1029/2004JC002601.
- De Souza et al., (1996) Seasonal variability in oxygen and nutrients in the central and eastern Arabian Sea, *Current Science*, **71**(11), 847-851
- DiTullio G.R. and Laws E.A. (1991) Impact of an atmospheric-oceanic disturbance on phytoplankton community dynamics in the North Pacific Central Gyre, *Deep Sea Res*, **38**, 1305-1329.
- Dore J. E. and Karl D. M. (1996) Nitrification in the euphotic zone as a source of nitrite, nitrate, and nitrous oxide at station ALOHA, *Limnology and Oceanography*, **41**(8), 1619-1628.
- Dugdale, R.C., and Goering, J. J., (1967) Uptake of new and regenerated forms of nitrogen in primary productivity, *Limnology and Oceanography*, **12**, 196-206.
- Dugdale, R.C. and Wilkerson, F. P., (1986) The use of ^{15}N to measure nitrogen uptake in eutrophic oceans: experimental considerations, *Limnology Oceanography*, **31**, 673-689
- Dugdale R.C., Wilkerson F.P., Barber R. T. and Chavez F.P. (1992) Estimating new production in the Equatorial Pacific Ocean at 150° W, *Journal of Geophysical Research*, **97**(C1), 681-686.
- Ducklow H.W. and Harris R. (1993) Introduction to the JGOFS North Atlantic Bloom Experiment, *Deep Sea Research II*, **40**, 1-8.
- Ducklow H.W. (1995) Ocean Biogeochemical fluxes: New production and export of organic matter from the upper ocean, *Review of Geophysics*, Supplement, 1271-1276.
- Dupelssy J.C, (1982) Glacial to interglacial contrasts in the northern Indian Ocean, *Nature*, **295**, 319-321.
- Dwivedi R.M. et al., (2006) Influence of northeasterly trade winds on intensity of winter bloom in the northern Arabian Sea, *Current Science*, **90**(10), 1397-1406

- Emerson S., Quay P., Karl d., Winn C., Tupas L. and Landry M. (1997) Experimental determination of organic carbon flux from open Ocean surface waters, *Nature*, **389**, 951-954.
- Eppley R.W., Sharp J.H., Renger E.H., Perry M.J. and Harrison W.G. (1977) Nitrogen assimilation by phytoplankton and other microorganism in the surface waters of the central North Pacific Ocean, *Mar. Biol.*, **39**, 111.
- Eppley R.W. and Peterson B.J. (1979) Particulate organic matter flux and planktonic new production in the deep ocean, *Nature*, **282**, 677-680.
- Falkowski P.G. et al., (1998) Biogeochemical controls and feedbacks on ocean primary production, *Science*, **281**, 200-206.
- Falkowaski P.G. et al., (2000) The global carbon cycle: A test of our knowledge of Earth as a system, *Science*, **290**, 291-296.
- Falkowski P.G., Laws E.A., Barber R.T. and Murray J.W. (2003) Phytoplankton and their role in primary new and export production, In: *Ocean Biogeochemistry* (Eds) M.J.R. Fasham, 99-121, Springer, Heideberg.
- Fernandez C., et al., (2005), An estimation of annual new production and carbon fluxes in the northeast Atlantic Ocean during 2001. *Journal of Geophysical Research* **110**, C07S13, doi:10.1029/2004JC002616.
- Field C.B. et al., (1998) Primary production of the biosphere: Integrating terrestrial and oceanic components, *Science*, **281**, 237-240.
- Fischer J., Schott F.A., and Stramma L., (1996) Currents and transports of the Great Whirl-Socotra Gyre system during the summer monsoon August 1993, *Journal of Geophysical Research*, **101**, 3573-3587.
- Gall et al., (2001) Phytoplankton processes. Part 1: Community structure during the Southern Ocean Iron RElease Experiment (SOIREE), *Deep Sea Research II*, **48**, 2551-2570
- Geider, R. J., and Roche, J. La., (1994) The role of Iron in phytoplankton photosynthesis and the potential of iron limitation of primary productivity in the sea, *Photosynthetic Research*, **39**, 275-301.
- Gervais F. and Riebesell U., (2002) Changes in the primary productivity and chlorophyll-a in the response to iron fertilization in the southern frontal zone, *Limnology and Oceanography*, **47**(5), 1324-1335.

- Gilbert P. M. et al., (1982) Isotope dilution models of uptake and re-mineralization of ammonium by marine phytoplankton, *Limnology and Oceanography*, **27**(4), 639-650
- Godfrey J.S., (1996) The effect of the Indonesian throughflow on ocean circulation and heat exchange with the atmosphere: A review, *J. Geophys. Res.*, **101**, 12217-12238.
- Goes J et. al., (2005) Warming of the Eurasian landmass is making the Arabian Sea more productive, *Science*, **308**, 545-547.
- Godfrey J S., (1996) The effect of the Indonesian throughflow on ocean circulation and heat exchange with the atmosphere: A review, *Journal of Geophysical Research*, **101**, 12,217–12,237
- Godfrey, J. S., Johnson, G. C., McPhaden, M. J., Reverdin, G., & Wijffels, S. (2001). The tropical ocean circulation. In J. Church, J. Gould, & G. Siedler (Eds.), *Ocean circulation and climate* pp. 215–245 London: Academic Press.
- Gordon A. and Fine R., (1996) Pathways of water between the Pacific and Indian Oceans in the Indonesian seas, *Nature*, **379**, 146-149.
- Gregg et al., (2002) Ocean primary production and climate: Global decadal Changes, *Geophysical Research Letters*, **30**(15), doi:10.1029/2003GL016889
- Gregg W. W., N. W. Casey, C. R. McClain (2005), Recent trends in global ocean chlorophyll, *Geophys. Res. Lett.*, **32**, L03606, doi:10.1029/2004GL021808.
- Hall T. M. et al., (2004) Estimates of anthropogenic carbon in the Indian Ocean with allowance for mixing and time-varying air-sea CO₂ disequilibrium, *Global Biogeochemical Cycle*, **18**, doi:10.1029/2003GB02120
- Hansell D.A., Whitledge T.E. and Goering J.J. (1993) Patterns of nitrate utilization and new production over the Bering -Chukchi Shelf, *Continental Shelf Research*, **13**, 601-627.
- Hansen P.J. et al., (2004) Green *Noctiluca Scintillans*: a dinoflagellate with its own greenhouse, *Marine Ecology Progress Series*, **275**, 79-87.
- Harrison W. G. et al., (1987) *f*-ratio and its relationship to ambient nitrate concentration in coastal waters, *Journal of plankton research*, **9**(1), 235-248).
- Hellerman S. and Rosenstein M. (1983) Normal monthly wind stress over the world ocean with error estimates, *Journal of Physical Oceanography*, **13**, 1093–1104.

- Hood R. R. et al., (2006) Carbon Cycling and biogeochemical variability in the Indian Ocean, *CLIVER Exchanges*, **11**(4), 24-28.
- Holm-Hansen O. and Mitchell B.G.(1991) Spatial and temporal distribution of phytoplankton and primary production in the western Bransfield Strait region, *Deep Sea Research*, **38**, 961-980,1991.
- Honjo S. and Manganini S.J. (1993) Annual biogenic particle fluxes to the interior of the North Atlantic Ocean studied at 34°N, 21°W and 48°N, 21°W, *Deep Sea Research II*, **40**, 587-607.
- Huntley M., Karl D.M., Niller P. and Holm-Hansen O. (1991) Research on Antarctic Coastal Ecosystem Rates (RACER): An interdisciplinary field experiment, *Deep Sea Research*, **38**, 911-941.
- Hutchins D. A., (1995) Iron and the marine phytoplankton community, *Prog. Phycol. Res.*, **11**, 1-49.
- Intergovernmental Panel on Climate Change (IPCC) report no. IV, (2007) Cambridge University Press, ISBN 978-0-521-88009-1
- Ittekkot V. (1991) Particle flux studies in the Indian Ocean, *EOS*, **72**(47), 527-530.
- JGOFS Report No. 19. (1996) Protocol for the Joint Global Ocean Flux Study (JGOFS) core measurements, 145-150, SCOR, Bergen, Norway.
- Karl D. et al., (1997) The role of nitrogen fixation in biogeochemical cycling in the subtropical north Pacific Ocean, *Nature*, **388**, 533-538.
- Levitus et al., (2000) Warming of the world Ocean, *Science*, **287**, 2225-2229
- Levitus S., Burgett R. and Boyer T.P. (1994) World Ocean Atlas 1994, Vol. 5, Salinity. NOAA Atlas NESDIS, Vol. 3, US Government Printing Office, Washington DC, 99pp.
- Lohrenz S.E. et al. (1992) Seasonal variability in primary production and particle flux in the northwestern Sargasso Sea: U.S. JGOFS Bermuda Atlantic Time Series Study, *Deep Sea Research*, **39**, 1373-1391.
- Madhupratap M et. al., (1996) Mechanism of the biological response to winter cooling in the Northeastern Arabian Sea, *Nature*, **386**, 549-552.
- Martin, J H. et al., (1991) The case of Iron, *Limnology Oceanography*, **36**(8), 1793-1802.

- Martin J. H. and Fitzwater S.E., (1988) Iron deficiency limits phytoplankton growth in the north-east subarctic, *Nature*, **331**, 341-343.
- Martin J.H., Gordan R.M. and Fitzwater S.E., (1990) Iron in Antarctic waters, *Nature*, **345**, 156-158
- Martin J., et al., (1991) The case of Iron, *Limnology and Oceanography*, **36**(8), 1793-1802.
- Malone T.C., Pike S.E., Conley, D.J. (1993) Transient variations in phytoplankton productivity at the JGOFS Bermuda time series station, *Deep Sea Research*, **40**, 903-924.
- Marinov et al. (2006) The Southern Ocean biogeochemical divide, *Nature*, **441**, doi:10.1038/nature04883.
- McCarthy J.J., Garside C., Nevins J.L. and Barber R.T. (1996) New production along 140°W in the equatorial Pacific during and following the 1992 El Nino event, *Deep Sea Research II*, **43**, 1065-1093.
- McCarthy J.J., Garside C. and Nevins J. (1999) Nitrogen dynamics during the Arabian Sea northeast monsoon, *Deep Sea Research II*, **46**, 1623-1664.
- Mengesha S. et al., (1998) Seasonal variations of phytoplankton community structure and nitrogen uptake regime in the Indian sector of the Southern Ocean, *Polar Biology*, **20**, 259-172.
- Michaels A.F., Siegel D.A., Johnson R.J., Knap A.F. and Galloway J.N. (1993) Episodic inputs of atmospheric nitrogen to the Sargasso Sea: Contribution to new production and phytoplankton blooms, *Global Biogeochemical Cycles*, **7**, 339-351.
- Michaels A.F., Bates N.R., Buesseler K.O., Carlson C.A., Knap H.H. (1994) Carbon cycle imbalances in the Sargasso Sea, *Nature*, **372**, 537-540.
- Miller C.B. et al. (1991) Ecological dynamics in the subarctic Pacific, a possibly iron limited ecosystem, *Limnology and Oceanography*, **36**, 1600-1615.
- Miller C.B. (1993) Pelagic production processes in the subarctic Pacific, *Progress in Oceanography*, **32**, 1-15.
- Minas J. H. et al., (1986) Productivity in upwelling areas deduced from hydrographic and chemical fields, *Limnology and Oceanography*, **31**, 1182-1206.
- Mitchell, G., et al. (1991) Light limitation of phytoplankton biomass and macronutrient utilization in the Southern Ocean, *Limnology and Oceanography*, **36**(8), 1662-1677.

- Miyama T et al., (2003) Structure and dynamics of the Indian Ocean cross equatorial cell, *Deep Sea Research II*, **50**, 2023-2047.
- Mullin M.M. et al., (1975) Nutrient regeneration by oceanic zooplankton: a comparison of methods, *Mar. Sci. Comm.*, **1**, 1-13
- Murray J.W., The 1988 Black Sea Oceanography Expedition: Introduction and Summary, *Deep-Sea Res*, **38** (Supplement 2) (1991): S655-S661
- Murtugudde R., Signorini S., Christian J., Busalacchi A., McLain C. and Picaut J. (1999) Ocean color variability of the tropical Indo-Pacific basin observed by SeaWiFS during 1997–98, *Journal of Geophysical Research*, **104**, 18351–18366.
- Nair R.R. et al., (1989) Increased particle flux to the deep ocean related to monsoons, *Nature*, **338**, 749-751.
- Naqvi et al., (1982) Denitrification in the Arabian Sea, *Deep Sea Research*, **29**, 459-469.
- Naqvi, S.W.A. and Jaykumar, D.A., (2000) Ocean biogeochemistry and atmospheric composition: Significance of the Arabian Sea, *Current Science*, **78**, 289-299.
- Neess, J.C., R.C., Dugdale, and J.J., Goering, (1962) Nitrogen metabolism in lakes, Measurement of nitrogen fixation with ^{15}N , *Limnology and Oceanography*, **7**, 163-169.
- O'Reilly J. et. al., (1998) Ocean colour chlorophyll algorithms for SeaWiFS, *Journal of Geophysical Research*, **103**, 24,937-24,953.
- Oslo R.J. (1980) Nitrate and Ammonium uptake in Antarctic waters, *Limnology and Oceanography*, **25**, 1064-1074.
- Owens N. J. P. and Rees A. P. (1989) Determination of nitrogen-15 at sub-microgram levels of nitrogen using automated continuous-flow isotope ratio mass spectrometer, *Analyst*, **114**, 1655-1657.
- Owens N. J. P. et al. (1993) Size-fractionated primary production and nitrogen assimilation in the northwestern Indian Ocean, *Deep Sea Research II*, **40(3)**, 607-709.
- Parab S. G. et al., (2006) Monsoon driven changes in phytoplankton populations in the eastern Arabian Sea as revealed by microscopy and HPLC pigment analysis, *Continental Shelf Research*, **26**, 2538-2558.

Pfannkuche O. and Lochte K., (2000) The biogeochemistry of the deep Arabian Sea: overview, *Deep Sea Research II*, **47**, 2615-2628.

Platt T., and Sathyendranath S., (1988) Oceanic primary production: estimation by remote sensing at local and regional scales, *Science*, **241**, 1613-1620.

Poisson A., N Metzl., C. Brunet, B. Schauer, B. Bres, D. Ruiz-Pino and F. Louanchi, (1994) Variability of sources and sinks of CO₂ in the Western Indian and Southern Oceans during the year 1991, *Journal of Geophysical Research*, **98**, 22,759-22,778.

Prasanna Kumar S. et al., (2001a) High biological productivity in the central Arabian Sea during the summer monsoon driven by Ekman pumping and lateral advection, *Current Science*, **81(12)**, 1633-1638

Prasanna Kumar S., et al., (2001b) High biological in the central Arabian Sea during the summer monsoon driven by Ekman pumping and lateral advection, *Current Science*, **81(12)**, 1633-1638

Prasanna Kumar S. and Prasad T.G., (1996) Winer cooling in the northern Arabian Sea, *Current Science*, **71**, 834-841.

Probyn T.A., and Painting S.J., (1985) Nitrogen uptake by size-fractionated phytoplankton population in Antarctic surface waters, *Limnology and Oceanography*, **30(6)**, 1327-1332.

Raimbault P. et al., (1999) Carbon and nitrogen uptake and export in the equatorial Pacific at 150W: evidence of an efficient regenerated production cycle, *Journal of Geophysical Research*, **104(C2)**, 3341-3356.

Ramaswamy V., Sarin M. M. and Rengarajan R., (2005) Enhanced export of carbon by salps during the northeast monsoon period in the northern Arabian Sea, *Deep Sea Research II*, **52**, 1922-1929.

Rao, R. R , Molinari, R. L. and Festa, J., (1989) Evolution of the near surface thermal Structure of the tropical Indian Ocean. Part I: Description of mean monthly mixed layer depth and surface temperature, surface current and surface meteorological field. *J. Geophys. Res.*, **94**, 10801-10815.

Reay et al., (2001) Regulation by low temperature of phytoplankton growth and nutrient uptake in the southern Ocean, *Marine Ecology Progress Series*, **219**, 51-64.

Redfield A.C. (1934) On the proportions of organic derivatives in seawater and their relation to the composition of plankton, *James Johnstone Memorial Volume*, Liverpool, 176p.

Rees A. P. et. al., (2002) Size-fractionated nitrogen uptake and carbon fixation during a developing coccolithophore bloom in the North Sea during June 1999, *Deep-Sea Research II*, **49**, 2905-1927.

Rees A.P., Woodward E.M.S., and Joint I. (2006). Concentrations and uptake of nitrate and ammonium in the Atlantic Ocean between 60°N and 50°S. *Deep Sea Research II*, **53(14-16)**, 1649-1665.

Roman M.R., Dam H.G., Gauzens, A.L. and Napp J.M. (1993) Zooplankton biomass and grazing at the JGOFS Sargasso Sea time series station, *Deep Sea Research*, **40**, 883-901.

Sabine C. L. et al., (2000) Seasonal CO₂ fluxes in the tropical and sub-tropical Indian Ocean, *Marine Chemistry*, **72**, 33-53.

Sahayak S. et al., (2005) Red tide of *Noctiluca milliaris* off south of Thiruvananthapuram subsequent to the 'stench event' at the southern Kerala coast, *Current Science*, **89(9)**, 1472-1473.

Sambrotto R.N., Martin J.H., Broenkow W.W., Carlson C.A. and Fitzwater S.E. (1993) Nitrate utilization in surface waters of the Iceland Basin during spring and Summer of 1989, *Deep Sea Research II*, **40**, 441-457.

Sambrotto R. N., and Mace B. J. (2000) Coupling of biological and physical regimes across the Antarctic Polar Front as reflected by nitrogen production and recycling, *Deep Sea Research II*, **47**, 3339-3367.

Sambrotto R. N., (2001) Nitrogen production in the Arabian Sea during spring intermonsoon and southwest monsoon seasons, *Deep Sea Research II*, **48**, 1173-1198.

Sanjeev Kumar and Ramesh R., (2005) Productivity measurements in the Bay of Bengal using the ¹⁵N tracer: Implications to the global carbon cycle, *Indian Journal of Marine Sciences*, **34(2)**, 153-162.

Sanjeev Kumar et al., (2004) High new production in the Bay of Bengal: Possible causes and implications, *Geophysical Research Letters*, **31**, L18304, doi:10.1029/2004GL021005.

Sanjeev Kumar et al., (2008) Effect of winter cooling on nitrogen uptake in the northeastern Arabian Sea, *AGU Monograph*, (under review).

Sarangi R. K., Prakash Chauhan and Nayak S.R., (2005) Inter-annual variability of phytoplankton blooms in the northern Arabian Sea during winter monsoon

period (February-March) using IRS-P4 OCM data, *Indian Journal of Marine Sciences*, **34**, 163-173.

Sarkar A., Ramesh, R., Bhattacharya, S.K., and Rajagopalan, G.S., (1990) Oxygen isotope evidence for a stronger winter monsoon current during the last glaciation, *Nature*, **343**, 548-551.

Sarin M. M., Rengarajan R., and Ramaswamy V., (1996) ^{234}Th scavenging and particle export fluxes from the upper 100 m of the Arabian Sea, *Current Science*, **71**, 888-893.

Sarmiento J. L. et al., (2003) High-latitude controls the thermocline nutrients and low latitude biological productivity, *Nature*, **247**, doi:10.1038/nature02127.

Sarmiento J.L., and Gruber N., (2002) Sinks for Anthropogenic Carbon, *Physics Today*, **8**, 30-36.

Sathyendranath S., (2000) Remote sensing of Ocean Colour in coastal, and other optically complex waters, Reports of the International Ocean-Colour Coordinating group, Report No. 3.

Savoye N et al., (2004) Regional variations of spring N-uptake and new production in the Southern Ocean, *Geophysical Research Letters*, **31**, L03301, doi:10.1029/2003GL018946.

Schott F.A. et al., (2002) The shallow overturning circulation of the Indian Ocean, *Progress in Oceanography*, **53**, 57-103.

Schott F.A. and McCreary P. Jr. (2001) The monsoon circulation of the Indian Ocean, *Progress in Oceanography*, **51**, 1-123.

Schott F. A., & Fischer J., (2000), Winter monsoon circulation of the northern Arabian Sea and Somali Current. *Journal of Geophysical Research*, **105**, 6359–6376.

Semeneh M. et al., (1998) Nitrogen uptake regime and phytoplankton community structure in the Atlantic and Indian sectors of the Southern Oceans, *Journal of Marine Systems*, **17**, 159-177.

Shankar D, Vinayachandran P.N., and Unnikrishnan A.S., (2002) The monsoon currents in the north Indian Ocean, *Progress in Oceanography*, **52**, 63-120.

Slawyk G., (1979) ^{13}C and ^{15}N uptake by phytoplankton in the Antarctic upwelling area: Results from the Antipod I cruise in the Indian Ocean sector, *Aust. J. Mar. Freshwater Res.*, **30**, 431-448.

- Smith W.O. and Nelson D.M. (1990) Phytoplankton growth and new production in the Weddell Sea marginal ice zone in the austral spring and autumn, *Limnol. Oceanogr.*, **35**, 809-821.
- Smith W.O. et al., (1997) New production in the northeast water Polynya, *Journal of Marine Systems*, **10**, 199-209.
- Smith S.L., (2001) Understanding the Arabian Sea: Reflections on the 1994-1996 Arabian Sea expedition, *Deep Sea Research II*, **48**, 1385-1402.
- Sparrow M.D., and Heywood, K. J., (1996) Current Structure of the south Indian Ocean, *Journal of Geophysical Research*, **101(C3)**, 6377-6391.
- Stramma, L., (1992) The South Indian Ocean Current, *Journal of Physical Oceanography*, **22**, 421-430.
- Srivastava R., Ramesh R., Satya Prakash, N. Anil Kumar, M. Sudhakar (2007) Oxygen isotope and salinity variations in the Indian sector of the Southern Ocean, *Geophys. Res. Lett.*, **34**, L24603, doi:10.1029/2007GL031790
- Sullivan C.W., Arrigo K.R., McClain C.R., Comiso J.C. and Firestone J. (1993) Distribution of phytoplankton blooms in the Southern Ocean, *Science*, **262**, 1832-1837.
- Sweeney B.M. (1971) Laboratory studies of a green *Noctiluca* from New Guinea, *Journal of Phycology*, **7**, 53-58
- Takahashi et al., (2002) Global sea-air CO₂ flux based on climatological surface ocean pCO₂, and seasonal biological and temperature effects, *Deep Sea Research II*, **49**, 1601-1622.
- Toggweiler J.R., (1999) An ultimate limiting nutrient, *Nature*, **400**, 511-512.
- Townsend D.W., Keller M.D., Sieracki M.E. and Ackleson S.G. (1992) Spring phytoplankton blooms in the absence of vertical water column stratification, *Nature*, **360**, 59-62.
- Treguer, P., and Jacques, G., (1992) Dynamics of nutrients and phytoplankton, and fluxes of carbon, nitrogen and silicon in the Antarctic Ocean, *Polar Biology*, **12**, 149-162.
- Tyrell T. (1999) The relative influence of nitrogen and phosphorus on oceanic primary production, *Nature*, **400**, 525-531
- Tyrell T and Law C.S., (1997) Low Nitrate: Phosphate ratio in the global Ocean, *Nature*, **387**, 793-796.

Van Cappellen P. and Ingall E., (1994) Benthic phosphorus regeneration, net primary production, and ocean anoxia: A model of the coupled marine biogeochemical cycles of carbon and phosphorus, *Paleoceanography*, **9**(5): doi: 10.1029/94PA01455

Van Leeuwe M. A., et al., (1997) Iron enrichment experiment in the Southern Ocean: physiological responses of plankton communities, *Deep Sea Research II*, **44**, 189-207.

Varela D. E. and Harrison P. J. (1999) Seasonal variability in nitrogenous nutrition of phytoplankton assemblages in the northeastern subarctic Pacific Ocean, *Deep Sea Research II*, **46**, 2505-2538.

Villareal T.A., Altabet M.A. and Culver-Rymsza K. (1993) Nitrogen transport by vertically migrating diatom mats in the North Pacific Ocean, *Nature*, **363**, 709-712.

Vinayachandran et al., (2004) Biological response of the sea around Sri Lanka to summer monsoon, *Geophysical Research Letters*, **31**: doi:10.1029/2003GL018533

Vyas N.K., et al., (2007) Utility of OCEANSAT-1 OCM data in deciphering Antarctic features, *Current Science*, **93**(3), 292-294.

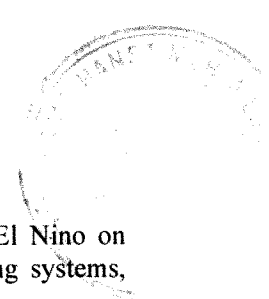
Watts L.J. and Owens N.J.P. (1999) Nitrogen assimilation and f-ratio in the northwestern Indian Ocean during an Intermonsoon period, *Deep Sea Research II*, **46**, 725-743.

Wiebe P.H., Boyd S. and Cox J.L. (1975) Relationship between zooplankton displacement volume, wet weight, dry weight, and carbon, *Fishery Bulletin*, **73**(4), 777-786.

Wheeler P. A. and Kokkinakis S. A. (1990) Ammonium recycling limits nitrate use in the oceanic subarctic Pacific, *Limnology and Oceanography*, **35**, 1267-1278.

Wiggert J. D. et al., (2000) The Northeast Monsoon's impact on mixing, plankton biomass and nutrient cycling in the Arabian Sea, *Deep-Sea Research II*, **47**, 1353-1385

Wiggert et al., (2002) Processes controlling interannual variations in wintertime (Northeast Monsoon) primary productivity in the central Arabian Sea, *Deep-Sea Research II*, **49**, 2319-2343

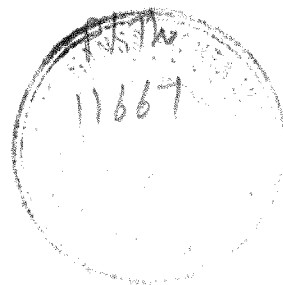


Wilkerson F.P., Dugdale R.C. and Barber R.T., (1987) Effects of El Nino on new, regenerated and total production in eastern boundary upwelling systems, *Journal of Geophysical Research*, **92**, 14347-14353.

Wyrski K., (1973) An equatorial jet in the Indian Ocean, *Science*, **181**, 262-264.

Wyrski K., (1988) Oceanographic Atlas of the International Indian Ocean Expedition, Amerind Publishing Co. Pvt. Ltd., New Delhi, India.

P/Th
11667



**A Summary of the thesis on
“Role of the Ocean in
the Global Carbon Cycle”**

Submitted to

**The Maharaja Sayajirao University of Baroda
Vadodara, India**

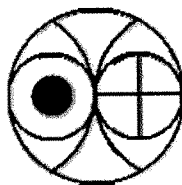
For the degree of

Doctor of Philosophy in Geology

By

Satya Prakash

April, 2008



**Planetary and Geosciences Division
Physical Research Laboratory,
Navrangpura, Ahmedbad-380 009,
India**

Chapter 1. INTRODUCTION

Biogeochemical processes including the marine carbon cycle are the key factors in global change. During the last 150 years the concentration of CO₂ in the atmosphere has increased by 35% compared to the pre-industrial level (from 280ppm in pre-industrial era to 379ppm in 2005) (IPCC AR IV-2007) and is projected to double in the coming century, mainly due to anthropogenic activity such as fossil fuel burning, deforestation and change in the land use pattern. This has lead to an increase in the global temperature by 0.74±0.18°C during the last century (IPCC AR IV-2007). The observed growth rate of CO₂ in the atmosphere is less than that expected. This is because a major part, approximately 104.9 Gt/yr, of this is taken up by the terrestrial and oceanic biota. In the oceanic photic zone, microscopic plants (phytoplankton) convert inorganic carbon through photosynthesis into particulate organic carbon. When these plankton die, they tend to sink to the deep and thus a large part of biologically fixed carbon gets exported to the deep. This is known as the “Biological Pump” and it plays an important role in the ocean's ability to absorb atmospheric carbon. In this way the ocean works as a net sink for this greenhouse gas. The rate at which inorganic CO₂ is converted into organic carbon by phytoplankton is called primary productivity, measured in units of mgCm⁻²d⁻¹ or mgCm⁻²y⁻¹.

Nitrogen plays a key role in oceanic productivity and its unavailability can be a limiting factor. On the basis of the source of nitrogen into the euphotic zone, primary productivity can be subdivided into two: new productivity and regenerated productivity (Dugdale and Goering 1967). New productivity is defined as a fraction of primary productivity supported by the newly borne nitrate into the euphotic zone and regenerated productivity as that supported by the recycled nutrients within the same zone. The ratio of the new productivity to the total productivity is called the *f*-ratio (Eppley and Peterson 1979). Integrated over an annual time scale, new productivity approximates the exportable productivity and thus, measuring new productivity allows us to quantify the amount of atmospheric carbon being removed by different regions of the ocean i.e., the strength and efficiency of the oceans biological pump.

As oceans play a major role in the global carbon cycle, it is required to quantify the amount of inorganic carbon taken up by the individual ocean basins. Also the

assessment of different ocean basins as source/sink of carbon is important. The present study was carried out using the ^{15}N tracer technique (Dugdale and Wilkerson 1986) which gives total production as a sum of new production (nitrate uptake) and regenerated production (ammonium and urea uptakes). The advantage of this technique lies in the quantification of new productivity which is a measure of carbon removed from the surface for significantly longer time periods ($>1000\text{yrs}$). The present work is a comprehensive study of primary productivity in different regions of the Indian Ocean such as the Arabian Sea, equatorial Indian Ocean and Southern Indian Ocean. Though some study has been carried out previously in some selected parts of the Arabian Sea, most of them are concentrated on the north-western and central Arabian Sea. No study has been done in the equatorial Indian Ocean and Southern Indian Ocean. The present study concentrates on the north-eastern Arabian Sea and is the *first* to measure primary productivity in the *equatorial Indian* and *Southern Indian Oceans*.

Chapter 2: Sampling Locations, Seasons and Experimental Techniques

The main aim of this thesis is to characterize the Indian Ocean on the basis of new production and f -ratio and to evaluate its role in the Global Carbon Cycle. To achieve this goal, three different methods are used:

1. Ocean color studies of northeastern Arabian Sea
2. ^{15}N based measurements in the some region of the Arabian Sea. Measurements were also done in the equatorial and the southern Indian Ocean
3. Small scale iron enrichment experiment in the southern Indian Ocean

Recent observations based on ocean colour show that the summer productivity in the western Arabian Sea has been increasing during the last seven years, reportedly due to the warming of the Eurasian landmass (Goes et al., 2005). Ocean color data from SeaWiFS (Sea-viewing Wide Field of view Sensor) for the eastern Arabian Sea were analyzed by me to asses the role of global climate change on the productivity of the eastern Arabian Sea.

For ^{15}N based measurements four cruises were undertaken: two cruises in the eastern Arabian Sea and one each in the equatorial Indian Ocean and the Southern Indian Ocean.

The details of the cruises with the region of study, cruise number and duration are described in detail in this chapter.

2.1 Ocean colour studies

The only possible way to monitor the variation in the biological properties of the ocean on a larger spatial scale is by remote sensing. Chlorophyll-*a*, which is the main photosynthetic constituent in the phytoplankton, absorbs more in blue than in green; as the concentration of phytoplankton increases, the backscattered light progressively shifts towards the green. This property is successfully used to derive the Chl-*a* concentration with the help of a sensor in a satellite. In the tropics, where variation in sunlight is not significant on an interannual scale, variation in chlorophyll concentration can indicate the variation in primary production. Satellite ocean colour data provides the spatial and temporal variations in phytoplankton biomass and hence in the primary production on a larger scale. Since the launch of SeaWiFS (Sea-viewing Wide Field of view Sensor) in August 1997, global ocean colour data are available to the science community on a regular basis. For present study, monthly composites Level-3 Version 4 9-km resolution mapped SeaWiFS chlorophyll images were taken. From these images chlorophyll values were obtained using SEADAS software (provided by NASA for ocean colour image processing).

The seasonality of the north-east Arabian Sea SST (Sea Surface Temperature) is also inspected over the same region for the same time period in order to analyse the effect of sea surface cooling due to upwelling on the chlorophyll-*a* concentration. Monthly composite SST data are taken from AVHRR (Advanced Very High Resolution Radiometer) pathfinder version 5 (June-1997 to Dec-2004) and MODIS (Moderate Resolution Imaging Spectro-radiometer) data (Jan-2005 to June-2005). We also analyzed version-3 QuickScat data in order to monitor change, if any, in wind speed over past 6 years (1999-2005).

The remote sensing studies were done for the eastern Arabian Sea. We have divided the eastern Arabian Sea into two zones: Zone 1 extends from 20°N to 25°N and 62°E to 75°E and zone 2 extends from 20°N to 10°N and 62°E to 75°E. This division (into two different zones) is based on the observed physical forcing responsible for the high production in each zone.

2.2 Primary Production

Joint Global Ocean Flux Study (JGOFS) protocol was followed for the estimation of total primary production which is the sum of new and regenerated production. For the present study nitrate uptake rate is considered as new production and a sum of ammonium and urea uptake rates as regenerated production. New production is measured as the uptake rate of ^{15}N -labelled nitrate by the phytoplankton during deck incubation and regenerated production as a sum of ^{15}N -labelled ammonium and urea uptake rates.

Experimental Procedures

The depth of the photic zone i.e., the depth at which light falls to 1% of the surface level, was estimated using an underwater radiometer (Satlantic Inc.). Based on these light measurements six different depths were chosen for collecting water samples for ^{15}N and chlorophyll measurements. These, six depths, correspond to light levels 100, 80, 64, 20, 5 and 1% of the surface value, cover the entire photic zone (except at two stations: PP 5 and PP 6). Water samples were collected using clean Go-Flo bottles (General Oceanic, Miami, Florida, USA) attached to a CTD rosette. 100 ml of each sample was separately collected for nutrient measurement using a SKALAR autoanalyzer. 1 L of water sample from each depth was also collected for chlorophyll measurement and filtered on 47 mm GF/F 0.7 μm pore size filter under low vacuum. Chlorophyll was then extracted using 10ml of 90% acetone (AR) grade and was measured using Turner Design fluorometer. Individual seawater samples were taken in duplicates in polycarbonate Nalgene bottles, for measurement of nitrate (2L), ammonium (2L) and urea (1L) uptakes rates. Appropriate neutral density filter were put on the bottles, immediately after the collection of samples, to simulate the same light condition that was present at the corresponding depths. This was followed by the addition of ^{15}N enriched (99 atom% ^{15}N) $\text{Na}^{15}\text{NO}_3$, $^{15}\text{NH}_4\text{Cl}$, and $\text{CO}(^{15}\text{NH}_2)_2$ (obtained from SIGMA ALDRICH USA) tracers to the individual samples taken for the measurement of nitrate, ammonium and urea uptake rates. The amount of nutrient tracer added corresponded to less than 10% of the ambient nutrient concentration. After the addition of tracers, the samples were incubated for 4 hrs symmetrical to the local noon on the deck. Sea water, pumped from a depth of 4 m was continuously circulated to maintain the temperature

during incubation. Subsequently all samples were filtered subsequently under low pressure (<100mm Hg) through precombusted (4 hrs at 400°C) 47mm diameter and 0.7µm pore size Whatman GF/F filter, then dried in oven at 60°C overnight and brought to the shore for mass-spectrometric analysis. The samples were analysed using a *CarloErba* elemental analyser interfaced via conflo III to a *Finnigan Delta Plus* mass spectrometer, using a technique for sub-microgram level ^{15}N determination (Owens and Rees, 1989).

Analysis was done using a Finnigan Delta Plus stable isotope ratio mass spectrometer. The aim was to measure the total organic nitrogen content of natural and enriched samples and the atom% ^{15}N . For this, the mass spec is calibrated using some standard material, inorganic as well as organic, of known nitrogen content. Main standards used are: Potassium nitrate, ammonium sulphate, acetylene, Casein and BSA (an organic compound) which contains 13.8, 21.2, 10.3 and 17.8% nitrogen respectively. ^{15}N atom % estimation has an error of less than 0.5%. Uptake rates were calculated using the equation given by Dugdale and Wilkerson (1986).

Quality Control

Special care was taken during experiments to avoid any contamination. For collection of samples Teflon coated Go-Flo bottles were used to avoid any trace metal contamination. These bottles were rinsed thoroughly before using them for sample collection. Samples were directly transferred from Go-Flo bottles to polycarbonate Nalgene bottles. No other plastic cans or pipes were used as a precautionary measure to avoid contamination. Always new and separate pipette tips were used for adding different tracers. Continuous running seawater was maintained during incubation to maintain the temperature. Samples were immediately transferred to the ship-board laboratory after incubation and kept covered under dark clothes till the filtration was over. Filtration cups were thoroughly washed with milliQ water before the filtration and were rinsed properly once the filtration of each sample was over. This was done to restrict cross contamination. Filter papers were handled using well cleaned and separate forceps for each tracer. After filtration each bottles were washed thoroughly using 10% HCl for the

next experiment. For the mass spectrometric analysis samples were packed in clean silver foils. Blanks with silver foils were run in the mass spectrometer during every batch.

Chapter 3. The Northeastern Arabian Sea

The northern Indian Ocean is divided into two major ocean basins by the Indian Peninsula: The Arabian Sea in the west and the Bay of Bengal in the east. The Arabian Sea has a unique geographical setting: it is surrounded by the Arabian and African continents on its north and west and by the Indian peninsula on its east. The Arabian Sea is one of the most biologically productive region of the world ocean (Madhupratap et al., 1996; Smith, 2001) and is characterized by a range of biogeochemical provinces, based on atmospheric forcing due to the seasonally reversing southwest (summer) and northeast (winter) monsoons (Bange et al., 2000; Wiggert et al., 2000; Kumar et al., 2001a). Both trigger high biological production, but have different underlying mechanisms. During the winter monsoon, cool dry air from the Himalaya enhances evaporation in the northern Arabian Sea causing convective mixing. This deepens the upper mixed layer causing entrainment of nutrients from the deeper to the upper layers and triggers high primary production (Kumar et al., 2001b), sometimes leading to the initiation of phytoplankton bloom. The total production during this period can reach up to $\sim 3 \text{ gCm}^{-2}\text{d}^{-1}$ (Sanjeev Kumar et al., 2007). The bloom during the late winter monsoon is dominated by *Noctiluca scintillans*, a large and conspicuous dinoflagellate, commonly found in coastal areas worldwide. Its most widely spread form is completely heterotrophic and is red in colour, survives on a wide range of prey such as phytoplankton and micro-zooplankton (Hansen et al., 2004). Heterotrophic *Noctiluca scintillans* had been reported from the eastern Arabian in the month of September i.e., during the late summer monsoon (Sahayak et al., 2005). In the tropical and subtropical areas of the Southeast Asia, particularly in the northeastern Arabian Sea during late winter monsoon, a green form of *Noctiluca scintillans* is also found which can do photosynthesis and survive on itself under light for at least a month (c.f Sweeney 1971). The appearance of *Noctiluca* bloom in the northeast Arabian Sea is well documented in the literature (Dwivedi et. al., 2006, Parab et al., 2006) but data available on the nitrogen uptake and *f*-ratios is limited (Sanjeev Kumar et al., 2008).

The rates of nitrogen uptake, integrated over euphotic zone, varied from 2.7 $\text{mmolNm}^{-2}\text{d}^{-1}$ to 23.0 $\text{mmolNm}^{-2}\text{d}^{-1}$ over the study area. The higher rates were measured at the stations in the north (PP9, 10 and 11), whilst the lower rates were associated with the southern stations. The same spatial variability in the nitrogen uptake was also reported by Owens et al., (1993) *i.e.*, the lower uptake in the south and the higher in the north with an overall increasing trend from south to north. Euphotic zone integrated nitrate uptake rate or new production during the late winter monsoon in the eastern Arabian Sea showed significant variation in new production; it varied from 0.63 $\text{mmolNm}^{-2}\text{d}^{-1}$ to 20.91 $\text{mmolNm}^{-2}\text{d}^{-1}$. It was low in the southern sector of the sampling area but was significantly higher in the northern sector. The mean new production in the southern sector or the non bloom area was 2.1 $\text{mmolNm}^{-2}\text{d}^{-1}$ whereas in the bloom area it was 15.7 $\text{mmolNm}^{-2}\text{d}^{-1}$, almost eight fold higher than the non-bloom area. The present study indicates the presence of two different biogeochemical provinces in the eastern Arabian Sea during the late winter monsoon: less productive southern and more productive northern regions. The southern sector was characterized by low column N-uptake and low new production. The column integrated total N-uptake rates, although low, increased progressively towards north. This increase may be the effect of more intense winter cooling towards the north. The northern part was a highly productive zone, with very high N-uptake and new production.

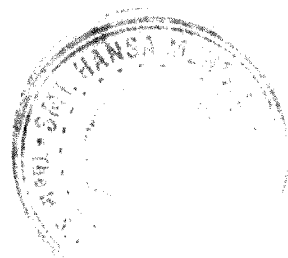
During the early winter monsoon (*i.e.*, in the month of December) the rates of nitrogen uptake varied from 4.07 $\text{mmolNm}^{-2}\text{d}^{-1}$ to 23.31 $\text{mmolNm}^{-2}\text{d}^{-1}$. Unlike the late winter monsoon when higher uptake rates were measured at stations in the southern part of the eastern Arabian Sea, during the early winter monsoon no such pattern was seen in N-uptake rates at different stations in the same region. New production during early winter monsoon 2004 varied from 1.95 $\text{mmolNm}^{-2}\text{d}^{-1}$ to 19.70 $\text{mmolNm}^{-2}\text{d}^{-1}$. In comparison to the rates of nitrate uptake measured during the late winter monsoon, new production during December month is thrice that of the same in a non-bloom (2.1 $\text{mmolNm}^{-2}\text{d}^{-1}$) region but is less than half of that (15.7 $\text{mmolNm}^{-2}\text{d}^{-1}$) in the bloom area. These clearly suggests that the productivity pattern has lots of heterogeneity over space and time in the eastern Arabian Sea but still this part of the world ocean has a potential of high new productivity.

Chapter 4. The Equatorial and Southern Indian Ocean

The equatorial region of the Indian Ocean is distinctly different from the other two major oceans in a sense that it does not possess equatorial upwelling regimes like the Pacific and Atlantic. Ocean upwelling does not occur along the equator as it occurs in the Pacific and the Atlantic ocean but in the north, along Somalia and Oman coast and also along western Indian coast, and this upwelling takes place only during the summer monsoon. Though it is now reasonably established, though dependent of season and direction of trade winds, that equatorial upwelling does take place in the Indian Ocean, yet no data exists on the productivity of this important basin. The equatorial Indian Ocean is still a virgin area and the present data set is the first set of data from this important basin. The rates of nitrogen uptake, integrated over the photic zone, span more than an order of magnitude over the study area and it varied from $19.1 \text{ mmolNm}^{-2}\text{d}^{-1}$ to $171.1 \text{ mmolNm}^{-2}\text{d}^{-1}$. Though higher uptake rates were measured at almost all the stations, the N-uptake rates were low in the upper mixed layer and increased tremendously below mixed layer. Most of the productivity was confined below the mixed layer. This was mainly because nitrate concentration was below detection limit in the mixed layer, and in the absence of nitrate ammonium and urea were the preferred nutrient. But below the mixed layer, where the concentration of ambient nitrate increased dramatically, nitrate uptake also increased. The mixed layer integrated N-uptake rates were very low and were similar to the rates reported from the other oligotrophic regions around the world ocean. It varied from $0.81 \text{ mmolNm}^{-2}\text{d}^{-1}$ to $2.23 \text{ mmolNm}^{-2}\text{d}^{-1}$ over the study area. The mixed layer integrated nitrate uptake rates were very low: it varied from a minimum of $0.12 \text{ mmolNm}^{-2}\text{d}^{-1}$ to a maximum of $0.84 \text{ mmolNm}^{-2}\text{d}^{-1}$. The mean new production over the study area was $0.32 \text{ mmolNm}^{-2}\text{d}^{-1}$. It was very low ($0.20 \text{ mmolNm}^{-2}\text{d}^{-1}$) along 77°E transect but was more the twice ($0.43 \text{ mmolNm}^{-2}\text{d}^{-1}$) along 83°E transect. Capability of the equatorial ocean for export production is low as compared to that of Arabian Sea (present study), Bay of Bengal (Sanjeev Kumar et al., 2004) and the Southern Ocean (present study). The slope of the regression equation between new and total production suggests that along 77°E transect only 9% of the total mixed layer production can be exported to the deep where the export production along 83°E transect may be as high as 38%, almost 4-fold more, of the mixed layer integrated total production.

The Southern Ocean, of which the Indian Sector constitutes ~39% by area (Mengesha et al., 1998), plays an important role in the global carbon cycle and climate regulation by acting as a net sink, *via* solubility and biological pump, for the atmospheric CO₂ (Chisholm, 2001). The biogeochemistry of the Southern Ocean is controlled by two major current systems: the eastward flowing Antarctic Circumpolar Current (ACC) and the westward flowing Antarctic Coastal Current (Constable et al., 2003). The strong westerly wind generates upwelling of nutrient rich deep water in this region. According to an estimate (Anderson, 2003) only half of the upwelled nutrients are consumed by phytoplankton present here and the rest are carried back into the deep sea via formation of Antarctic intermediate water (AAIW) and Antarctic bottom water (AABW). Global and low latitude export production is controlled by the amount of intermediate and deep water formed at subantarctics (Sarmiento et al, 2003; Marinov et al, 2006). The uniqueness of the Southern Ocean is that while its surface water harbors significant amounts of macronutrients e.g., nitrate, silicate and phosphate to support high primary production, yet the productivity in this region is quite low. Because of this property this region is described as a “High Nutrient Low Chlorophyll” or HNLC region (Minas et. al., 1986). Several causes including low temperature, low specific growth rate, grazing control, sun-light limitation, trace metal toxicity and Fe-limitation, have been proposed to explain “HNLC” condition. During the last decade, a number of large scale Fe-enrichment experiments were carried out to test the hypothesis of Fe-limitation in such regions (de Baar et al., 2005). More recently it has been proposed that natural iron fertilization due to upwelling of nutrient rich water, which contains Fe as well, from deep leads to development of bloom near the Kerguelen plateau sector of the Southern Indian Ocean (Blain et al., 2007). As a consequence of these experiments now it is well established that iron addition could cause increased carbon sequestration through enhanced marine productivity but studies pertaining to the nitrogen uptake rates are limited.

The rates of total N-uptake, integrated over the photic zone showed a significant variation in the Southern Indian Ocean. Euphotic zone integrated total N-uptake rate varied from 1.73 mmolNm⁻²d⁻¹ to 12.26 mmolNm⁻²d⁻¹ in the Southern Indian Ocean; highest uptake rate was at a station (PP1) in the Antarctic coastal zone and the lowest at



58°S. Nitrate uptake rate was more than ammonium and urea uptake rates at all the stations except at a station north of STF (sub-tropical front) at 35°S where ammonium uptake was more than nitrate uptake. Our mean column N-uptake rate in this zone ($1.17 \pm 0.36 \text{ mmolNm}^{-2}\text{d}^{-1}$) is significantly less than those reported by Savoye et al., (2004) (mean = $5 \text{ mmolNm}^{-2}\text{d}^{-1}$) from the Australian sector of the Southern Ocean on similar latitudes. The decrease in productivity in this zone has been attributed to the strong stratification due to the melting of sea ice in summer by Treguer and Jacques, (1992). In late austral summer the whole Southern Indian Ocean is characterized by high nitrate uptake and hence high new production: new production during late austral summer in the Indian sector of the Southern Ocean varied from $0.92 \text{ mmolNm}^{-2}\text{d}^{-1}$ to $7.7 \text{ mmolNm}^{-2}\text{d}^{-1}$. The highest new production of $616 \text{ mgCm}^{-2}\text{d}^{-1}$ was observed at the Antarctic coast and lowest of $73.6 \text{ mgCm}^{-2}\text{d}^{-1}$, the lowest observed during the present study, at a station at 58°S. The plot of total N-uptake (on x-axis) and nitrate uptake (on y-axis) shows very significant correlation between the two: $y = (0.63 \pm 0.06) x - (0.66 \pm 0.42)$ (coefficient of determination, $r^2 = 0.95$). The slope of line of regression suggests the maximum possible value of f -ratio (0.63) for this zone. This large area is traditionally regarded as a low productive area where for some reason or the other the surface nutrients are not utilized fully. Our measurements show that even though the productivity over a large area of the Southern Ocean is low, the f -ratio is moderately high. This signifies that a large part of production could get transported to deeper ocean and thus this area has the potential to play a significant role in atmospheric carbon sequestration.

Chapter 5. Conclusions and Scope for future work

Biogeochemical processes including the marine carbon cycle are the key factors in global change. The ocean works as a net sink for CO_2 , a potential greenhouse gas, through biological pump. The present study brings new data on oceanic productivity using ^{15}N tracer technique which not only gives total productivity but also categorise it into new and regenerated productivity; new productivity indirectly gives an estimation of the export production i.e., amount of carbon that is getting removed from the atmosphere for a sufficiently longer time scale through biological activities. For the first time, ^{15}N based productivity has been measured in the equatorial Indian Ocean. It also provides

comprehensive data on new and regenerated productivity and *f*-ratios of the northeastern Arabian Sea and the southern Indian Ocean and has made an effort to assess the role of the Indian Ocean in the Global Carbon Cycle. The important results that have emerged from this study are as follows:

- The Arabian Sea was characterized by the presence of two different biogeochemical provinces during the late winter monsoon: low productive southern province and highly productive northern province with an overall increasing trend from the south to the north.
- Total productivity in the southern region averaged around $5.5 \text{ mmolNm}^{-2}\text{d}^{-1}$ ($440 \text{ mgCm}^{-2}\text{d}^{-1}$) whereas in the north it was $19 \text{ mmolNm}^{-2}\text{d}^{-1}$ ($1520 \text{ mgCm}^{-2}\text{d}^{-1}$); increase in productivity from the south to north was more than three fold. New productivity also increased on south-north transect, from $2.1 \text{ mmolNm}^{-2}\text{d}^{-1}$ ($168 \text{ mgCm}^{-2}\text{d}^{-1}$) in the south to $15.7 \text{ mmolNm}^{-2}\text{d}^{-1}$ ($1256 \text{ mgCm}^{-2}\text{d}^{-1}$) in the north. Increase in new productivity was more than 7-fold.
- During the early winter monsoon total productivity varied from $4.07 \text{ mmolNm}^{-2}\text{d}^{-1}$ ($326 \text{ mgCm}^{-2}\text{d}^{-1}$) to $23.31 \text{ mmolNm}^{-2}\text{d}^{-1}$ ($1865 \text{ mgCm}^{-2}\text{d}^{-1}$) with a mean of $8.65 \text{ mmolNm}^{-2}\text{d}^{-1}$ ($692 \text{ mgCm}^{-2}\text{d}^{-1}$). Productivity during this season was almost half of that during the bloom but was more than the productivity in the south during the late winter monsoon. New productivity showed a large variation; it varied from a low of $1.95 \text{ mmolNm}^{-2}\text{d}^{-1}$ ($156 \text{ mgCm}^{-2}\text{d}^{-1}$) to a high of $19.70 \text{ mmolNm}^{-2}\text{d}^{-1}$ ($1576 \text{ mgCm}^{-2}\text{d}^{-1}$).

In general, results from the present study suggest almost three fold increase in the total productivity during the developing phase of the *Noctiluca* bloom. This increase was more than seven fold in new productivity. During early winter monsoon total and new productivity was less than those during the bloom but was more compare to non-bloom southern regions. The most important finding of the present study for the eastern Arabian Sea is the identification of two different biogeochemical provinces during the late winter monsoon where the northern province was four times more productive than the southern.

The present study was the first step towards understanding the biogeochemistry of the equatorial Indian Ocean. The results from this region suggest that mixed layer has greater control on the productivity. Total and new production were very less in this layer and so the f -ratio. Reduced forms of nitrogen were preferred over nitrate. Some important results are:

- Total N-uptake was very less: it varied from $0.66 \text{ mmolNm}^{-2}\text{d}^{-1}$ to $2.23 \text{ mmolNm}^{-2}\text{d}^{-1}$. Mean N-uptake was $1.32 \text{ mmolNm}^{-2}\text{d}^{-1}$ ($105.6 \text{ mgCm}^{-2}\text{d}^{-1}$)
- New production along 77°E transect was $0.20 \text{ mmolNm}^{-2}\text{d}^{-1}$ ($16 \text{ mgCm}^{-2}\text{d}^{-1}$), almost half of the same $0.43 \text{ mmolNm}^{-2}\text{d}^{-1}$ ($34.4 \text{ mgCm}^{-2}\text{d}^{-1}$) along 83°E transect.
- The f -ratio was low though it showed considerable spatial variation: it varied from 0.14 to 0.40. The f -ratio was low along 77°E (mean = 0.18) transect but was relatively high along 83°E (mean = 0.29).

While a large area of the Southern Indian Ocean is not highly productive, it appears capable of moderate export productivity and thus could be significant in removing atmospheric CO_2 on longer time scales. Relatively high productivity was measured in Antarctic coastal zone, STF and equatorial Indian Ocean. A large part of the southern Ocean, HNLC region, is less productive but can have high export production, almost 50% of the total. A mean f -ratio of 0.50 in the southern ocean indicates that the autotrophic community uses nitrate as well as regenerated nutrients equally. Compared to other data from similar regions (Mengesha et al., 1998, Savoye et al., 2004) the present study shows a shift in productivity regime from regenerated nutrient based production to nitrate based production, in the last 12 years possibly due to global warming. This means a slightly greater export production in this region than before. These results are first comprehensive estimates of nitrogen based productivity in a large area in the Southern Indian Ocean.

- Euphotic zone integrated total uptake rate varied from $1.73 \text{ mmolNm}^{-2}\text{d}^{-1}$ ($138 \text{ mgCm}^{-2}\text{d}^{-1}$) to $12.26 \text{ mmolNm}^{-2}\text{d}^{-1}$ ($981 \text{ mgCm}^{-2}\text{d}^{-1}$) in the Southern Indian Ocean; the highest rate was measured in the Antarctic coastal zone (69°S).

- New productivity varied from $0.92 \text{ mmolNm}^{-2}\text{d}^{-1}$ ($73.6 \text{ mgCm}^{-2}\text{d}^{-1}$) to $7.7 \text{ mmolNm}^{-2}\text{d}^{-1}$ ($616 \text{ mgCm}^{-2}\text{d}^{-1}$). The Antarctic coastal zone, equatorial region and STF had more new production compared to other regions of the Southern Ocean.
- Mean total uptake in a large part of the Southern Ocean was very low. It was $1.73 \text{ mmolNm}^{-2}\text{d}^{-1}$ ($138 \text{ mgCm}^{-2}\text{d}^{-1}$), almost one-seventh of the Antarctic coastal zone.

Scope for the future work

Despite having some major programme such as JGOFS and BOBPS, a large part of Indian Ocean still remains unexplored particularly the Bay of Bengal, equatorial Indian Ocean and the Southern Indian Ocean. Even though the Arabian Sea has received some attention of oceanographers all over the world for being dynamic in space and time, the major emphasis has been given to the central and western Arabian Sea; the northeastern Arabian Sea is relatively less studied. In order to understand the role of Indian Ocean, as a whole, in the global carbon cycle we need much more comprehensive understanding of the primary and export productions taking place in this part of the world ocean and for this we need more such observations pertaining to the estimation of new production and the f -ratio.

High productivity events of the Arabian Sea are followed by formation of oxygen minimum zone in sub-surface layer which leads to significant denitrification.

Quantification of denitrification, is important to estimate the carbon and nitrogen budget and hence its needs to be incorporated in the future studies

Quantification of N_2 fixation by these cyanobacterium is important to understand marine nitrogen cycle as it is a source of new nitrogen to the marine cycle.

^{15}N tracer technique can be effectively combined with ^{13}C . A coupled tracer techniques for the estimation of primary and new production may give a better understanding of the productivity regimes and nutrients kinetics and so quantification of new productivity using this technique should be the course of research in the near future.